UMS
UNIVERSITI MALAYSIA SABAH

BORNEO SCIENCE

The Journal of Science and Technology

ONLINE ISSN : 2231-9085 | ISSN : 1394- 4339

BORNEO SCIENCE

A JOURNAL OF SCIENCE AND TECHNOLOGY

BORNEO SCIENCE is a journal of science and technology published twice a year. It publishes original articles on all aspects of research in science and technology of general or regional interest particularly related to Borneo. Manuscripts submitted must not have been published, accepted for publication, or be under consideration elsewhere. Borneo Science welcomes all categories of papers: full research papers, short communications, papers describing novel methods, review papers and book reviews. Views expressed in the articles do not represent those of the Editorial Board and the University.

BORNEO *SCIENCE* *merupakan jurnal sains dan teknologi yang diterbitkan dwitahunan. Jurnal ini menerbitkan artikel asli dalam kesemua bidang sains dan teknologi secara umum mahupun dalam kepentingan serantau, terutamanya yang berkaitan dengan Borneo. Manuskrip yang dihantar bukan yang telah diterbitkan, telah diterima untuk diterbitkan, atau sedang dipertimbangkan untuk diterbitkan. Borneo Science mengalu-alukan semua jenis kertas kerja sama ada hasil penyelidikan, komunikasi pendek, penjelasan suatu kaedah, ulasan kertas kerja atau ulasan buku. Pandangan yang ditulis dalam artikel Borneo Science tidak menggambarkan pendapat Sidang Editor dan Universiti.*

DOI: https://doi.org/10.51200/bsj.v46i2

BORNEO SCIENCE

A JOURNAL OF SCIENCE AND TECHNOLOGY

BORNEO SCIENCE

A JOURNAL OF SCIENCE AND TECHNOLOGY

ONLINE ISSN 2231-9085 | ISSN 1394-4339

BORNEO SCIENCE

A JOURNAL OF SCIENCE AND TECHNOLOGY
JURNAL SAINS DAN TELNOLOGI

Volume 46 Issue 2

September 2025

CONTENT
KANDUNGAN

Page
Muka
Surat

ORIGINAL ARTICLES

BORNEO SCIENCE

A JOURNAL OF SCIENCE AND TECHNOLOGY

RESEARCH ARTICLE

BORNEO SCIENCE
THE JOURNAL OF SCIENCE & TECHNOLOGY

Journal homepage: https://jurcon.ums.edu.my/ojums/index.php/borneo-science

GROWTH AND HEAVY METAL CONTENT IN TWO ROSELLE VARIETIES CULTIVATED UNDER DIFFERENT TYPES OF SOIL MEDIA

Siti Aishah Mohd Ali, Sahibin Abd. Rahim, Rohana Tair, and Tan Wei Hsiang*

Faculty of Science and Technology, Universiti Malaysia Sabah, Jln UMS, 88400 Kota Kinabalu, Sabah, Malaysia.

***Correspondence:**
tan@ums.edu.my

Received: 4 June 2025
Revised: 3 July 2025
Accepted: 4 July 2025
Published online: 29 September 2025

DOI:

10.51200/bsj.v46i2.6468

Keywords:
Roselle; Heavy metal; Plant growth; Ultrabasic soil; Clay soil

ABSTRACT. *Recent increases in anthropogenic activities have contributed to elevated levels of heavy metals in the environment. These metals can bioaccumulate within ecosystems and be absorbed by plants. Therefore, this study was carried out to investigate the influences of different soil type treatments (ultrabasic, clay, and organic soil) on plant growth, phenolic constituents' production, and selected heavy metal content (Zn, Cd, Co, Cu, Ni, Cr, Pb, and Mn) in two Roselle varieties (H. sabdariffa L. and H. sabdariffa var. UMKL-1). The growth parameters, including plant height, stem diameter, number of branches, and leaf count, were recorded. Roselle calyx extract was analyzed for heavy metal concentrations using Inductively Coupled Plasma - Optical Emission Spectrometry. The results showed no statistically significant effects of soil type ($p > 0.05$) or variety on growth parameters. Overall, growth parameters increased steadily over the 84 days after transplanting in both varieties. In addition, heavy metal results indicated that Mn and Zn were the predominant heavy metals accumulated in both varieties. Roselle grown in ultrabasic soil showed higher levels of Mn, Co, Ni, and Pb, while clay soil resulted in higher concentrations of Zn, Cu, Cr, and Cd. In contrast, organic soil had the lowest heavy metal content. In conclusion, both roselle varieties grown in organic soil demonstrated better growth and lower heavy metal accumulation in the calyces.*

INTRODUCTION

In recent years, the issue of environmental contamination by heavy metals has gained significant attention due to human activities. There is growing concern about the bioaccumulation of these metals in the environment, particularly as they are absorbed by plants. Heavy metals present in water and soil can be taken up by plants, eventually accumulating in their tissues (Nnaji *et al*., 2023). This accumulation can negatively impact the nutritional value of plants, leading to deficiencies in essential nutrients (Khan *et al*., 2015). While some heavy metals are required by plants for growth, excessive levels can become highly toxic (Chibuike & Obiora, 2014). Therefore, it is crucial to monitor the heavy metal concentrations in plants to assess potential risks related to their consumption.

Roselle, scientifically known as *Hibiscus sabdariffa L.*, is a subtropical plant belonging to the Malvaceae family. In Malaysia, it is commonly referred to as "asam paya," "asam kumbang," or "asam susur" and is widely recognized for its versatile uses. The edible calyces of Roselle are harvested for a variety of food and traditional medicinal applications, including herbal teas, ice creams, jams, and jellies (Avela *et al*., 2021). Due to its numerous health benefits, Roselle is extensively used for its medicinal

properties. This herbaceous shrub is known for its antioxidant, antibiotic, antihypertensive, antidiabetic, cardioprotective, and anticancer effects (Abou-Sreea *et al*., 2022). The calyx extract contains a range of beneficial compounds, including phenolic acids, anthocyanins, flavonoids, alkaloids, terpenes, phenols, cardiac glycosides, steroids, saponins, tannins, and anthraquinone (Nerdy *et al.*, 2022).

This study involved two varieties of Roselle: *Hibiscus sabdariffa L.* and *H. sabdariffa* var. UMKL-1. The former, commonly known as the Arab variety, is widely grown in Malaysia and is distinguished by its deep red calyces. It was introduced to the country in the early 1990s by the Department of Agriculture in Terengganu (Mohamad *et al*., 2011). The UMKL-1 variety, often referred to as the Terengganu variety, was developed by Universiti Malaya (UM) for commercial cultivation. This variety is noted for its dark green leaves and red calyces. Compared to UMKL-1, the Arab variety generally produces a higher yield of calyces per plant and exhibits more vigorous growth (Mohamad *et al.*, 2011).

Currently, there aren't many studies on how Roselle accumulates heavy metals when cultivated using different soil media. It is essential to understand how different types of soil media may affect Roselle's reactions to metal uptake. Therefore, this study aims to investigate the influences of different soil media treatments (ultrabasic, clay, and organic soil) on the growth of two Roselle varieties, calyces (*H. sabdariffa* L. and *H. sabdariffa* var. UMKL-1), and evaluating the selected heavy metals concentrations (Zn, Cd, Co, Cu, Ni, Cr, Pb, Mn) in soil and Roselle calyces using Inductively Coupled Plasma - Optical Emission Spectrometry (ICP-OES).

MATERIALS AND METHODS

Plant Samples and Treatments

Two roselle varieties were evaluated in three types of soil media (ultrabasic, clay, and organic soil) at Universiti Malaysia Sabah from December 2021 to April 2022. Healthy roselle seeds were first sown in seed trays filled with organic soil. After two weeks, seedlings measuring 6–8 cm in height were selected and transplanted into 20 × 20 cm nursery polyethylene bags containing 15 kg of the respective soil media. Irrigation was provided via a drip system at a rate of 1.72 L per plant per day, applied twice daily, following the optimal recommendation for roselle growth reported by Nur Amirah *et al*. (2015). All plants received the same commercial fertilizer regime (NPK Green 15:15:15 and NPK + Mg Blue 12:12:17:2) along with organic matter/compost. Fertilizers were applied every two weeks after transplanting. Manual weeding was conducted regularly, and pesticides were used when needed. Calyces were harvested 35–40 days after flowering from four individual plants per treatment, serving as biological replicates. Figure 1 illustrates the roselle cultivation process.

Sample Collection

The collection of calyces started at the end of February until April 2022. Fresh calyces were placed in zip-lock bags and kept in a cooler for transport to the laboratory. Each calyx was washed with water, drained, the seeds were removed, and then the calyces were air-dried at room temperature for three days. The dried calyces were sealed in zip-lock bags and stored in a refrigerator at -20 °C until extraction. Roselle calyx extract was prepared following the method of Chumsri *et al.* (2008). Briefly, dried calyces were extracted with water at a 1:10 ratio in a water bath at a constant temperature of 50 °C for 30 minutes. The extracts were then filtered using Whatman No. 1 filter paper, and the filtrates were dried with a freeze dryer.

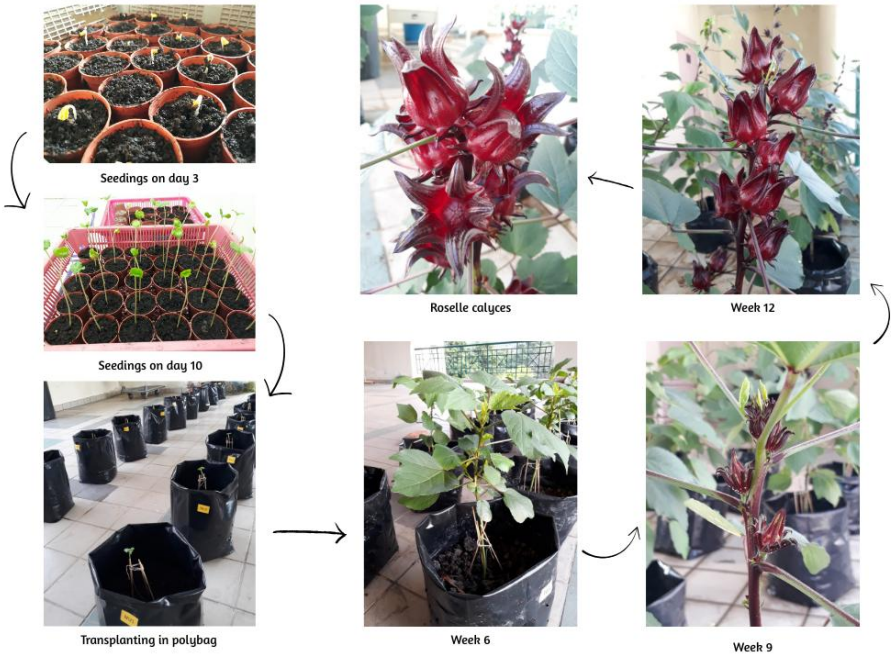

Figure 1. Cultivation process of *H. sabdariffa*.

Determination of Growth Traits

Growth parameters, including stem diameter (mm), plant height (cm), number of branches, and number of leaves (an indicator of physiological age), were recorded at seven-day intervals after transplanting. The number of branches was determined by counting the primary reproductive branches. Plant height was measured from ground level to the shoot tip along the main stem using a measuring tape. The number of leaves was counted and recorded for every visible leaf on the plant, including newly emerging leaf tips.

Heavy Metal Analysis

The soil and dry calyces' samples underwent heavy metals analysis (Zn, Cd, Co, Cu, Ni, Cr, Pb, and Mn). Using the digestion method, the heavy metals were extracted from the soil (Weldegebrial *et al.*, 2012). Briefly, 1 g of each soil sample was digested with a mixture of 5 mL HNO_3 and 10 mL HCl for at least 45 minutes at 160 °C. It was removed from the heated plate before it dried, chilled, diluted in a 200 mL volumetric flask with distilled water, agitated, and poured back into the beaker after 30 minutes of settling. The heavy metal concentrations in the samples were determined using ICP-OES, and the results were expressed in milligrams per liter (mg/L). Calibration was performed to ensure accurate and reliable measurements.

The dry calyces samples underwent heavy metal analysis using the wet digestion technique according to US EPA method 3050 B. Briefly, about 1 g of finely powdered dried calyx was combined with 10 mL of 65% nitric acid (HNO_3), then heated to a temperature of 95 °C $\pm$ 5 °C and subjected to reflux for a duration of 10 to 15 minutes, ensuring that boiling did not occur. After cooling, a volume of 5 mL of concentrated HNO_3 was introduced and refluxed for 30 minutes. The presence of brown fumes showed that oxidation had taken place due to the addition of HNO_3. Subsequently, 5 mL concentrated nitric acid was added dropwise until no more brown fumes were produced by the sample. After the mixture had cooled down, about 2 mL of water and 3 mL of 30% hydrogen peroxide (H_2O_2) were added to the sample. Subsequently, the flask was sealed with a watch glass and subjected to further heating to trigger the peroxide reaction. The sample combination was heated until the bubbling ceased and then chilled. A 1 mL portion of 30% hydrogen peroxide (H_2O_2) was introduced into the flask. The sample was subjected to heat until the effervescence reached a minimum level. The maximum volume of 30%

H_2O_2 that may be added is 10 mL. The acid-peroxide sample was thereafter placed under a watch glass and subjected to heating at a temperature of 95 °C ± 5 °C, avoiding boiling, until the volume was decreased to roughly 5 mL. Subsequently, the sample was allowed to undergo a cooling process. The cooled sample was treated with 10 mL of 37% hydrochloric acid (HCl) solution. The mixture was then heated for 15 minutes. Subsequently, the initial sample combination was diluted by adding 100 mL of water. The particulates in the sample were separated by passing them through a membrane filter paper with a pore size of 0.45 µm. Subsequently, the material that had undergone filtration was subjected to analysis using ICP-OES.

Statistical Analysis

The mean value ± standard deviation collected data were subjected to analysis of variance using the Statistical Package for Social Science for Windows version 29.0 software (IBM SPSS Statistics). To find significant variations between treatments, a one-way analysis of variance (ANOVA) was used. Significantly different values are defined at the 5% level ($p < 0.05$).

RESULTS AND DISCUSSIONS

Growth Characteristics

Figure 2 presents the data for each growth parameter measured at seven-day intervals in roselle plants under different irrigation treatments. No statistically significant differences were observed among the irrigation treatments ($p > 0.05$). Overall, all growth parameters showed an increasing trend over the 84 days after transplanting across all treatments. Although the differences were not significant, both Roselle varieties grown in ultrabasic soil exhibited the lowest growth rates for all parameters except the number of branches, when compared to clay and organic soil. This may be attributed to the high mineral content of ultrabasic soil, which often results in increased acidity. Excessively acidic soils can negatively impact soil physical properties and reduce nutrient availability for plant growth (Xia *et al*., 2024).

These results are consistent with Shuhaimi *et al*. (2019) on *H. sabdariffa* L., Nur Amirah *et al.* (2015) on *H. sabdariffa* var. UMKL-1 and Azza *et al*. (2010) on *Jatropha curcas.* Nur Amirah *et al.* (2015) reported no statistically significant differences in UMKL-1 growth cultivated in Beach Ridges Interspersed with Swales (BRIS) soil with respect to leaf area index, plant height, stem diameter, or post-harvest quality. In contrast, Khalil and Abdel-Kader (2011) found that sandy soil significantly enhanced all growth characteristics in *H. sabdariffa* L. from Egypt compared to clay soil. Azza *et al*. (2010) suggested that sandy soil allows the root system to penetrate deeper and spread more widely than clay soil, promoting better root establishment. Metwally *et al*. (1972) highlighted that soil aeration, nutrient availability, water movement, and microbiological activity are highly dependent on soil pore structure. However, sandy soils may experience rapid leaching of nutrients and chemicals as they move downward with water (Roslan *et al.*, 2010).

Heavy Metal Concentration in Soil

The concentration of heavy metals in the soil followed the order: ultrabasic soil > clay soil > organic soil (Table 1). The highest concentration of heavy metals in ultrabasic soil is in descending order: Cr >Mn > Ni > Co > Cu > Zn > Pb > Cd. The high levels of Cr, Ni, and Mn in ultrabasic soil are likely due to the geological nature of ultrabasic formations, which are known to contain elevated concentrations of these metals (Siebecker, 2010). In contrast, Pb, Cu, and Zn were found at comparatively lower levels, while Cd was below the detection limit.

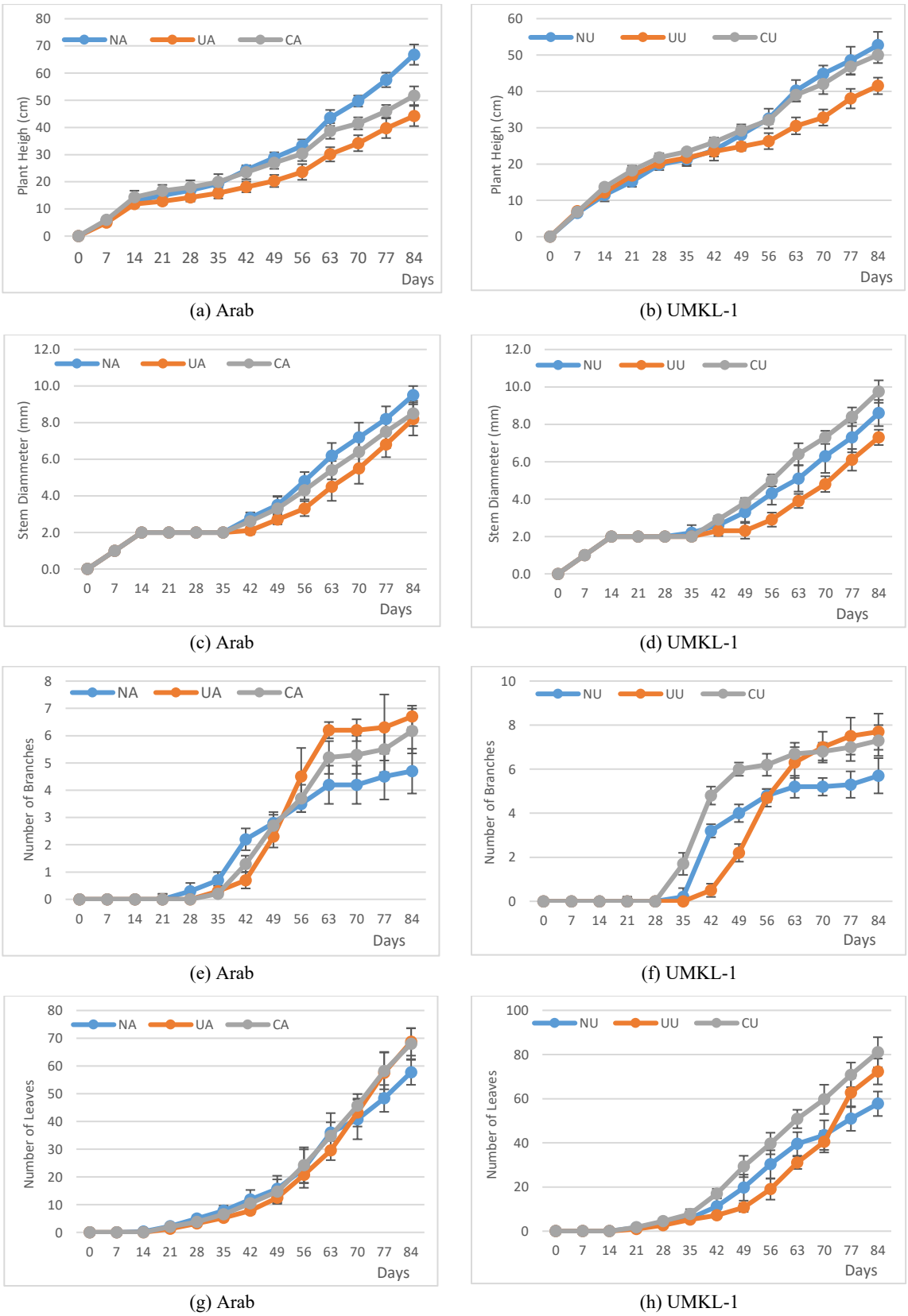

Arab: **NA** = Organic soil; **UA** = Ultrabasic soil; **CA** = Clay soil

UMKL-1: **NU** = Organic soil; **UU** = Ultrabasic soil; **CU** = Clay soil

Figure 2. The effect of soil media's treatment on Arab and UMKL-1 growth with different parameters: a-b) Plant height; c-d) Stem diameter; e-f) Number of branches, and g-h) Number of leaves. Data points are means of biological replicates (n = 4). The vertical bar represents the standard deviation.

Table 1. Heavy metal concentration in soils.

Heavy metal	Soil Sample (mg/kg)		
	Ultrabasic Soil	Clay Soil	Organic Soil
Zn	49.42 ± 4.58	29.23 ± 12.17	7.20 ± 1.73
Cd	BDL	BDL	BDL
Co	306.23±4.50	1.02±0.34	0.14 ± 0.12
Cu	80.57 ± 14.19	4.28 ± 2.41	1.07 ± 0.38
Ni	2023.60 ± 415.50	3.99 ± 1.95	1.00 ± 0.17
Cr	4402.80 ± 462.10	13.24 ± 5.09	7.33 ± 0.79
Pb	0.07 ± 0.12	2.86 ± 1.83	0.10 ± 0.12
Mn	2257±402	23.07±5.67	14.75±2.11

BDL = Below Detection Limit; Values represent the mean of four replicates ± Standard deviation

Ultrabasic soil has a rich mineral composition and generally exhibits a high pH. The findings are consistent with the known influence of soil minerals on metal retention, as the mineral content in ultrabasic soil can affect the availability and mobility of heavy metals in the environment (Wuana & Mbasugh, 2013). In clay soil, heavy metals were present in the descending order: Zn > Mn > Cr > Cu > Ni > Pb > Co > Cd. Clay is characterized by fine particles and high water-holding capacity. Its mineral structure may restrict the accumulation of heavy metals, suggesting that factors beyond mineral composition also influence metal retention (Tiwari & Lata, 2018).

In addition, organic soil contains heavy metals in descending order: Mn > Cr > Zn > Cu > Ni > Co > Pb > Cd. The high organic matter content in this soil type can affect metal availability and binding, contributing to the relatively lower uptake of heavy metals observed (Abubakari *et al*., 2017). All measured heavy metal concentrations were well below WHO limits, indicating that all soil types fall within acceptable ranges for agricultural use and pose minimal risk related to excessive heavy metal content (U.S. Environmental Protection Agency, 1996; 2002).

Accumulation of Heavy Metals in Roselle Calyces

Tables 2 and 3 show the heavy metal concentrations in the Roselle Arab and UMKL-1 varieties. Both Roselle calyces show similar heavy metal content, in the descending order: ultrabasic soil > clay soil > organic soil. Mn and Zn are the highest in concentration, followed by Cu, Cr, and Ni, while Co, Cd, and Pb are almost below the detection limit. The heavy metal concentrations in Roselle calyces for all elements did not violate the permissible limits of World Health Organization (WHO) guidelines for vegetable crops (Bigdeli & Seilsepour, 2008). Thus, the low amounts of heavy metals in roselle plant tissues show that the fruits are safe to be consumed.

Table 2. Heavy metal concentration in the Roselle Arab variety.

Heavy metal	Soil Sample (mg/kg)		
	Ultrabasic Soil	Clay Soil	Organic Soil
Zn	36.42 ± 3.32	46.01 ± 2.34	39.66 ± 1.03
Cd	BDL	BDL	BDL
Co	1.34±0.01	BDL	BDL
Cu	9.52 ± 0.01	9.31 ± 0.11	7.44 ± 0.32
Ni	5.36 ± 0.01	1.45± 0.01	1.03 ± 0.12
Cr	9.67 ± 0.22	9.47 ± 0.12	4.43 ± 0.32
Pb	BDL	BDL	BDL
Mn	150.45±6.32	97.33±3.67	68.73±2.11

BDL = Below Detection Limit; Values represent the mean of four replicates ± Standard deviation.

Table 3. Heavy metal concentration in the Roselle UMKL-1 variety.

Heavy metal	Soil Sample (mg/kg)		
	Ultrabasic Soil	**Clay Soil**	**Organic Soil**
Zn	36.77 ± 3.58	56.11 ± 8.17	50.22 ± 5.73
Cd	BDL	BDL	BDL
Co	1.21±0.01	BDL	BDL
Cu	8.43 ± 0.01	9.39 ± 0.17	8.49 ± 0.52
Ni	5.89 ± 0.01	2.45± 0.01	1.73 ± 0.11
Cr	6.91 ± 0.12	7.23 ± 2.12	3.73 ± 0.12
Pb	BDL	BDL	BDL
Mn	134.45±6.32	102.53±4.69	89.73±1.34

BDL = Below Detection Limit; Values represent the mean of four replicates ± Standard deviation.

Roselle, like many leafy vegetables, is classified as a hyperaccumulator plant. Hyperaccumulators are capable of storing higher concentrations of heavy metal ions in their shoots than in their roots and possess greater tolerance to heavy metals compared to other plant species (Saleem *et al*., 2020). Roselle is also an important source of minerals, including K, Ca, and Mg, as well as trace elements such as Fe, Mn, Zn, and Cu. These minerals play a crucial role in promoting health by acting as antioxidants or being involved in the functioning of antioxidant enzymes (Mitra *et al.,* 2022). According to Getso *et al.* (2018), the Roselle plant can accumulate a high concentration of Mn from mineral fertilizers, exceeding the tolerable daily intake but within the permissible limit. Similarly, Younes *et al*. (2016) found that roselle can remove up to 8 µM Mn from contaminated soil. Abou El-Seoud *et al*. (1997) observed that certain heavy metals (Fe, Mn, Zn, and Co) accumulated in roselle calyces at varying concentrations when plants were grown in soil amended with organic waste compost. Consistent with these findings, Shuhaimi *et al.* (2019) reported that Pb, Cd, and Cu levels in roselle crops remained very low.

Herrera-Estrella *et al.* (1999), in their study on heavy metal adaptation, explained that genotypic evolution and natural selection enabled accumulator species to adapt over time to habitats with high endogenous metal concentrations. The key mechanisms involved include metabolic adaptability, complexation, and compartmentalization. As a result, metal tolerance in plants may arise through fundamental strategies such as metal exclusion or metal accumulation, depending on the species. Therefore, metal toxicity in plants is often a complex and subtle phenomenon rather than a clearly visible, isolated issue. It may result from intricate interactions among major toxic ions, other essential or non-essential ions, and various environmental factors.

CONCLUSION

Cultivation of both roselle varieties in different soil media showed an overall increasing growth trend over the 84 days after transplanting. However, no statistically significant differences ($P > 0.05$) were observed in most growth parameters. For heavy metal accumulation, both varieties and soil types followed the descending order: ultrabasic soil > clay soil > organic soil. Therefore, it can be concluded that both varieties grown in organic soil may achieve better growth, particularly in height and stem diameter, while also exhibiting lower heavy metal content in the calyces. Future research could explore the influence of environmental variables beyond soil conditions to provide a more comprehensive understanding of the factors affecting plant growth and bioactive compound production. Such an approach could enhance knowledge of Roselle cultivation in Malaysia and help optimize conditions to maximize its health-promoting properties.

ACKNOWLEDGEMENT

The authors gratefully acknowledge the facility support from the Faculty of Science and Technology, Universiti Malaysia Sabah. The authors also acknowledge the financial support of Universiti Malaysia Sabah under the *Skim Penyelidikan Bidang Keutamaan* grant (SBK0493-2021).

REFERENCES

Abou El-Seoud, M.A.A., Abd El-Sabour, M.F. & Omer, E.A. 1997. Productivity of roselle (*Hibiscus sabdariffa* L.) plant as affected by organic waste compost addition to sandy soil. *Bulletin of National Research Centre, Cairo*, 22(4), 495-505.

Abou-Sreea, A.I.B., Roby, M.H., Mahdy, H.A., Abdou, N.M., El-Tahan, A.M., El-Hack, M.E.A., Taha, A.E. & El-Saadony, F.M. 2022. Improvement of selected morphological, physiological, and biochemical parameters of roselle (*Hibiscus sabdariffa* L.) grown under different salinity levels using potassium silicate and *Aloe saponaria* extract. *Plants*, 11 (4): 497.

Abubakari, M., Abu, M., Nyarko, G. & Dawuda, M.M. 2017. Heavy metal concentrations and risk assessment of Roselle and Jute Mallow cultivated with three compost types. *Annals of Agricultural Sciences*, 62 (2): 145–150.

Avela, B.S., Bahadhur, V., Kerketta, A., Singh, R. & Tayde, A. R. 2021. Varietal evaluation, calyces yield, and jam preparation from roselle (*Hibiscus sabdariffa* L.). *Indian Journal of Pure Applied Biosciences,* 9(3): 257-261.

Azza, A.M., Nahed, G.A. & El-Habba, E. 2010. Impact of different soil media on growth and chemical constituents of *Jatropha curca* L. seedlings grown under water regime. *Journal of American Science* 6(8): 549-556.

Bigdeli, M. & Seilsepour, M. 2008. Investigation of metal accumulation in some vegetables irrigated with wastewater in Shahre Rey, Iran, and toxicological implications. *Journal of Agriculture and Environmental Science,* 4(1): 86–92.

Chibuike, G.U. & Obiora, S.C. 2014. Heavy metal-polluted soils: effect on plants and bioremediation methods. *Applied and Environmental Soil Science*, 2014(1): 1-12.

Chumsri, P., Airichote, A. & Itharat, A. 2008. Studies on the optimum conditions for the extraction and concentration of roselle (*Hibiscus sabdariffa* Linn.) extract. *Songklanakarin Journal of Science and Technology,* 30(1): 133-139.

Getso, M.M., Sallau, M.S., Abechi, S.E. & Uba, S. 2018. The influence of mineral fertilizers in nutrient supplementation and qualitative calyx production of roselle (*Hibiscus sabdariffa* L.). *Bayero Journal of Pure and Applied Sciences*, 11(2): 198-204.

Herrera-Estrella, L.R., Guevara-García, A.A. & López-Bucio, J. 1999. Heavy metal adaptation. *Encyclopedia of Life Science*, 1-5.

Khalil, S.E. & Abdel-Kader, A.A.S. 2011. The influence of soil moisture stress on growth, water relations, and fruit quality of *Hibiscus sabdariffa* L. grown within different soil types. *Nature and Science,* 9(4): 62-74.

Khan, A., Khan, S., Khan, M.A., Qamar, Z. & Waqas, M. 2015. The uptake and bioaccumulation of heavy metals by food plants, their effects on plant nutrients, and associated health risk: a review. *Environmental Science and Pollution Research*, 22(18): 13772-13799.

Metwally, M.M., Afify, M.M., Wahba, H.E., Makarem, A.M., Eraki, M.A., Metwally, S.S.Y., Hamdi, H., Abdel Samie, A.G., Hilal, M.H. & Mabrouk, S. 1972. A study on the porosity of compacted soils. *Egyptian Journal of Soil Science,* 12(1): 107-118.

Mitra, S., Chakraborty, A., Tareq, A.M., Emran, T.B., Nainu, F., Khusro, A., Idris, A.M., Khandaker, M.U., Osman, H., Alhumaydhi, F.A. & Simal-Gandara, J. 2022. Impact of heavy metals on the environment and human health: Novel therapeutic insights to counter the toxicity. *Journal of King Saud University - Science*, 34 (3): 101865.

Mohamad, O., Saberi, S., Nezhadahmadi, A., Hossain, Z. & Golam, F. 2013. Development and evaluation of fruit-related morphological and physico-chemical characteristics in three roselle mutants. *Pensee Journal,* 75(9): 332–339.

Nerdy, N., Barus, B.R., El-Matury, H.J., Ginting, S., Zebua, N.F. & Bakri, T.K. 2022. Comparison of flavonoid content and antioxidant activity in calyces of two Roselle varieties (*Hibiscus sabdariffa* L.). *IOP Conference Series: Earth and Environmental Science,* 956 (1): 012001.

Nnaji, N.D., Onyeaka, H., Miri, T. & Ugwa, C. 2023. Bioaccumulation for heavy metal removal: A review. *SN Applied Sciences*, 5: 125.

Nur Amirah, Y., Alias, A.A. & Wan Zaliha, W.S. 2015. Growth and water relations of roselle grown on BRIS soil under partial root zone drying. *Malaysia Applied Biology,* 44(1): 63-67.

Roslan, I., Shamshuddin, J., Fauziah C.I. & Anuar, A.R. 2010. Occurrence and properties of soils on sandy beach ridges in the Kelantan-Terengganu plains, Peninsular Malaysia. *Catena,* 83: 55-63.

Salem, M.A., Michel, H.E., Ezzat, M.I., Okba, M.M., El-Desoky, A.M., Mohamed, S.O. & Ezzat, S.M. 2020. Optimization of an extraction solvent for angiotensin-converting enzyme inhibitors from *Hibiscus sabdariffa* L. based on its UPLC-MS/MS metabolic profiling. *Molecules*, 25(10): 2307.

Shuhaimi, S. N., Kanakaraju, D. & Nori, H. 2019. Growth performance of roselle (*Hibiscus sabdariffa*) under application of food waste compost and Fe_3O_4 nanoparticle treatment. *International Journal of Recycling of Organic Waste in Agriculture*, 8: 299–309.

Siebecker, M. 2010. Nickel speciation in serpentine soils using synchrotron radiation techniques. Proceedings of the 19th World Congress of Soil Science, Soil Solutions for a Changing World, Aug. 1-6, DVD, Brisbane, Australia, 160-162.

Tiwari, S. & Lata, C. 2018. Heavy metal stress, signaling, and tolerance due to plant-associated microbes: An overview. *Frontiers In Plant Science*, 9: 452.

U.S. Environmental Protection Agency. 1996. *Soil Screening Guidance: Technical Background Document*, 2.

U.S. Environmental Protection Agency. 2002. National Recommended Water Quality Criteria: 2002.

Weldegebriel, Y., Chandravanshi, B.S. & Wondimu, T. 2012. Concentration levels of metals in vegetables grown in soils irrigated with river water in Addis Ababa, Ethiopia. *Ecotoxicology and Environmental Safety*, 77: 57–63.

Wuana, R.A. & Mbasugh, P.A. 2013. Response of roselle (*Hibiscus sabdariffa*) to heavy metals contamination in soils with different organic fertilisations. *Chemistry and Ecology*, 29(5): 437–447.

Xia, Y., Feng, J., Zhang, H., Xiong, D., Kong, L., Seviour, R. & Kong, Y. 2024. Effects of soil pH on the growth, soil nutrient composition, and rhizosphere microbiome *of Ageratina adenophora*. *PeerJ*, 12, e17231. https://doi.org/10.7717/peerj.17231.

Younes, M.A., Nicaise, L.A. & Bertrand, M.B. 2016. Polymerization degree of phytochelatin in contaminated soil phytoremediation of manganese in *Hibiscus sabdariffa* Linn var sabdariffa. *European Scientific Journal*, 12(33): 482- 492.

RESEARCH ARTICLE

BORNEO SCIENCE
THE JOURNAL OF SCIENCE & TECHNOLOGY

Journal homepage: https://jurcon.ums.edu.my/ojums/index.php/borneo-science

ADSORPTION BEHAVIOR OF Cu(II), Pb(II), AND Zn(II) ON SELECTED NATURAL SOILS IN SABAH

Tan Wei Hsiang[1], Noumie Surugau[1], Awang Bono[2], Mohd Hardyianto Vai Bahrun[3], Nurika Atiqah Widdie[1], Nur Athirah Suhaimy[1] and Siti Aishah Mohd Ali[1]*

[1] Faculty of Science and Technology, Universiti Malaysia Sabah, Jln UMS, 88400 Kota Kinabalu, Sabah, Malaysia
[2] GRISM Innovative Solutions, 88400 Kota Kinabalu, Sabah, Malaysia
[3] School of Chemical Engineering, Engineering Campus, Universiti Sains Malaysia, 14300 Seri Ampangan, Nibong Tebal, Pulau Pinang, Malaysia

*** Correspondence:**
ctaishah@ums.edu.my

Received: 8 September 2025
Revised: 31 October 2025
Accepted: 2 November 2025
Published online: 3 November 2025

DOI: 10.51200/bsj.v46i2.6789

Keywords:
Adsorption capacity; Adsorption isotherm models; Pb^{2+}; Cu^{2+}; Zn^{2+}

ABSTRACT. *Heavy metals in soil can reduce plant fertility and may pose health risks to those who consume the affected plants. Therefore, understanding the soil's ability to retain heavy metals is essential. This study explores the adsorption behaviors of Cu(II), Pb(II), and Zn(II) ions in selected natural soil samples from Sabah, providing insights into their retention capacities and potential environmental implications. The adsorption isotherms were measured using the conventional batch adsorption technique. The results indicate that the adsorption isotherms are satisfactorily described by both the Langmuir and the Freundlich models, with R^2 values mostly exceeding 0.93. Hilltop soil (clay loam) demonstrated the greatest adsorption capacity, exhibiting a distinct metal ion affinity sequence of $Cu^{2+} > Pb^{2+} > Zn^{2+}$. In contrast, clayey sand soils from orchards, rubber plantations, and foothill regions showed a preferential adsorption for Zn^{2+} over Pb^{2+} and Cu^{2+}. Despite sharing similar soil classifications, these variations highlight the influence of site-specific properties on metal ion adsorption behavior. It is found that soil adsorption behavior is shaped by mineralogical composition, particle size distribution, organic matter content, cation exchange capacity, pH, specific surface area, and land management practices. These elements influence both the availability of adsorption sites and the order in which adsorption takes place, ultimately determining the soil's capacity to retain and immobilize substances like heavy metals.*

INTRODUCTION

Soils are the major environmental reservoir for pollutants and waste materials, including heavy metals released through various anthropogenic activities (Naveedullah *et al*., 2013). Due to their nondegradable nature, heavy metals tend to accumulate in soil over time, leading to localized increases in concentration. Uptake of heavy metals from soil to plants is caused by their remaining in food chains, thus becoming a serious issue which may disrupt the balance of the ecosystem (Ayangbenro & Babalola, 2017). The presence of heavy metals also impairs the biodegradation of organic pollutants by disrupting the physiological and ecological functions of microorganisms responsible for organic matter breakdown (Olaniran *et al.*, 2013). Elevated concentrations of heavy metals in soil threaten ecosystem health through direct ingestion, consumption of contaminated water, and bioaccumulation in living organisms.

Furthermore, heavy metal contamination alters soil properties such as pH, porosity, color, and chemical composition, ultimately leading to a decline in overall soil quality (Musilova *et al.,* 2016).

Soil composition plays a pivotal role in regulating its physicochemical properties, particularly pH and cation exchange capacity (CEC), which in turn influence nutrient availability and contaminant mobility. Soil pH can be acidic or basic depending on the parent material during soil formation, while CEC reflects the soil's ability to retain and exchange cations, a function largely attributed to clay minerals and organic matter. Clay particles, with their high surface area and negative charge, exhibit a strong affinity for heavy metal ions such as Pb^{2+}, Cu^{2+}, and Zn^{2+}, facilitating their immobilization through sorption processes (Chen *et al.,* 2023). The presence of organic matter in soil contributes significantly to metal adsorption through complexation and chelation mechanisms (Chenu *et al.,* 2024). Organic compounds possessing functional groups such as carboxyl and phenolic hydroxyls have the capacity to bind metal ions, reducing their mobility and bioavailability. Soil rich in organic content tends to retain heavy metals more effectively, particularly in environments with slightly acidic to neutral pH levels, where these functional groups maintain their reactivity.

Past research has shown that several types of soil were used to adsorb heavy metals (Ali *et al*., 2023; Bai *et al*., 2024). Soil is able to adsorb or retain heavy metals from various sources and accumulates in the soil body. From an environmental perspective, when large quantities of heavy metals are accidentally introduced into the environment, whether through improper waste disposal, accidental spills, or activities like mining and ore smelting, there is concern about whether soils, such as clay-rich soils, can effectively adsorb these metals before they migrate to uncontaminated areas like streams or groundwater. This raises the critical need to assess the adsorption capacity of soils, as their composition significantly influences their ability to retain heavy metals. Soil is a complex matrix composed of various components, each contributing differently to its overall adsorption potential. Even within a single soil component, such as clay minerals, there can be substantial variation in surface area, reactive sites, and mineralogical composition. Clays differ in their chemical structure and arrangement, which affects their interaction with metal ions. Additionally, soil organic matter derived from a wide range of organisms adds another layer of variability, with diverse organic compounds influencing metal binding through various functional groups. Given these complexities, it is important to study the adsorption capacity of soil components in understanding their role in adsorption.

Thus, this study investigates the adsorption behavior of heavy metal ions (Cu^{2+}, Pb^{2+}, and Zn^{2+}) in selected soil samples from Sabah. The batch adsorption technique was used to investigate the adsorption. The adsorption isotherm is described by the most common use models: the Freundlich and Langmuir isotherms.

MATERIALS AND METHODS

Materials and Sampling Sites

Copper (II) ions as copper (II) nitrate trihydrate ($Cu(NO_3)_2.3H_2O$; AR grade, (99%), lead (II) ions as lead (II) nitrate ($Pb(NO_3)_2$; AR grade, (99.0%) and zinc (II) ions as zink (II) nitrate hexahydrate ($Zn(NO_3)_2.6H_2O$; AR grade, (98%). All these reagents were purchased from Sigma-Aldrich. The adsorbents used in this study consist of four soil samples collected from two areas: Kota Marudu and Sepanggar, Sabah. Farm areas (orchard & rubber plantation, Kota Marudu) and areas of different elevations (hilltop & foothill of Botak Hill, Sepanggar) were selected as sites to excavate soil samples. The topsoil layer (about 5 cm) and any discernible plant matter were meticulously removed before the soil samples were obtained from the surface to a depth of 20 cm (ASTM E1727-20). To obtain a representative composite sample, five discrete samples from each station were mixed. All soil samples were dried in an oven for 24 hours at 105 °C and then passed through a sieve (2.0 mm). Table 1 shows the chemical compositions, pH, and organic matter of soil samples.

Table 1. Properties of soil samples.

Soil samples	Chemical composition				pH	Organic matter content (%)
	SiO_2	Al_2O_3	Fe_2O_3	etc		
Orchard	84.20	8.88	4.29	2.62	5.13 ± 0.02	4.38 ± 0.03
Rubber Plantation	85.31	7.81	3.54	3.33	5.22 ± 0.04	1.99 ± 0.01
Hilltop	75.86	15.38	4.86	3.82	4.82 ± 0.09	5.92 ± 0.02
Foothill	81.51	9.35	7.76	1.38	4.41 ± 0.01	4.68 ± 0.03

Particle Size Distribution Analysis

Particle size distribution of sample was determined using the hydrometer method according to ASTM D7928-21E1. The dried samples were subsequently separated based on particle size using a Ro-Tap RX-29 Sieve Shaker. The samples were then transferred to the 2 mm sieve in the Sieve Shaker. With the size of sieves set from the range of 2 mm to 63 µm, the soil samples were separated into their specific size ranges. The percentage of clay, sand, and silt in the soil sample was calculated using Equation 1.

$$\text{Percentage clay/ sand/ silt} = \frac{Mass\ of\ clay,silt\ or\ sand\ in\ soil\ sample\ (g)}{mass\ of\ soil\ sample\ (g)} \times 100\% \quad (1)$$

Surface Area Analysis

Surface area and pore size of the sample were determined using the total surface area (S_t) equation (Equation 2) and the BET equation (Equation 3) (ISO 9277:2010(E)). The samples were degassed at 200 °C for 1 hour to remove the moisture. Soil samples were analyzed at 79 distinct points to obtain detailed information on pore size distribution and surface area.

$$S_t = N_m A_{CS} \quad (2)$$

Where N_m is the product of the number of molecules of adsorbate in a monolayer and A_{CS} is the effective cross–sectional area of the adsorbate molecule.

$$\frac{1}{W((P/P_o)-1)} = \frac{1}{W_m C} + \frac{C-1}{W_m C}\left(\frac{P}{P_o}\right) \quad (3)$$

Where W is the weight of gas adsorbed (g) at a relative pressure, P/P_o, and W_m is the weight of adsorbate (g) in a monolayer of surface coverage. The term C is the BET constant that is related to the energy of adsorption in the first adsorbed layer, and consequently, its value is an indication of the magnitude of the adsorbent/adsorbate interactions.

Cation Exchangeable Capacity (CEC) Analysis

Cation exchangeable capacity of soil samples was determined by following the SW-846 Test Method 9080. About 3.0 g of the sample was added to a 500 mL Erlenmeyer flask. Then 25 mL of the 1 M ammonium acetate (NH_4OAc) was added and shaken thoroughly, and allowed to stand overnight. The sample was filtered using No.2 filter paper and gently washed four times with 25 mL additions of the NH_4OAc. The leachate was discarded, and the sample was then washed with eight separate additions of 95% ethanol to remove excess saturating solution. Again, the leachate was discarded, and the receiving flask was cleaned. The adsorbed NH_4 was extracted by leaching the sample with eight separate 25 mL additions of 1M potassium chloride (KCl). The leachate was transferred to a 250 mL volumetric flask and diluted to volume with additional KCl. The concentration of NH_4-N in the KCl extract (20 mL) was determined by the Kjeldahl Method (distillation and titration). NH_4-N levels in the original KCl extracting solution (blank) were also measured to account for potential contamination present in the reagent. The CEC value was calculated using Equation 4.

$$\text{CEC (cmol}_c\text{/kg)} = V_a \times N \times V_{KCl} / S \times 100\text{g}/M_s \quad (4)$$

Where V_a is the volume of 0.01N HCl solution (mL) used in titrating the sample, N is the normality of 0.01N HCl solution, S is the volume of filtrate used for distillation (mL), V_{KCl} is the total volume of KCl used to substitute NH_4^+ (mL), and M_s is the weight of the sample used (g).

Adsorption Study

The adsorption study employed a standard approach for calculating adsorption isotherms, through certain modifications made considering previous research (Tan *et al*., 2021; Tan *et al*., 2023). Individual adsorbate solutions (Cu^{2+}/Pb^{2+}/Zn^{2+}) with concentrations ranging from 10 to 100 mg/L were prepared. The weight ratio between the adsorbent and the adsorbate solution was fixed at 1:50. All samples were prepared in triplicate. Each sample was placed in a 250 mL sealed conical flask in an incubator shaker for 24 h at 30 °C and at 100 rpm to achieve equilibrium. The samples were then centrifuged, and the concentrations of the solutions before and after adsorption were determined using inductively coupled plasma-optical emission spectrometry (ICP-OES). If necessary, a series of dilutions was performed to match the ICP-OES instrument's detection limit.

Adsorption Isotherms Analysis

For the analysis and interpretation of adsorption isotherms, two commonly used isotherm models, the Langmuir and Freundlich isotherms, were utilised to analyse the equilibrium data. The Langmuir adsorption model describes the surface as homogeneous with the assumption that maximum adsorption relates to a saturated monolayer of solute molecules occupied on the adsorbent's surface sites, with no lateral interaction between the adjacent adsorbed molecules, and the energy of adsorption is constant during the adsorption process (Benjelloun *et al.,* 2021). The Langmuir adsorption model is expressed as Equations 5 and 6.

$$q_e = \frac{q_m K_L C_e}{1 + K_L C_e} \quad (5)$$

$$R_L = \frac{1}{1 + (1 + K_L C_e)} \quad (6)$$

Where q_e is the amount of adsorbate adsorbed (mg/g), C_e is the concentration of adsorbate at equilibrium (mg/L), q_m is the maximum adsorption capacity (mg/L), K_L is the Langmuir constant related to the energy of adsorption and R_L is a separation factor which indicates the nature of the adsorption process to be either unfavorable ($R_L > 1$), linear ($R_L = 1$), favorable ($0 < R_L < 1$), or irreversible ($R_L = 0$). The linearization of the Langmuir equation (Equation 7) can be used to determine the adsorption parameters.

$$\frac{C_e}{q_e} = \frac{1}{q_m K_L} + \frac{C_e}{q_m} \quad (7)$$

When C_e/q_e is plotted against C_e, a straight line with a slope of $1/q_m$ and an intercept of $\frac{1}{q_m K_L}$ is determined. The Freundlich adsorption isotherm model is widely applied for non-ideal adsorption on heterogeneous surfaces and describes the multilayer adsorption due to solute-solute interaction in the system. Freundlich isotherm also assumes the enthalpy of adsorption is independent of the amount adsorbed (Benjelloun *et al.,* 2021). The Freundlich model is expressed by Equation 8.

$$q_e = K_f C_e^{1/n} \quad (8)$$

Where, q_e is the amount of adsorbate adsorbed, C_e is the concentration of the adsorbate at equilibrium, K_f is the intercept at zero equilibrium concentration, and n is adsorption intensity. The linearization form of Equation 8 is given as Equation 9.

$$\log q_e = \log K_f + \frac{1}{n} \log C_e \quad (9)$$

The slope 1/n is a measure of adsorption intensity or surface heterogeneity, becoming more heterogeneous as its value gets closer to zero. A steep slope that is value of 1/n close to 1 reflects high sorption capacity at high equilibrium concentration, which decreases rapidly at lower equilibrium concentration. Whereas a flat slope with 1/n << 1 represents that the sorption capacity is slightly reduced at lower equilibrium concentration.

RESULTS AND DISCUSSION

Particle Size Distribution Analysis

Soil particle size distribution is crucial for understanding its effects on soil texture coarsening, degradation of soil structure and properties, as well as the movement of water and migration of solutes within the soil (Hailemariam *et al*., 2023). It also significantly affects the soil's adsorption capacity, as variations in particle composition determine the soil's ability to retain and bind ions, molecules, and pollutants (Yu *et al*., 2023). In the rubber plantation, orchard, and foothill areas, sand is the predominant component, ranging from 51.70 ± 0.05% to 42.11 ± 0.03%, classifying these soils as clayey sand (Table 2). The overall texture defined by the proportions of sand, clay, and silt can be interpreted through the chemical composition presented in Table 1. In contrast, hilltop soil is characterized as clay loam, with the highest clay content (39.87 ± 0.46%), followed by sand (37.81 ± 0.30%) and silt (22.32 ± 0.22%). This soil tends to experience minimal erosion due to stable vegetation cover, which promotes the gradual accumulation of finer particles like clay and silt, leading to the formation of clay loam. As soil materials move downslope, heavier sand particles tend to settle at the foothill, while lighter clay particles are more likely to be carried further by water or wind. This process results in a coarser soil texture at the base of the hill, forming clayey sand. Additionally, the orchard and rubber plantation soils undergo minimal mechanical disturbance due to infrequent tilling, which helps preserve their structure and maintain a relatively stable composition over time.

Table 2. Particle size distribution of soil samples.

Soil Texture	Rubber Plantation	Orchard	Hilltop	Foothill
Sand (%)	51.70±0.05	46.56±0.05	37.81±0.30	42.11±0.03
Clay (%)	30.24±0.04	27.32±0.02	39.87±0.46	36.75±0.01
Silt (%)	17.40±0.04	25.37±0.04	22.32±0.22	21.14±0.37

Surface Area Analysis

Table 3 shows the obtained results of the BET surface area, pore volume, and pore size of the studied adsorbents. All soil samples predominantly contain mesopores, with average pore sizes ranging from 12.61 to 24.07 nm. Hilltop soil exhibited a greater BET surface area (8.0020 m^2/g) and total pore volume (0.03343 cm^3/g) than foothill soil (7.0127 m^2/g, 0.02749 cm^3/g). This difference is likely attributed to the higher organic matter content in hilltop soil (Table 1), which reflects greater structural heterogeneity and influences both the original soil structure and its physicochemical properties. Rubber plantation soil possesses the lowest pore volume of 0.00070 cm^3/g, which might be influenced by the presence of low organic matter content. In contrast, orchard soil, despite having the largest pore size, maintains a higher pore volume than rubber plantation soil, likely a result of its richer organic matter and clay content. Soil specific surface area is closely related to particle size distribution, as a decrease in particle size leads to an increase in surface area. Clay particles, being smaller than sand, offer a significantly higher specific surface area. This expanded surface area enhances the soil's adsorption capacity by providing more surface for interactions with metals and other contaminants. A larger specific surface area also facilitates greater interaction between soil particles and ions or water molecules (Sepaskhah *et al.*, 2010). Therefore, soil with high specific surface areas has high adsorption capacity.

Table 3. Pore volume distribution and surface area of soil samples.

Adsorbent	BET surface area (m^2/g)	Total pore volume (cm^3/g)	Pore size (nm)
Orchard	4.3006	0.01462	24.07
Rubber Plantation	3.3249	0.00070	18.78
Hilltop	8.0220	0.03343	14.23
Foothill	7.0127	0.02749	12.61

The nitrogen (N_2) adsorption and desorption isotherm curves along with pore size distribution data, were analyzed to compare the adsorption behavior across four soil types. As illustrated in Figure 1, the isotherms correspond to a typical Type II profile, indicative of unrestricted monolayer to multilayer adsorption. The adsorption/desorption isotherm curves exhibited a very low adsorption and desorption in low relative pressure region; and a steep monolayer adsorption are found above the partial pressure (P/P_0) around 0.5– 0.9 suggesting the presence of mesopores in the soil samples. The desorption isotherm curves for all soil samples exhibit the characteristic H3 hysteresis loop (capillary condensation occurs) given by non-rigid aggregates of plate-like particles which further indicate the existence of mesopores in the studied adsorbents.

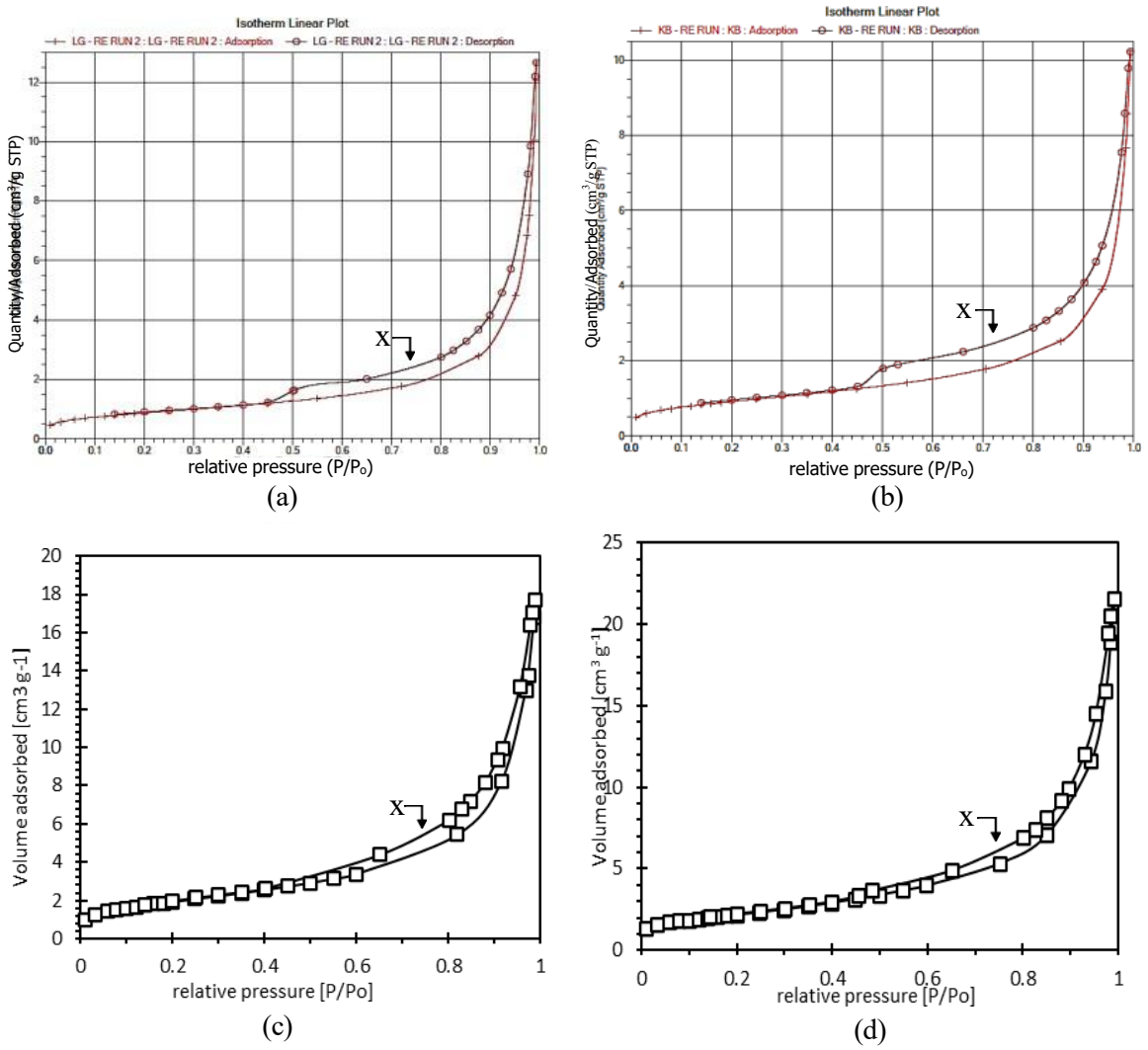

Note: x – desorption

Figure 1. N_2 adsorption/desorption isotherms of (a) orchard soil, (b) rubber plantation soil, (c) hilltop soil, and (d) foothill soil.

Cation Exchangeable Capacity (CEC) Analysis

It is found that the clay loam soil (hilltop) exhibited the highest CEC value of 35.060 ± 0.004 $cmol_c$ /kg compared to clayey sand soils (24.170 ± 0.002, 20.285 ± 0.001, and 12.371 ± 0.002 $cmol_c$/kg) from other sampling sites (Table 4). Clayey sand soils exhibit lower cation exchange capacity (CEC) due to their larger particle size (reflected in the higher sand content shown in Table 2) and reduced negative surface charge. This larger size produces a smaller surface-to-volume ratio, reducing the availability of negative sites to attract cations, including heavy metal ions in this context (Abegunde *et al.*, 2020). Theoretically, clayey sand soils exhibit lower adsorption capacity due to their coarse texture leads to larger pore spaces. As soil particle size increases, adsorption tends to decrease; conversely, finer particles exhibit greater adsorption capacity. Clay particles possess a high surface area and elevated CEC, enabling them to retain more positively charged ions such as nutrients and metals. Therefore, soils with higher clay content typically demonstrate enhanced adsorption capacity for these ions (Chen *et al*., 2023). The adsorption capacity of soil is expected to rise with increasing clay composition.

Table 4: CEC value of soil samples.

Soil Samples	CEC ($cmol_c$ /kg)
Orchard	20.285 ± 0.001
Rubber Plantation	12.371 ± 0.002
Hilltop	35.060 ± 0.004
Foothill	24.170 ± 0.002

Organic matter plays a crucial role in enhancing the soil's cation exchange capacity (CEC). It contains functional groups such as oxidized carboxylate and phenolate, which generate negative charges, particularly under higher pH conditions, making organic matter a significant contributor to CEC. Despite having similar chemical compositions and particle size distributions, orchard soil demonstrates a notably higher CEC value (20.285 ± 0.001 $cmol_c$/kg) than rubber estate soil, largely due to its substantially greater organic matter content (4.38 ± 0.03%) compared to that of rubber estate soil (1.99 ± 0.01%) (Table 1). In the case of hilltop versus foothill soils, elevation differences lead to distinct temperature regimes. Higher elevations experience cooler temperatures, which promotes the accumulation of organic matter in hilltop soils (Kumar *et al.,* 2019). These lower temperatures suppress microbial and enzymatic activity, thereby slowing the decomposition of organic material. Consequently, the reduced biological breakdown at high altitudes is a key factor driving the elevated organic matter content in hilltop soils.

Adsorption Isotherms

The amounts of adsorbed heavy metals, q_e, and the equilibrium concentrations, C_{eq} are plotted and shown in Figure 2. The amount of adsorption toward heavy metals increases with rising equilibrium concentrations. The adsorption isotherm curve clearly showed that the adsorption rate of Cu^{2+}, $Pb^{2+,}$ or Zn^{2+} in the soil sample was rapid at lower concentrations and gradually decreased to reach a maximum value. This behavior explains that in lower concentrations, heavy metal ions exhibit high mobility and therefore, enhance their interaction with soil samples (adsorbents). However, as the concentrations increase, the binding centers of the soil samples become saturated because the amount of heavy metal ions exceeds the number of available adsorption sites, preventing further adsorption (Sangiumsak & Punrattanasin, 2014). Besides, the increase in heavy metal ion concentration has affected the amount of heavy metal ions adsorbed due to the increased driving force of these ions towards the active sites of soil samples. Therefore, the adsorption rate is getting lower as the concentration of heavy metal ions increases.

The Langmuir and Freundlich isotherms were adopted to describe the adsorption isotherm. Table 5 shows the parameters of both Langmuir and Freundlich isotherms. Both adsorption isotherms exhibited R^2 values predominantly above 0.93, indicating that both models can accurately describe the isotherm behavior. Analysis revealed that the Freundlich isotherm performs equally well as the

Langmuir isotherm in modeling adsorption behavior. The consistency of the Langmuir isotherm implies that adsorption occurred in the form of a monolayer of metal particles on the soil surface.

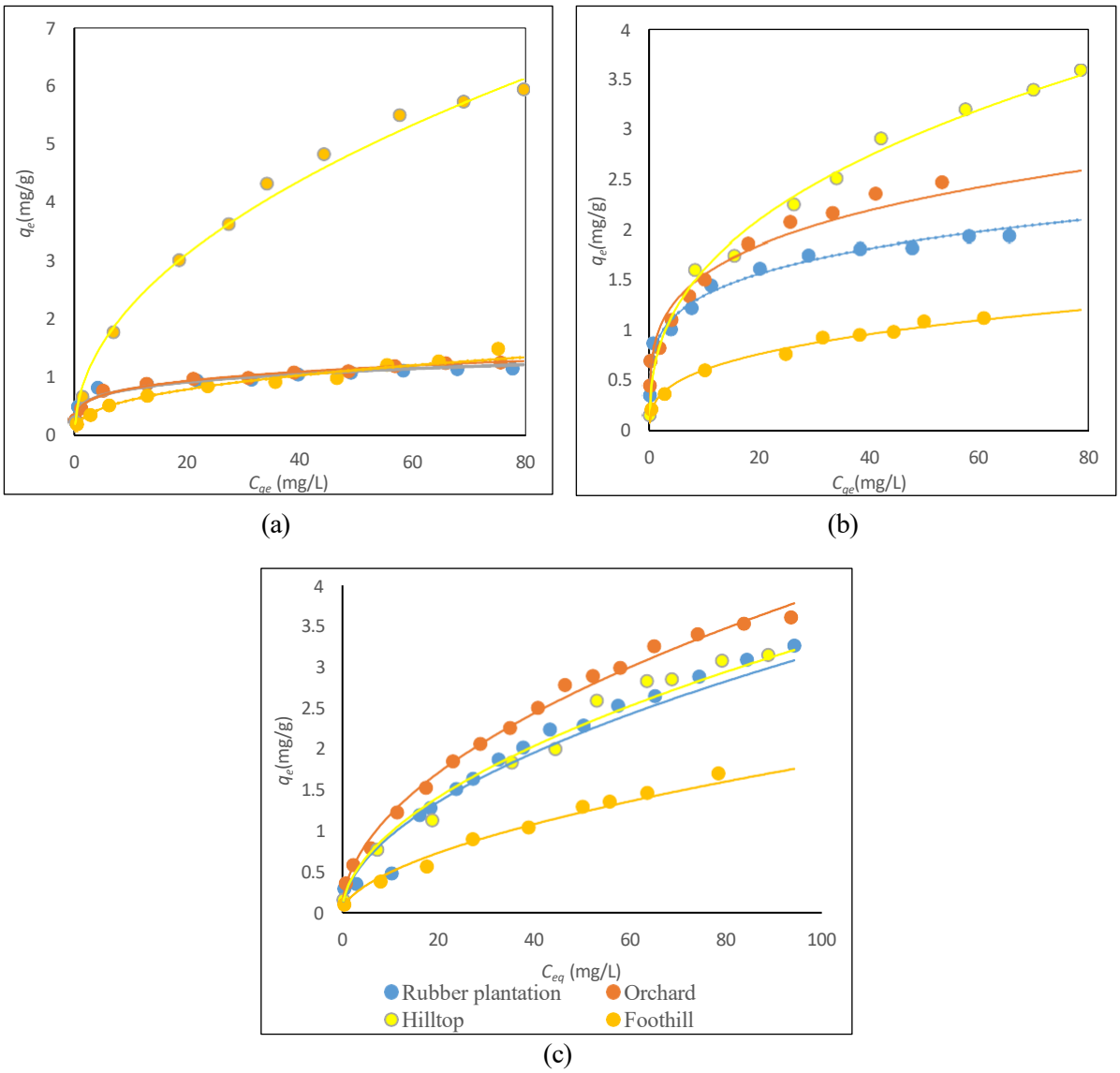

Figure 2. Adsorption isotherm of (a) Cu^{2+}, (b) $Pb^{2+,}$ and (c) Zn^{2+}.

The clay loam soil from the hilltop exhibited the highest adsorption capacity, with the metal ion affinity following the order of $Cu^{2+} > Pb^{2+} > Zn^{2+}$. In contrast, clayey sand soils from orchards, rubber plantations, and the foothill region exhibited a preference for Zn^{2+} over Pb^{2+} and Cu^{2+}, indicating a distinct adsorption pattern despite sharing a similar soil classification. This variation implies that metal adsorption behavior in clayey sand soils is influenced not only by soil type but also by other factors such as mineral composition, organic matter levels, and land management practices.

The hilltop soil, classified as clay loam and exhibiting a higher proportion of clay particles (Table 2), offers more binding sites for heavy metal ions, resulting in a greater overall adsorption capacity compared to clayey sand soil. The particle size of clay is smaller than sand particles and produces a greater specific surface area relative to their size (Table 3). High clay content also provides higher cation exchange capacity (CEC). Moreover, the presence of organic matter further supports adsorption by forming stable organo-metallic complexes. In contrast, clayey sand soils (orchard, rubber plantation, and foothill soils) display distinct mineralogical compositions, particularly in the types of clay minerals and iron/ aluminium oxides present (Table 1). Differences in land use and topography also

result in variations in soil organic matter content and pH, even within similar textural classes. These factors influence the availability of sites for adsorption and the sequence in which adsorption occurs, thereby affecting the adsorption capacity of the soil, which reflects its ability to retain and immobilize substances such as heavy metals.

Table 5: Parameters of Langmuir and Freundlich.

Soil	Metal	Langmuir				Freundlich		
		q_m	K_L	R_L	R^2	n	K_f	R^2
Orchard	Cu^{2+}	1.261	0.233	0.046	0.9881	4.422	0.720	0.9805
	Pb^{2+}	2.560	0.381	0.028	0.9959	2.978	0.891	0.9643
	Zn^{2+}	3.743	0.033	0.251	0.9379	1.751	0.535	0.9957
Rubber Plantation	Cu^{2+}	1.137	0.583	0.022	0.9907	6.230	0.782	0.9669
	Pb^{2+}	2.151	0.770	0.016	0.9989	3.481	0.908	0.9349
	Zn^{2+}	3.350	0.053	0.192	0.9455	1.991	0.608	0.9453
Hilltop	Cu^{2+}	6.139	0.003	0.666	0.9957	1.021	0.033	0.9813
	Pb^{2+}	3.792	0.035	0.159	0.9387	3.831	0.874	0.9361
	Zn^{2+}	3.451	0.014	0.328	0.9326	1.489	0.099	0.9303
Foothill	Cu^{2+}	1.403	0.469	0.030	0.9833	1.021	0.033	0.9413
	Pb^{2+}	1.134	0.160	0.082	0.9352	2.115	0.196	0.9336
	Zn^{2+}	1.859	0.006	0.824	0.9408	1.145	0.080	0.9409

CONCLUSION

The adsorption characteristics of the studied soils were effectively described by both Freundlich and Langmuir isotherm models. Clay loam soil (hilltop) exhibited higher adsorption capacity, whereas clayey sand soils (orchard, rubber plantation, and foothill) demonstrated the lowest. All soils showed measurable sorptive potential, with distinct metal ion affinities governed by their physicochemical properties. Adsorption capacity was primarily influenced by factors such as mineralogical composition, particle size distribution, organic matter content, cation exchange capacity, pH, and specific surface area. A comprehensive understanding of these soil attributes is essential for accurately predicting adsorption behavior and conducting site-specific evaluations of heavy metal retention potential.

ACKNOWLEDGEMENT

The authors gratefully acknowledge Universiti Malaysia Sabah (UMS) for the funding with grant number SBK0486-2021.

REFERENCES

Abegunde, S.M., Idowu, K.S., Adejuwon, O.M. & Tinuade, A., 2020. A review on the influence of chemical modification on the performance of adsorbents. *Resources, Environment and Sustainability,* 1:100001.

Ali, J.K., Ghaleb, H., Arangadi, A.F., Le, T.P.P., Moraetis, D., Pavlopoulos, K. & Alhseinat, E. 2023. Comprehensive assessment of the capacity of sand and sandstone from aquifer vadose zone for the removal of heavy metals and dissolved organics. *Environmental Technology & Innovation*, 29: 102993.

ASTM D7928-21E1: Standard Test Method for Particle-Size Distribution (Gradation) of Fine-Grained Soils Using the Sedimentation (Hydrometer) Analysis.

ASTM E1727-20: Standard Practice for Field Collection of Soil Samples for Subsequent Lead Determination

Ayangbenro, A.S. & Babalola, O.O., 2017. A new strategy for heavy metal polluted environments: a review of microbial biosorbents. *International Journal of Environmental Research and Public Health,* 14: 94; doi:10.3390/ijerph14010094.

Bai, B., Bai, F. & Hou, J. 2024. The migration process and temperature effect of aqueous solutions contaminated by heavy metal ions in unsaturated silty soils. *Heliyon*, 10(9): e30458.

Benjelloun, M., Miyah, Y., Evrendilek, G. A., Zerrouq, F. & Lairini, S. 2021. Recent advances in adsorption kinetic models: Their application to dye types. *Arabian Journal of Chemistry*, 14(4): 103031.

Chen, J., Yuan, J., Tong, H., Fang, Y. & Gu, R. 2023. Mechanism study on the soil mechanical behavior of the mixed soil based on energy multi-scale method. *Frontiers in Materials*, 10.

Chenu, C., Rumpel, C., Védère, C. & Barré, P. 2024. Methods for studying soil organic matter: nature, dynamics, spatial accessibility, and interactions with minerals. *In Elsevier eBooks* (pp. 369–406).

Hailemariam, M.B., Woldu, Z., Asfaw, Z. & Lulekal, E. 2023. Impact of elevation change on the physicochemical properties of forest soil in South Omo Zone, southern Ethiopia. *Applied and Environmental Soil Science*, 1–17.

ISO 9277:2010(E). Determination of the specific surface area of solids by gas adsorption - BET method.

Kumar, S., Suyal, D.C., Yadav, A., Shouche, Y. & Goel, R. 2019. Microbial diversity and soil physiochemical characteristics of higher altitude. *Plos One*, 14(3).

Musilova, J., Arvay, J., Vollmannova, A., Toth, T. & Tomas, J., 2016. Environmental contamination by heavy metals in region with previous mining activity. *Bulletin of Environmental Contamination and Toxicology*, 97: 569-575

Naveedullah, Hashmi, M.Z., Yu, C.N., Shen, H., Duan, D.C., Shen, C.F., Lou, L.P. & Chen, Y.X., 2013. Risk assessment of heavy metals pollution in agricultural soils of siling reservoir watershed in Zhejiang Province, China. Hindawi Publishing Corporation. *BioMed Research International,* Volume 2013, Article ID: 590306, 10 pages http://dx.doi.org/10.1155/2013/590306

Olaniran, A.O., Balgobind, A. & Pillay, B. 2013. Bioavailability of heavy metals in soil: impact on microbial biodegradation of organic compounds and possible improvement strategies. *International Journal of Molecular Sciences*, 14: 10197-10228

Sangiumsak, N. & Punrattanasin, P. 2014. Adsorption behavior of heavy metals on various soils. *Polish Journal of Environmental Studies.,* 23(3): 853-865

Sepaskhah, A.R., Tabarzad, A. & Fooladman, H.R., 2010. Physical and empirical models for estimation of specific surface area of soils. *Archives of Agronomy and Soil Science*, 56: 325–335.

SW-846 Method 9080: 1986. Cation-Exchange Capacity of Soils (Ammonium Acetate), Part of Test Methods for Evaluating Solid Waste, Physical/Chemical Methods.

Tan, W.H., Surugau, N., Bahrun, M.H.V. & Bono, A. 2021. Heavy metal Cu(II) and Pb(II) retention on clay soil. In *Proceedings of the Seminar on Science and and Technology 2021*, pp. 42-44, Sabah, Malaysia.

Tan, W.H., Surugau, N., Bono, A., Bahrun, M.H.V., Idris, R., Ali, S.A.M., Tair, R. & Rahim, S.A. 2023. Effect of soil composition in copper (II), lead (II), and zinc (II) ion adsorption capacity. *Science, Engineering and Health Studies*, 17: 23020001.

Yu, H., Li, C., Yan, J., Ma, Y., Zhou, X., Yu, W., Kan, H., Meng, Q., Xie, R. & Dong, P. 2023. A review on adsorption characteristics and influencing mechanism of heavy metals in farmland soil. RSC Advances, 13(6): 3505 – 3519.

RESEARCH ARTICLE

BORNEO SCIENCE
THE JOURNAL OF SCIENCE & TECHNOLOGY

Journal homepage: https://jurcon.ums.edu.my/ojums/index.php/borneo-science

BIOGAS RECOVERY AND WASTE REDUCTION FROM SELECTED KITCHEN FOOD WASTE (SHALLOTS AND CABBAGE) BY USING ANAEROBIC DIGESTION

Newati Wid*[1,2], Rey Tiburtius[2] and Razak Mohd Ali Lee[3]

*[1]Preparatory Centre for Science and Technology, Universiti Malaysia Sabah, Jalan UMS, 88400, Kota Kinabalu, Sabah, Malaysia.
[2]Faculty of Science and Technology, Universiti Malaysia Sabah, Jalan UMS, 88400, Kota Kinabalu, Sabah, Malaysia.
[3]Faculty of Engineering, Universiti Malaysia Sabah, Jalan UMS, 88400, Kota Kinabalu, Sabah, Malaysia.

Correspondence:
newati@ums.edu.my

Received: 23 April 2025
Revised: 28 October 2025
Accepted: 31 October 2025
Published online: 3 November 2025

Doi:
10.51200/bsj.v46i2.6358

Keywords:
Anaerobic Digestion; Biogas Recovery; Kitchen Food Waste; Waste Reduction.

ABSTRACT. *Kitchen food waste is defined as food that is left over or wasted during the production, processing, distribution, procurement, preparation, and consumption processes. About 50% of all food waste is reportedly to originate from kitchens and since it can decompose, food waste is regarded as degradable kitchen waste. It is reported about 15,000 tonnes per day kitchen food waste generated in Malaysia and has the potential to produce hazardous gases, leachate, air pollution from food decay and quickly expanding landfills. In this study, kitchen food waste was used to recover biogas using anaerobic digestion. Additionally, the volume of waste reduced was also investigated to prove that anaerobic digestion is not only to recover resources, but also to reduce waste generation. The anaerobic digestion was performed at pH value of 6.8-7.2 and temperature 37°C for 15 days. Two (2) different samples of kitchen waste were used namely, shallots and cabbage. The biogas recovery was determined using water displacement technique. Kitchen food waste was also characterised before and after anaerobic digestion in terms of total solids, volatile solids and pH value. It is found that the percentage of total solids for shallots and cabbage before anaerobic digestion were 19.9% and 16.8%, respectively, and the percentage of volatile solids before anaerobic digestion were 88.1% and 95.6%, respectively. After anaerobic digestion, the percentage of total solids for shallots and cabbage were 15.5% and 13.6%, respectively, and the percentage of volatile solids were 21.0% and 15.2%, respectively. This suggests that the total and volatile solids of shallots and cabbage were reduced with 22.11% and 19.5%, and 76.14% and 84.14%, respectively, after performing anaerobic digestion. While, 168mL and 52mL of biogas can be recovered from shallots and cabbage, respectively, throughout 15 days anaerobic digestion. This shows that anaerobic digestion is not only to recover biogas but also to reduce waste.*

INTRODUCTION

Biogas, produced through anaerobic digestion, has gained attention as a promising method for converting organic waste into energy. Biogas is a mixture of mostly methane, CH_4 (50%-70%) and carbon dioxide, CO_2 (30%-50%) with some trace gases (1%-5%) (Ramaraj & Dussadee, 2015). The

methane in biogas can be used to produce renewable heat, electricity or cooling (Sibilo *et al*., 2017), thereby reducing dependence on fossil fuel energy.

Among the many sources of biogas, food waste stands out as a significant contributor to municipal solid waste, especially in urban households. According to the Food and Agriculture Organization (FAO), more than 30% of the food produced globally is wasted, contributing significantly to environmental issues (Safdie, 2023). In Malaysia, it is estimated 15,000 tonnes of food waste generated daily which mostly originating from households, including kitchen food waste (KFW) (Shukla *et al*., 2024; Abd Ghafar, 2017). KFW, a significant fraction of municipal solid waste, is primarily biodegradable. Improper disposal of KFW poses environmental risks, including the generation of methane and other harmful greenhouse gases, as well as soil contamination from leachate. Converting KFW into biogas offers a promising solution to these issues. KFW can be converted into biogas because it is rich in organic, biodegradable matter with high moisture content, making it ideal for anaerobic digestion by microbes.

Previous research highlights the potential of anaerobic digestion to reduce the environmental impact of food waste while simultaneously producing renewable energy (Xu *et al*., 2024). One of the widely studied method in converting waste into biogas is anaerobic digestion (AD) which includes four (4) prominent steps, namely, hydrolysis, acidogenesis, acetogenesis and methanogenesis. AD is a biological process that breaks down organic material in the absence of oxygen, transforms organic waste into biogas, composed mainly of methane (CH_4) and carbon dioxide (CO_2), and a nutrient-rich digestate. This process reduces the volume of waste sent to landfills and mitigates methane emissions, making it an environmentally friendly solution. The efficiency of AD depends on several factors, including the composition of the waste, temperature, pH, and moisture content. The AD process is increasingly being used worldwide to convert organic waste into biogas, which can be used as a source of energy for heating, electricity, or as vehicle fuel (Shukla *et al*., 2024). In addition, AD reduces greenhouse gas emissions by preventing the release of methane from landfills.

Therefore, this research aims to explore the potential of KFW for biogas recovery, focusing on shallots and cabbage, the commonly consumed food items at the café of Faculty of Science and Technology, Universiti Malaysia Sabah, where the samples were collected. This study assessed the production of biogas using anaerobic digestion over a 15-day period as well as the amount of waste reduced after performing anaerobic digestion. This research not only contributes to the growing knowledge on waste-to-energy solutions but also promotes the use of sustainable waste management practices.

MATERIALS AND METHODS

Sample Collection and Preparation

The kitchen food waste (KFW) samples, namely, shallots and cabbage were collected after lunch hour from the student's café of Faculty of Science and Technology, Universiti Malaysia Sabah, when needed. The samples were cleaned using tap water and ground using a mortar to make it ready for anaerobic digestion and were stored at 4°C prior to use (APHA, 2005). The sediment sludge was collected from a lake at Universiti Malaysia Sabah and used as inoculum for AD process. The sludge was stored in a Schott Duran glass bottles and allowed to degasify in a water bath at 37°C for seven (7) days. The level of the water bath was raised slightly above the level of sludge in the Duran bottle. The bottle top was opened at least once a day to allow any gas that might escape from the sludge. After the degasification process was completed, the sludge was kept in a water bath at 37°C until it was needed for the AD treatment (Wid *et al*., 2017).

Determination of Physical Properties of Kitchen Food Waste

The physical properties that were determined including total solids (TS), volatile solids (VS) and pH value. The total solids (TS) and volatile solids (VS) of the samples were determined using standard

procedures outlined by APHA (2005). TS was determined by drying the samples at 105°C for 24 hours, followed by VS analysis by igniting the dried samples at 550°C for four (4) hours in a furnace. The determination of TS and VS were carried out before and after anaerobic digestion. While the pH of the samples was also determined according to the standard method of APHA (2005). The raw samples of KFW were placed in a 250mL of Duran and distilled water was added to the bottle in a ratio of 1:10. The Duran bottle was then shaken in an orbital shaker at 100rpm for 24h in room temperature. The pH of the solution was then measured.

Anaerobic Digestion Setup

The AD process was conducted using biomethane potential (BMP) method according to the procedures outlined by Owen *et al*., (1979) and Wid & Sualin (2018) with slight modification. 250 mL Schott Duran reactors were used, sealed with rubber stoppers to maintain anaerobic conditions. In total there were three sample bottles including shallots, cabbage and a control sample that contained only inoculum to create the resulting biogas formation that would be subtracted from the biogas production from the studied sample bottles (Figure 1).

Figure 1. The anaerobic reactors of shallots, cabbage and control samples used in this study

This study used the effective volume of 200 mL and ratio of 1.5:1 food waste to inoculum to increase the kinetic effect of biogas production (Selaman & Wid, 2019). The inoculum was used to maximise sample conversion into final products as it contains high number of microorganisms and bacteria present in the sludge. The reactors were placed in a water bath maintained at 37°C because it is a mesophilic temperature in the anaerobic digestion process and bacteria are very active at this temperature. The reactor was shaken daily to ensure an even temperature inside the reactor. The pH was controlled between 6.8 – 7.2 using sodium hydroxide (NaOH) and hydrochloric acid (HCl) (Li *et al*., 2024; Jiraprasertwong *et al*., 2019; Owen *et al*., 1979). Biogas production was monitored daily using water displacement method for 15 days (Wid *et al*., 2017).

RESULTS AND DISCUSSION

The determination of the physical properties is crucial in order to understand the organic and inorganic content of the sample to maximise the utilization of the sample during anaerobic digestion. This is also important to study waste reduction analysis after performing anaerobic digestion. While for pH, it is important to determine the value to make sure the anaerobic digestion process is carried out within the optimum conditions for anaerobic bacteria.

Total Solids, Volatile Solids and Waste Reduction

From this study, it was found that the initial total solids (TS) for shallots (before AD) was 19.9%, while cabbage had an initial TS value of 16.8%. After AD, these values reduced to 15.5% and 13.6%, respectively, indicating substantial degradation of the organic matter. Similarly, the volatile solids (VS) for shallots decreased from 88.1% to 21.0%, and for cabbage from 95.6% to 15.2%.

The initial TS values before AD indicate that KFW of shallots and cabbage were suitable to be used in AD. Recent studies have reported that TS contents between 15% and 25% support favorable microbial activity and biogas production, provided that VS content is sufficiently high (Akter *et al*., 2021). However, some anaerobic digesters can handle total solids concentrations as high as 20% to 30% or more, depending on the type of digester and the specific substrate being used. According to Li *et al*., (2024) TS content more than 8% is not only hindering dissolution but also leading to generation of antimicrobial by-products that significantly affect methane production. In addition, the increase in molecular weight of organic matter is an important reason for prolonging the start-up time of anaerobic digestion. While the high initial VS values indicate high organic content in the KFW samples. The reduction in TS and VS suggests the effectiveness of AD in breaking down organic materials. The higher initial VS in cabbage beans compared to shallots suggests that cabbage contained more organic material available for decomposition.

In terms of waste reduction, the TS values for shallots and cabbage were reduced to 15.5% and 13.6%, suggesting that 22.11% and 19.05% of waste reduction, respectively. While for VS, the organic content of shallots and cabbage reduced significantly with 76.14% and 84.14% reduction, respectively, after anaerobic digestion. This indicated that AD is able to reduce the amount of waste as well as stabilise organic wastes by degrading organic matter. This may divert waste from landfill, the most common disposal technique in Malaysia, by reducing the amount of waste sent to landfill. Consequently, preventing the release of greenhouse gases into the atmosphere. Similar VS reduction rates have been observed in recent studies on vegetable and kitchen waste digestion, where reductions above 80% are associated with high substrate biodegradability (Mehmood *et al*., 2023; Mollah *et al*., 2023). Additionally, the nutrient-rich digestate produced during AD can be used as fertiliser, further promoting sustainability by recycling nutrients back into the ecosystem.

Biogas Recovery from Kitchen Food Waste

The biogas recovery from kitchen food waste was measured over the 15 days of anaerobic digestion. Figure 2 illustrates the daily production of biogas from shallots and cabbage where biogas production from control was subtracted from both samples. Generally, there was a daily increase of biogas production from shallots and cabbage, with the highest production was 20mL and 7mL, at day 3 and 10, respectively. A high production at the early stage of AD for shallots primarily because of the rapid hydrolysis, acidogenesis, and methanogenesis of easily biodegradable carbohydrates in the food waste samples. Figure 2 also shows fluctuation in both samples which may tributed to the large fluctuation in the levels of methanogenic population bacteria, as volatile fatty acids were accumulated and then subsequently consumed. This may be due to the inconsistency of food waste composition or any sudden changes in pH values or carbon to nitrogen ratio during AD. Similar trends were reported by previous studies (Al-Wahaibi *et al*., 2020; Griffin *et al*., 1998).

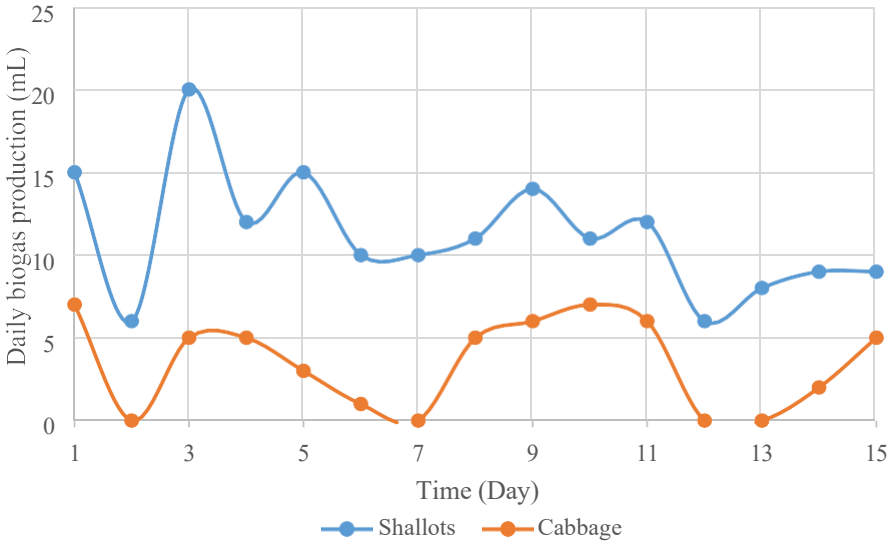

Figure 2. Daily biogas production of biogas throughout 15 days anaerobic digestion of shallots and cabbage

The cumulative biogas production is shown in Figure 3. The cumulative biogas production from shallots and cabbage were 168mL and 52mL, respectively. The cumulative production from shallots was higher than cabbage, and steadily increased until day 15, indicating that anaerobic digestion was not complete and still producing biogas. Therefore, it can be suggested that anaerobic digestion can be prolonged to allow more biogas production. The cumulative production from cabbage was lower, maybe due to suppression factors such as high fixed solid concentration and difficulty in digesting the composition present in the sample. This may also be attributed to the lower total solids content in cabbage, which may affect microbial activity and substrate instruction due to high moisture content. Shallots produced significantly more biogas (168 m L) than cabbage (52 mL), which is consistent with findings by Gulhane *et al*., (2024), who noted that vegetables with higher carbohydrate content and lower acidity tend to produce higher methane yields. Overall, this finding shows both KFW samples were suitable to be used as a source for biogas recovery, though, the results were highly depending on the physical and chemical properties of the food waste substrates.

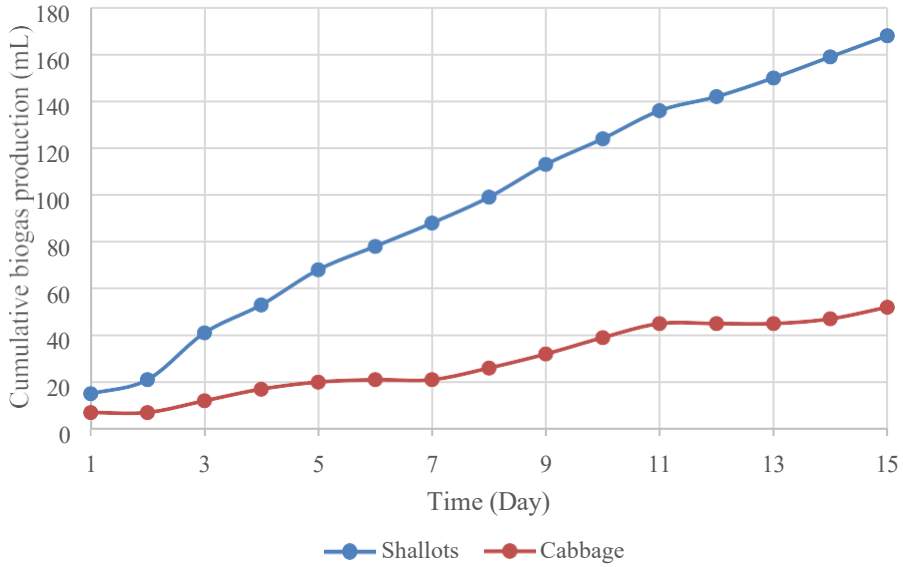

Figure 3. Cumulative production of biogas throughout 15 days anaerobic digestion of shallots and cabbage

CONCLUSION

Anaerobic digestion has drawn considerable attention due to its ability to convert waste into products. This study demonstrates the feasibility of biogas recovery from kitchen food waste over a 15-day anaerobic digestion (AD) period. The physical characterisation showed total solids (TS) and volatile solids (VS) contents of 19.9% and 16.8%, for shallots and cabbage, respectively, were within the optimal range for efficient anaerobic digestion, which supported by recent studies that this range is favorable for microbial activity and biogas production. Shallots produced significantly more biogas (168 mL) than cabbage (52 mL), which is consistent with previous findings, particularly for kitchen food waste with higher carbohydrate content. The reduction in total solids and volatile solids with 22.11% and 19.5%, as well as 76.14% and 84.14%, for shallots and cabbage, respectively, further supports the effectiveness of anaerobic digestion in breaking down and stabilising organic material. Overall, the results of this study underscore the potential of kitchen food waste as a renewable energy source. By adopting anaerobic digestion as a waste management strategy, this can reduce landfill waste, lower greenhouse gas emissions and promote sustainable environment. Future research should focus on optimising anaerobic digestion conditions, such as pre-treatment methods and co-digestion with other waste streams, to enhance biogas yields.

ACKNOWLEDGEMENT

The authors would like to acknowledge Universiti Malaysia Sabah for the financial support (GUG0119-1/2017) and the Faculty of Science and Technology, Universiti Malaysia Sabah for the technical assistance.

REFERENCES

Abd Ghafar, S.W. 2017. Food waste in Malaysia: trends, current practices and key challenges. Centre of Promotion Technology, MARDI, Persiaran MARDI-UPM.

Akter, N., Akter, T. & Nizamuddin, M. 2021. Kinetic study and optimization of total solids for anaerobic digestion of kitchen waste in Bangladesh. *Water Science and Technology*, 84(5): 1136–1147.

Al-Wahaibi, A., Osman, A.I., Al-Muhtaseb, A.H., Alqaisi, O., Baawain, M., Fawzy, S. & Rooney, D.W. 2020. Techno-economic evaluation of biogas production from food waste via anaerobic digestion. *Nature Research, Scientific Reports*, 10.1038/s41598-020-72897-5.

American Public Health Association, APHA. 2005. Standard methods for the examination of water and wastewater. *American Public Health Association* (APHA): 21st ed, Washington, DC, USA.

Griffin, M.E., McMahon, K.D., Mackie, R.I. & Raskin, L. 1998. Methanogenic population dynamics during start-up of anaerobic digesters treating municipal solid waste and biosolids. *Biotechnology, Bioengineering*, 57: 342–355.

Gulhane, M., Poddar, B.J. & Chelani, A. 2024. Assessment of biomethanation potential and batch kinetics of the anaerobic digestion of vegetable market waste in serum bottles. *Biomass Conversion and Biorefinery*, 14: 9805–9820.

Jiraprasertwong, A., Maitriwong, K. & Chavadej, S. 2019. Production of biogas from cassava wastewater using a three-stage upflow anaerobic sludge blanket (UASB) reactor. *Renewable Energy*, 130: 191-205.

Li, Z., You, Z., Zhang, L. & Chen, H. 2024. Effect of total solids content on anaerobic digestion of waste activated sludge enhanced by high-temperature thermal hydrolysis. *Journal of Environmental Management*, 359: 120980.

Mehmood, M. A., Ahmed, A., Qyyum, M. A. & Raja, M. A. 2023. Anaerobic co-digestion of food waste: Optimization, energy yield, and kinetic modeling. *Bioengineering*, 10(8): 437.

Mollah, M. Y. A., Hasan, M. R., Roy, P. K. & Rana, M. S. 2023. Evaluation of anaerobic digestion performance of organic kitchen waste and sewage sludge using lab-scale digester. *Environmental Health Insights*, 17: 11786302231191743.

Owen, W. F., Stuckey, D.C., Healy Jr, J.B., Young, L.Y. & Mccarty, P.L. 1979. Bioassay for monitoring biochemical methane potential and anaerobic toxicity. *Water Research*, 13(6): 485-492.

Ramaraj, R. & Dussadee, N. 2015. Biological Purification Processes for Biogas Using Algae Cultures: A Review. *International Journal of Precision Engineering and ManufacturingGreen Technology*, 4(1-1): 20-32.

Safdie, B. 2023. Global Food Waste in 2024. Greenly. https://greenly.earth/en-us/blog/ecologynews/global-food-waste-in-2022.

Selaman, R. & Wid, N. 2019. Effects of substrate to inoculum ratio on Phosphorus Recovery from Different Composition of Food Waste using Anaerobic Batch Digestion. *Journal of Physics: Conference Series*, 1358 012030.

Shukla, K., Abu Sofian, ADA., Singh, A., Chen, W.H., Show, P.L. & Chan, Y.J. 2024. Food waste management and sustainable waste to energy: Current efforts, anaerobic digestion, incinerator and hydrothermal carbonization with a focus in Malaysia. *Journal of Cleaner Production*, 448: 141457.

Sibilo, S., Rosato, A., Ciampi, G., Scorpio, M. & Akisawa, A. 2017. Building-integrated trigeneration system: Energy, environmental and economic dynamic performance assessment for Italian residential applications. *Renewable and Sustainable Energy Reviews*, 68 (2): 920933.

Wid, N., Selaman, S. & Jopony, M. 2017. Enhancing Phosphorus Recovery from Different Wastes by Using Anaerobic Digestion Technique. *Advanced Science Letters*, 23(2): 14371439.

Wid, N. & Sualin, F. 2018. Volatile Fatty Acids Production from Different Composition of Food Waste and Its Effect on Phosphorus Recovery. *ASM Science Journal*, 11, Special Issue 2, 2018 for SANREM: 272-277.

Xu, S., Bi, G., Zou, J., Li, H., Chen, M., Tang, Z., Yu, Q., Xie, J. & Chen, Y. 2024. Effect of hydrochar from biogas slurry co-hydrothermal carbonization with biomass on anaerobic digestion performance of food waste. *Industrial Crops and Products*, 221: 119361.

RESEARCH ARTICLE

BORNEO SCIENCE
THE JOURNAL OF SCIENCE & TECHNOLOGY

Journal homepage: https://jurcon.ums.edu.my/ojums/index.php/borneo-science

HEALTH RISK ASSESSMENT OF HEAVY METAL IN FISH TO THE POPULATION IN PETAGAS RIVER, SABAH

Muhammad Nur Rashidi Rosli[*1], Madihah Jaafar Sidik[2], Syerrien Shennen Jamiol[2], Mohd Razali Shamsuddin[1], and Nurashikin Abd Azis[3]

[1] Preparatory Center for Science and Technology, Universiti Malaysia Sabah, 88400 Kota Kinabalu, Sabah, Malaysia.
[2] Borneo Marine Research Institute, Universiti Malaysia Sabah, 88400 Kota Kinabalu, Sabah, Malaysia.
[*3] Faculty of Security and Governance, North Borneo University College, Wisma Angkatan Hebat, 1 Borneo, Jalan Sulaman, 88400 Kota Kinabalu, Sabah.

***Correspondence:**
mnrashidirosli@ums.edu.my

Received: 26 April 2025
Revised: 28 November 2025
Accepted: 18 December 2025
Published online: 31 December 2025

Doi:
10.51200/bsj.v46i2.6356

Keywords:
Bioaccumulation; Heavy metals; Inductive Coupled Plasma-Mass Spectrometry (ICP-MS); Recommended Dietary Allowance (RDA).

ABSTRACT. *The levels of heavy metals in marine environments and fish are crucial for assessing heavy metal contamination, which poses deleterious effects on communities, especially those in Petagas River. Four randomly caught fish species—Sagor Catfish, Indo-Pacific Tarpon, Spotted Catfish, and Nile Tilapia—from the river were dissected to obtain the fish flesh and prepared following the APHA (American Public Health Association) standard method (2017). The water and fish flesh samples were analyzed using Inductively Coupled Plasma Mass Spectrometry (ICP-MS) to determine the concentrations of potassium (K), arsenic (As), and lead (Pb). The highest average heavy metal concentration in the water sample was potassium (K) 10.04 µg/L, followed by arsenic (As) 0.46 µg/L and lead (Pb) 0.63 µg/L. For the fish samples, the highest average concentration was potassium (K) 14.28 µg/g, followed by arsenic (As) 1.33 µg/g and lead (Pb) 1.14 µg/g. The results were compared with the permissible limits set by the Malaysian Food Act and Regulation (MFAR 1983 & 1985), Malaysian Water Quality Standard (MWQS 2008), and FAO/WHO (1984, 2017). The study revealed that As and Pb concentrations in water exceeded the permissible limits of MWQS (2008) and FAO/WHO (2017), while K concentrations were within the acceptable range. In fish samples, As exceeded the permissible limits of MFAR (1983 & 1985) and FAO/WHO (1984), while Pb exceeded the FAO/WHO (1984) limit but not MFAR. These findings highlight potential health risks to consumers and underscore the need for continuous monitoring of aquatic ecosystems in Petagas River.*

INTRODUCTION

The contamination of fresh and marine waters with wide range of pollutants has become a major concern (Vutukuru, 2005). Rivers, including Petagas River in Sabah, are susceptible to contamination by heavy metals, primarily originating from industrial and agricultural activities, leading to detrimental effects on water, soil, and air quality. Due to their high toxicity and accumulative nature, pollutants released into the environment have a significant impact on the ecological balance of the environment, causing significant harm to aquatic organisms' lives and even mass extinction (Yasir *et al.,* 2008; Rosli *et al.,* 2018; Yamada & Inaba, 2021). According to Yunus *et al.* (2020), the concentrations of these metals in

seawater are naturally low, but when organisms accumulate more than they can excrete, there is a high risk of contamination in living tissue.

Additionally, it is often necessary to examine chemical contaminants in food from aquatic sources to understand their level of hazard. The release of pollutants, especially heavy metals, into the aquatic environment is known to have detrimental effects on such an environment and on living organisms, including humans when those pollutants are allowed to enter the food chain. One of the obvious issues is regarding fish accumulate high concentrations of heavy metals beyond the standard limit or permissible level and affect humans via ingestion. Therefore, establishing a dependable database of contaminant levels in readily accessible commercial fish is essential for evaluating the current extent of heavy metal contamination.

Presently, despite the government of Sabah expressing a desire to promote river tourism development, the river remains untapped as a tourism resource. Its advantageous location near Kota Kinabalu city allows for easy market access. There are various opportunities for tourism development, including cultural tourism centred around the Bajau sea gypsy traditions of the local communities, ecotourism highlighting the region's wildlife and scenic waterfront, and adventure tourism focused on river recreation such as canoeing (Younis *et al.,* 2021). Unfortunately, rivers are also occasionally used as a convenient location for the disposal of industrial and human waste, which seriously reduces a river's usefulness for tourism.

In this study, the fish species consumed by the locals are randomly selected by fishing or using gill net and water samples also will be collected at the Petagas River, Penampang, Sabah. There were four fish samples and three water samples that were analysed using the inductively coupled-plasma mass spectrometry (ICP-MS) to identify the heavy metal concentration that affecting the level of metal contaminants. As a result, this study is used to evaluate the selected heavy metal concentrations in fish flesh and spatial variation Arsenic (As), Lead (Pb) and Potassium (K) in relation to the maximum residual limit for human consumption.

MATERIALS AND METHODS

Sample Collection

The sampling site located at Petagas River (5°54'45"N 116°3'42"E) and it takes 8.8 km to the state capital of Kota Kinabalu as shown in Figure 1. It is one among several rivers in Sabah that holds potential for ecotourism. The fish samples collected from the Petagas River encompass a selection of species, including *Arius maculatus* (Spotted Catfish), popularly referred to as "Ikan Duri Tompok," *Hexanematichthys sagor* (Sagor Catfish), also known as "Ikan Belukang," *Mugil cephalus* (River Mullet), commonly recognized as "Ikan Belanak," *Megalops cyprinoides* (Indo – Pacific Tarpon), widely known as "Ikan Bulan," *Cyclichthys spilostylus* (Puffer Fish), known as "Ikan Buntal," and *Oreochromis niloticus* (Nile Tilapia), which bears the common name "Ikan Tilapia." All these fish species are abundantly found in the Petagas River. The fish samples will be catch, packed, labelled and then taken to the BMRI laboratory for cleaning and isolation of the fish flesh.

This study was conducted from March 2023 until February 2024, where the collection of fish samples and water samples was conducted in three sampling stations (Station 1: Downstream, Station 2: Midstream, Station 3: Upstream) at Petagas River. This sampling was a one-time visit to achieve the study's objectives of assessing the heavy metal concentration in the Petagas River. To prioritize safety and sample integrity, sample collection was carefully planned out and executed in favorable weather conditions and tide status. Thus, the sampling took place in August during low tides when the weather was suitable to allow easy access for the boat to the designated three sampling stations in the Petagas River.

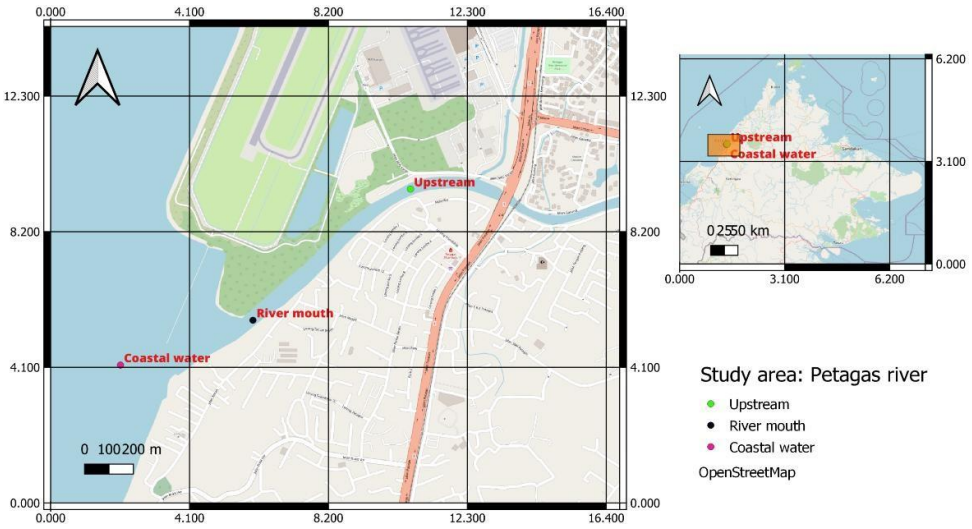

Figure 1. The map of Petagas River using QGIS 3.28.

Sample Treatment

The fish specimens were subjected to a thorough washing process using distilled water to eliminate any residual water. Subsequently, the head, viscera, gills, and flesh of the fish were separated. The fish flesh was dried in an oven at 105 °C for 24 hours or until the weight is constant. This method involving drying of fish flesh using oven also ensured all the water content was completely removed and to avoid residual unreacted fats, before proceeding with wet digestion. After that, the fish samples were milled with mortar and pestle to obtain fine grains of each sample of about size around 500 µm. A total of 0.1 g was mixed with 4.0 mL nitric acid, HNO_3 (65% analytical grade) and 6.0 mL hydrochloric acid, HCl. The mixed samples underwent the ICP-MS digestion method using microwave oven for 55 minutes until the solution was clear. Subsequently, the resulting solutions were filtered, and distilled water was added to bring the sample solution volumes to 100 mL, following the methodology outlined by Yasir *et al.* (2008).

Samples Analysis

The prepared samples, in the form of solutions, were subjected to analysis using Inductive Coupled Plasma-Mass Spectrometry (ICP-MS). The sample prepared following the APHA standard method (American Public Health Association, 2017). Accuracy and precision were validated using Standard Reference Material (SRM MA-A-2 Fish Flesh Homogenate) with recoveries between 93–106%. (Yasir *et al.,* 2008; Rosli *et al.,* 2018). To ensure accurate measurements and eliminate variations arising from differences in moisture content within organisms, the heavy metal concentrations in the tissues were calculated based on their dry weights. Additionally, control measures were implemented, including the use of blanks and replicates, to monitor and validate the precision and accuracy of the analytical procedure.

RESULTS AND DISCUSSION

Heavy Metal Content of Arsenic (As), Lead (Pb), Potassium (K) in the Fish Sample

Table 1 presents the metal contents in fish flesh from various species, including Sagor Catfish (downstream), Indo-Pacific Tarpon and Spotted Catfish (midstream), and Nile Tilapia (upstream). However, many factors, including gender, age, size, reproductive cycle, swimming pattern, feeding behaviour, and geographical location, can influence metal uptake and accumulation (Abdel-Baki *et al.,* 2011). Furthermore, different metal affinities to fish tissues, as well as different uptake, deposition, and excretion rates, result in varying levels of bioaccumulation in the fish body. Food consumption is the

most likely primary route of exposure to trace elements among the various modes of metal accumulation (ingestion, inhalation, and skin contact) for the great majority of people (Ahmed *et al.,* 2019). Fish are advantageous as bioindicators because they are long-lived and incorporate fluctuations in pollutants over time, allowing for continuous monitoring of the presence of pollutants while also allowing for spatial integration of pollutant data, and they are easily sampled (Ayodele *et al.,* 2020). The metal content of fish flesh was measured due to its importance in human consumption (Taweel *et al.,* 2013). The average metal concentration in fish flesh was K (14.28 µg/g), followed by As (1.33 µg/g) and Pb (1.14 µg/g).

Table 1. Heavy metal concentration in samples.

Station	Species	Heavy metal concentration in samples (µg/g)		
		As	Pb	K
Downstream	Sagor Catfish	1.38 ± 0.12	1.71± 0.49	14.68± 0.76
Midstream	Indo-Pacific Tarpon	1.25 ± 0.11	0.66± 0.33	13.45± 0.71
	Spotted Catfish	1.20 ± 0.11	0.91± 0.48	13.87± 0.71
Upstream	Nile Talapia	1.47 ± 0.13	1.29± 0.46	15.11± 0.78
Mean heavy metal concentrations by fish species ± SD		1.33 ± 0.12	1.14 ± 0.46	14.28 ± 0.76
Permissible limit MFAR (1983 & 1985)		1.0	2.0	nd

In this study, the Sagor Catfish accumulated the highest Pb concentration (1.71 µg/g) and was also high in K (14.68 µg/g). The Indo-Pacific Tarpon was found to have high concentrations of As (1.25 µg/g) and K (13.45 µg/g). The Spotted Catfish contained high concentrations of K (13.87 µg/g) and As (1.20 µg/g). The Nile Tilapia had the highest concentration of K (15.11 µg/g) and As (1.47 µg/g) compared to other fish species. According to the permissible limit established by FAO/WHO (1984), the K concentration exceeded the standard limit (1.6 - 2.0 µg/g), however Malaysia's national guidelines did not publish data on the limit for K concentration. All fish species contain high concentrations of K because it is necessary for sustaining normal body growth, enhancing fish protein, building muscle, regulating electrical conductivity, and preserving the acid-base balance (Ayodele *et al.,* 2020). On the other hand, even at relatively low concentrations, ingesting certain others, like Pb and As, can be extremely harmful to humans. Table 1 shows that Nile Tilapia had the highest As concentration (1.47 µg/g), followed by Sagor Catfish (1.38 µg/g), Indo-Pacific Tarpon (1.25 µg/g), and Spotted Catfish (1.21 µg/g), all exceeding the permissible limit set by MFAR (1983 & 1985) and FAO/WHO (1984). Inorganic arsenic is more lethal than organic arsenic and can cause cancer in humans if consumed over time (Abdel-Baki *et al.,* 2011).

The highest Pb concentration was found in Sagor Catfish (1.71 µg/g), followed by Nile Tilapia (1.29 µg/g), Spotted Catfish (0.91 µg/g), and Indo-Pacific Tarpon (0.66 µg/g). Based on the findings, the range of Pb concentrations in each species did not pose a threat to human consumption within the permissible limits set by MFAR (1983 & 1985). However, it is safe to be aware of the risk of metal contamination when eating these fish because the Pb concentration has exceeded the permissible limit set by FAO/WHO (1984) of 0.2 µg/g. This is also because lead is one of the most common pollutants in the environment, occurring naturally in rocks, soils, and the hydrosphere. Pb is quickly absorbed by fish after it is released into the marine environment and builds up in their body tissues, bones, gills, kidneys, liver, and scales (Md Yunus *et al.,* 2014). The findings of this study revealed that different fish species accumulated varying Pb concentrations.

According to Praveena and Lin (2015), heavy metal residues in contaminated environments typically build up in microorganisms, aquatic fauna, and flora. Heavy metals enter rivers through a variety of natural and anthropogenic sources (Saher & Kanwal, 2019). Fish bioaccumulation of heavy metals is influenced by a variety of factors, the most important of which are feeding behavior, growth rate, temperature, hardness, salinity, age, sex, and metal interactions (Sivaperumal *et al.,* 2007; Sow *et al.,* 2019). As a result, heavy metals' uptake by long-term contaminated organisms causes severe diseases such as food poisoning, liver damage, cardiovascular disorders, and even death (Tair & Eduin, 2018;

Zulkipli *et al.,* 2021). Furthermore, because fish are abundant and susceptible to accumulating trace elements, they serve as bioindicators for assessing the status of the aquatic ecosystem.

Heavy Metal Content of Arsenic (As), Lead (Pb), Potassium (K) in the Water Sample

Results of heavy metal concentration in water were compared with the permissible limit that have been set by the Malaysian Interim Water Quality Standard (NWQS) (2008) and World Health Organization (WHO) and the Food and Agriculture Organization (FAO) for arsenic (As), lead (Pb), and potassium (K) in microgram per gram (µg/L) in Table 2. Based on the permissible limit set by NWQS (2008) and FAO/WHO (2017) in milligrams per litre (mg/L) unit for water sample, the As concentration in downstream (0.39 µg/L), midstream (0.56 µg/L) and upstream (0.42 µg/L) and Pb concentration in downstream (1.10 µg/L), midstream (0.32 µg/L) and upstream (0.48 µg/L) exceeded the permissible limit (0.05 µg/L) and (0.01 µg/L) for both heavy metal elements. The K concentration of all three sampling sites did not exceed the permissible limit set by FAO/WHO (12.0 µg/L) as shown for downstream (8.10 µg/L), midstream (11.49 µg/L), and upstream (10.52 µg/L), respectively.

Table 2. Heavy metal sample concentration detected by ICP-MS from a water sample.

Heavy Metal	Heavy Metal concentration (µg/L)			Mean Heavy Metal concentrations by site (µg/L)	Permissible limit NWQS (2008)	Permissible limit FAO/WHO (2017)
	Downstream	Midstream	Upstream			
Arsenic (As)	0.39	0.56	0.42	0.46	0.05	0.01
Lead (Pb)	1.10	0.32	0.48	0.63	0.01	0.01
Potassium (K)	8.10	11.49	10.52	10.04	nd	12.0

Water-Fish Transfer Factor

The water-fish transfer factor was calculated for As, Pb, and K, and if the result is < 1, it means that bioaccumulation of metal (As, Pb, and K) in the fish flesh is not from the water, and otherwise it means that the bioaccumulation of metal in fish is from water (Ayodele *et al.,* 2020). Based on Table 3, 4, and 5 show that all elements were > 1, suggesting bioaccumulation of metal in fish is from the water and pose risk of metal contaminant of humans consuming the fish.

Table 3. Transfer factor of Arsenic (As) between fish and water.

Station	Fish species	$M_{fish\ flesh}$	M_{water}	Transfer Factor (TF)
Downstream	Sagor Catfish	1.38	0.392	3.520
Midstream	Indo-Pacific Tarpon	1.247	0.559	2.230
Midstream	Spotted Catfish	1.204	0.559	2.153
Upstream	Nile Tilapia	1.467	0.423	3.466

Table 4. Transfer factor of Lead (Pb) between fish and water.

Station	Fish species	$M_{fish\ flesh}$	M_{water}	Transfer Factor (TF)
Downstream	Sagor Catfish	1.705	1.095	1.557
Midstream	Indo-Pacific Tarpon	0.659	0.321	2.052
Midstream	Spotted Catfish	0.912	0.321	2.840
Upstream	Nile Tilapia	1.289	0.482	2.674

Table 5. Transfer factor of Potassium (K) between fish and water.

Station	Fish species	$M_{fish\ flesh}$	M_{water}	Transfer Factor (TF)
Downstream	Sagor Catfish	14.679	8.096	1.813
Midstream	Indo-Pacific Tarpon	13.446	11.491	1.170
Midstream	Spotted Catfish	13.869	11.491	1.207
Upstream	Nile Tilapia	15.109	10.523	1.436

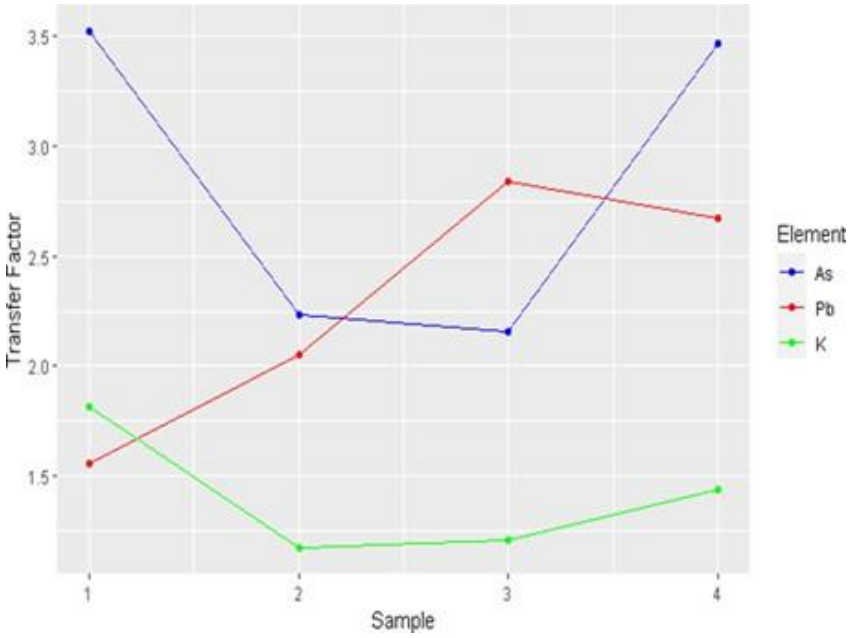

Figure 2. Transfer factor for As, Pb, and K between fish flesh and water.

Figure 2 depicts the amount of transfer factor of three elements (As, Pb, and K) in fish flesh versus water across four samples. The transfer factor determines how much of an element is transferred from the water to the fish tissue. A higher transfer factor indicated that more of the element was accumulated in the fish. Figure 2 shows that As follows, a fluctuating pattern, beginning with a high transfer factor, dropping in the second sample, rising again in the third, and peaking in the fourth. This implies that As uptake by fish is influenced by factors other than water concentration, such as fish species, size, diet, or metabolism. The first sample of Pb had a moderate transfer factor; the second sample showed a slight increase; the third sample showed a significant drop; and the fourth sample showed a sharp rise. This suggested that Pb was readily absorbed by fish from the water and accumulated in their tissue over time. K has a low transfer factor that remains stable across all samples. This suggested that fish regulate K and that there was less As and Pb buildup in their tissue.

According to this study, station 2 (midstream) had the highest concentration of heavy metal K in the water sample. Stations 3 (upstream) and 1 (downstream) had the next-highest concentrations, at 10.52 µg/L, 8.10 µg/L, and 11.49 µg/L, respectively. Pb levels were highest downstream (1.10 µg/L), followed by upstream (0.48 µg/L) and midstream (0.32 µg/L), while As levels were highest in midstream (0.56 µg/L), followed by upstream (0.42 µg/L) and downstream (0.39 µg/L). Overall, all heavy metal elements have exceeded the national and international guideline values established by NWQS (2008) and FAO/WHO (2017), as shown in Table 2, except for K concentration, which remains within the FAO/WHO (2017) standard limit.

Downstream had obvious dense riverside settlements along the Petagas River, providing communities with direct access to the river for economic benefits. Humans primarily contribute to the increase of pollutants that disrupt natural balance, such as organic substances, heavy metals, artificial agricultural fertilizers, detergents, radioactivity, pesticides, inorganic salts, artificially organic chemicals, and wastewater. For example, the houses in the riverside settlements of downstream do not have proper waste system and it will directly discharge in the river along with other solid waste that will increase metal contamination. According to the results, downstream has the highest concentration of Pb (1.10 µg/L), while midstream has the lowest concentration (0.32 µg/L). Based on this value, the Pb concentration exceeded the safe limits for human consumption established by the FAO/WHO (2017) and the NWQS (2008), both of which were set at 0.01 mg/L. According to Kamaruzzaman *et al.* (2011), this could be attributed to heavy metal accumulation at downstream, which was closer to the river mouth.

It is also possible that the presence of industrial and agricultural areas in the upstream contributes to the high Pb concentration at the downstream.

Meanwhile, there were agricultural and residential areas nearby at both stations 2 (midstream) and 3 (upstream). Metal contamination in river water occurs from a variety of sources, including metal-based pesticides, inorganic and organic fertilizers, industrial emissions, and transportation. Inorganic phosphate fertilizers may contain traces of As, Cd, Ni, and Pb (Liu *et al.,* 2015; Mat Amin *et al.,* 2018; Piddocke *et al.,* 2021). Midstream and upstream had the highest As concentrations (0.56 µg/L and 0.42 µg/L) due to their agricultural areas. The As concentration results show that it had exceeded the allowable limits set by FAO/WHO (2017) and NWQS (2008), which were 0.01mg/L and 0.05 mg/L, respectively. Stations 2 and 3 have K concentrations of 11.49 µg/L and 10.053 µg/L, respectively, which fall within the FAO/WHO (2017) standard limit of 12.0 µg/L. The environment is stressed by widespread and unplanned development for hotels, residential areas, deforestation, urbanization, and agriculture, particularly in river systems and water bodies (Pourang, 1995; Kamaruzzaman *et al.,* 2011).

CONCLUSION

The different values of heavy metal concentration in each of the stations correlated to the surrounding environment and human activities. It was found that the mean heavy metal concentration in water sample were higher for K (10.04 µg/L), followed by Pb (0.63 µg/L) and As detected lower (0.46 µg/L). This finding supported by other researchers which K naturally has higher concentration in all the station compared to As and Pb because it is required for fish growth and metabolism. However, the As and Pb concentration are influence by discharge of waste from riverside settlements (downstream) and agricultural area in midstream and upstream which uses arsenic or phosphate-based fertilizer and pesticide. The mean concentrations of heavy metals in randomly collected fish species were investigated, revealing higher levels of K (14.28 µg/g), followed by As (1.33 µg/g) and Pb (1.14 µg/g). Intrinsic factors like species, age, size, metabolic demand, and extrinsic factors such as heavy metal type, location, and environmental conditions were noted as influencing factors on the heavy metal content in various fish species. Overall, the results for heavy metals in water samples were compared to the permissible limits established by the NWQS (2008) and WHO/FAO. It shows that only the K concentration did not exceed the permissible limit of 12.0 mg/L. Meanwhile, the fish sample results were compared to the permissible limits set by MFAR (1983 & 1985) and FAO/WHO (1984). The As concentration has exceeded the permissible limit under both national and international guidelines. It is advised that the public exercise caution when consuming fish from the Petagas River because the Pb concentration was still below the FAO/WHO (1984) limit but above the MFAR (1983 & 1985) permissible limit of 2.0 µg/g. Although the permissible limit set by MFAR (1983 & 1985) did not include a limit for K concentration, caution should still be employed. As a result, there is a need to closely monitor industrial effluent and the wastewater system in the coastal area, as well as develop various strategies to prevent heavy metal accumulation in seafood, which may eventually reduce the chronic health risk to the exposed consumer. Nonetheless, additional research is necessary to guarantee that the same conclusions are made.

ACKNOWLEDGEMENT

The author expresses their sincere gratitude to the Universiti Malaysia Sabah (UMS) for financial support (Skim Penyelidikan Lantikan Baharu (SPLB) SLB2203 and Malaysian Fisheries Development Board (LKIM) for providing infrastructure facilities.

REFERENCES

Abdel-Baki, A.S., Dkhil, M.A. & Al-Quraishy, S. 2011. Bioaccumulation of some heavy metals in tilapia fish relevant to their concentration in water and sediment of Wadi Hanifah, Saudi Arabia. *African Journal of Biotechnology*, 10(13): 2541–2547. https://doi.org/10.5897/AJB10.1772

Ahmed, A. S., Sultana, S., Habib, A., Ullah, H., Musa, N., Hossain, M.B., Rahman, M.M. & Sarker, M.S. 2019. Bioaccumulation of heavy metals in some commercially important fishes from a tropical river estuary suggests higher potential health risk in children than adults. *PLOS ONE*, 14(10). https://doi.org/10.1371/journal.pone.0219336

Ayodele, O., Jegede, T., Oluwatimilehin, T.M., Olanipekun, E.O., Olorunfemi, T.E., Abolarinde, D.O., Ibimiluy, A.E., Aremo, O.E. & Ogundipe, B. S. 2020. Minerals assessment in water, sediment, and fish tissues obtained from earthen pond of Ekiti State University, Nigeria. *Carpathian Journal of Food Science and Technology*, 12(2): 112–124. https://doi.org/10.34302/crpjfst/2020.12.2.11

Kamaruzzaman, B.Y., Rina, Z., John, B.A. & Jalal, K.C.A. 2011. Heavy metal accumulation in commercially important fishes of South West Malaysian Coast. *Research Journal of Environmental Sciences*, 5: 595–602.

Liu, J.-L., Xu, X.-R., Ding, Z.-H., Peng, J.-X., Jin, M.-H., Wang, Y.-S., Hong, Y.-G. & Yue, W.-Z. 2015. Heavy metals in wild marine fish from South China Sea: Levels, tissue- and species-specific accumulation and potential risk to humans. *Ecotoxicology*, 24(7–8): 1583–1592. https://doi.org/10.1007/s10646-015-1451-

Mat Amin, N., Wan Omar, W.B., Abd Kadir, N.H., Mohd Razali, N.S., Mohd Ubaidillah, F.N.A. & Ikhwanuddin, M. 2018. Analysis of trace metals (Ni, Cu and Zn) in water, mud and various tissues of mud crab from Setiu wetlands, Terengganu, Malaysia. *Journal of Sustainability Science and Management*, 13.

Md Yunus, S., Hamzah, Z., Nik Ariffin, N.A. & Muslim, M.B. 2014. Cadmium, chromium, copper, lead, ferum and zinc levels in the cockles (*Anadara granosa*) from Selangor, Malaysia. *The Malaysian Journal of Analytical Sciences*, 18(3): 514–521.

Piddocke, T., Ashby, C., Hartmann, K., Hesp, A., Hone, P., Klemke, J., Mayfield, S., Roelofs, A., Saunders, T., Stewart, J., Wise, B. & Woodhams, J. 2021. Fishing methods. *Status of Australian Fish Stocks Reports*. https://www.fish.gov.au/fishing-methods

Pourang, N. 1995. Heavy metal bioaccumulation in different tissues of two fish species with regards to their feeding habits and trophic levels. *Environmental Monitoring and Assessment*, 35(3): 207–219. https://doi.org/10.1007/bf00547632

Praveena, S.M. & Lin, C.L.S. 2015. Assessment of heavy metal in self-caught saltwater fish from Port Dickson coastal water, Malaysia. *Sains Malaysiana*, 44(1): 91–99.

Rosli, M.N.R., Samat, S.B., Yasir, M.S. & Yusof, M.F.M. 2018. Determination of concentration activity natural radionuclide 232Th, 238U and 40K in fish at the coastal area of Terengganu, Malaysia. *Sains Malaysiana*, 47(9): 2151–2156.

Saher, N.U. & Kanwal, N. 2019. Assessment of some heavy metal accumulation and nutritional quality of shellfish with reference to human health and cancer risk assessment: A seafood safety approach. *Environmental Science and Pollution Research*, 26(5): 5189–5201. https://doi.org/10.1007/s11356-018-3764-6

Sivaperumal, P., Sankar, T.V. & Viswanathan, P. G. 2007. Heavy metal concentrations in fish, shellfish and fish products from internal markets of India vis-à-vis international standards. *Food Chemistry*, 102(3): 612–620. https://doi.org/10.1016/j.foodchem.2006.05.04

Sow, A.Y., Ismail, A., Zulkifli, S.Z., Amal, M.N. & Hambali, K.A. 2019. Survey on heavy metals contamination and health risk assessment in commercially valuable Asian swamp eel, *Monopterus albus* from Kelantan, Malaysia. *Scientific Reports*, 9(1). https://doi.org/10.1038/s41598-019-42753-2

Tair, R. & Eduin, S. 2018. Heavy metals in water and sediment from Liwagu River and Mansahaban River at Ranau, Sabah. *Malaysian Journal of Geosciences*, 2(2): 26–32. https://doi.org/10.26480/mjg.02.2018.26.32

Taweel, A., Shuhaimi-Othman, M. & Ahmad, A.K. 2013. Assessment of heavy metals in tilapia fish (*Oreochromis niloticus*) from the Langat River and Engineering Lake in Bangi, Malaysia, and evaluation of the health risk from tilapia consumption. *Ecotoxicology and Environmental Safety*, 93: 45–51. https://doi.org/10.1016/j.ecoenv.2013.03.031

Vutukuru, S.S. 2005. Acute effects of hexavalent chromium on survival, oxygen consumption, haematological parameters and some biochemical profiles of the Indian major carp, *Labeo rohita*. *International Journal of Environmental Research and Public Health*, 2: 456–462.

World Health Organization (WHO). 2017. *Guidelines for drinking-water quality: Fourth edition incorporating the first addendum*. Geneva: World Health Organization.

Yamada, S. & Inaba, M. 2021. Potassium metabolism and management in patients with CKD. *Nutrients*, 13(6): 1751. https://doi.org/10.3390/nu13061751

Yasir, M.S., Abd Majid, A., Ahmad Kabir, N. & Yahya, R. 2008. Kandungan logam berat dan radionuklid tabii dalam ikan, air, tumbuhan dan sedimen di bekas tapak lombong. *The Malaysian Journal of Analytical Sciences*, 12(1): 172–178.

Younis, E.M., Abdel-Warith, A.-W. A., Al-Asgah, N.A., Elthebite, S.A. & Rahman, M.M. 2021. Nutritional value and bioaccumulation of heavy metals in muscle tissues of five commercially important marine fish species from the Red Sea. *Saudi Journal of Biological Sciences*, 28(3): 1860–1866. https://doi.org/10.1016/j.sjbs.2020.12.038

Yunus, K., Zuraidah, M.A. & John, A. 2020. A review on the accumulation of heavy metals in coastal sediment of Peninsular Malaysia. *Ecofeminism and Climate Change*, 1(1): 21–35. https://doi.org/10.1108/efcc-03-2020-0003

Zulkipli, S.Z., Liew, H.J., Ando, M., Lim, L.S., Wang, M., Sung, Y.Y. & Mok, W.J. 2021. A review of mercury pathological effects on organ-specific functions of fishes. *Environmental Pollutants and Bioavailability*, 33(1): 76–87. https://doi.org/10.1080/26395940.2021.1920468

RESEARCH ARTICLE

BORNEO SCIENCE
THE JOURNAL OF SCIENCE & TECHNOLOGY

Journal homepage: https://jurcon.ums.edu.my/ojums/index.php/borneo-science

RECOMBINANT PHYTASE: ADVANCES IN PRODUCTION STRATEGIES AND INDUSTRIAL APPLICATIONS – A REVIEW

Kishor Biswas, Rima Akter, Tonima Rahman Tuli, and Sk Amir Hossain*

Biotechnology and Genetic Engineering discipline, Khulna University, Khulna 9208, Bangladesh.

***Correspondence:**
skamir@bge.ku.ac.bd

Received: 18 March 2025
Revised: 28 December 2025
Accepted: 28 December 2025
Published online:
31 December 2025

Doi:
10.51200/bsj.v46i2.6241

Keywords:
Yeast expression systems;
Recombinant enzymes;
Industrial biotechnology;
Recombinant phytase.

ABSTRACT. *Phytase has become an essential enzyme in modern biotechnology as global demand for sustainable and efficient feed and food production continues to increase. By catalyzing the hydrolysis of phytic acid, phytase improves phosphorus bioavailability, enhances nutrient utilization, reduces dependence on inorganic phosphate supplementation, and limits phosphorus discharge into the environment. These benefits have contributed to rapid market expansion, with the global phytase market valued at approximately USD 0.6–0.7 billion in 2023 and projected to exceed USD 1 billion by 2030. Recent advances in genetic engineering, protein engineering, and molecular biology have accelerated the development of phytase variants with improved catalytic efficiency, thermostability, and tolerance to acidic conditions. A range of microbial expression systems, including bacterial, fungal, and yeast platforms, has been extensively explored to optimize enzyme production and functionality under industrial settings. Recombinant DNA technologies now allow precise tailoring of phytase expression in intracellular, extracellular, and cell surface display formats, each offering specific advantages for industrial application. Notably, cell surface display systems are attracting growing interest due to their potential to simplify downstream processing and lower production costs. This review provides a comprehensive overview of contemporary recombinant phytase production strategies, critically examining host selection, expression formats, and key factors influencing large-scale production. By addressing both technological advances and production challenges, this review aims to support the development of efficient, cost-effective, and environmentally sustainable phytase production platforms.*

INTRODUCTION

Phytases, also known as myo-inositol hexakisphosphate phosphohydrolases, are enzymes that catalyze the hydrolysis of phytic acid, releasing inositol and inorganic phosphate (Gocheva *et al*., 2024). These enzymes play a pivotal role in improving the bioavailability of necessary minerals, such as calcium, iron, and zinc, which are otherwise bound to phytic acid, an anti-nutrient commonly found in plant-based feeds (Salim *et al.*, 2023). Due to their ability to enrich the nutritional value of animal feed, phytases are widely used in the livestock and poultry industries (El-Hack *et al*., 2018). Phytases are classified as 3-, 4-, and 5-phytases according to the location of the first phosphate group they hydrolyse (Meegoda *et al.*, 2018). This classification is crucial because it affects how well enzymes function in different environmental settings, such as temperature and pH, which are important considerations for both industrial operations and animal digestion (Ravindran, 2013). The need for phytases that maintain their activity throughout a wide range of pH and temperature conditions has prompted a great deal of

study on the stability and effectiveness of enzymes, especially for use in feed processing and the manufacture of biofuel (Rebello *et al.*, 2017). Phytases are produced by a broad range of species, including bacteria, plants, and animals. Singh *et al*. (2024) stated that microbial phytases, especially those derived from bacterial and fungal sources, are favored for industrial applications due to their high production yield, simplicity of genetic manipulation, and suitability to commercial fermentation techniques. Recombinant phytases provide improved enzymatic features, such as increased resistance to proteolysis, improved catalytic efficiency, and higher thermostability. Both wild-type and recombinant phytases are used in industrial settings (Venkataraman *et al*., 2024). The performance and production efficiency of recombinant phytases have been further enhanced using genetic engineering approaches such as cell surface display systems, powerful promoters, and codon optimization (Zhou *et al*., 2022). In commercial phytase synthesis, the cell surface display technique works especially well because it enables direct enzyme presentation on microbial cell surfaces, streamlining purification procedures while increasing enzyme stability and activity (Greenstein *et al*., 2020).

Interest in the industrial uses of phytases and recombinant phytases is rising due to the field's increasing research and the more than 30 patents that have been filed on them. In-depth examination of physiological roles of phytase enzyme, structural and catalytic mechanisms, industrial uses, and developments in production technologies are all included in this review (Outchkourov & Petkov, 2019). Through an examination of the relative importance of various production techniques, this review aims to highlight significant advancements in phytase biotechnology research and future directions (Handa *et al.*, 2020).

MATERIALS AND METHODS

This review was conducted through a comprehensive and systematic analysis of published literature focusing on recombinant phytase production strategies and their industrial applications. Relevant peer-reviewed research articles, reviews, book chapters, and doctoral theses were collected from major scientific databases, including Scopus, Web of Science, PubMed, Google Scholar, and ScienceDirect. The literature search covered publications primarily from 2000 to 2024, with emphasis on recent advances in recombinant DNA technology, enzyme engineering, and microbial expression systems.

Keywords used during the search included phytase, recombinant phytase, phytase production, cell surface display, yeast expression systems, fungal phytase, industrial enzymes, and phytase applications. Articles were selected based on their relevance to phytase classification, microbial sources, genetic engineering approaches, expression platforms (intracellular, extracellular, and surface display), biochemical properties, and industrial or environmental applications.

After initial screening of titles and abstracts, full-text articles were critically evaluated to extract information on enzyme characteristics, host systems, production strategies, and scalability. Only studies providing clear experimental data, comparative analyses, or significant technological insights were included. The selected literature was then categorized thematically to ensure structured discussion and critical comparison across different production platforms. This approach enabled an integrated assessment of current advancements, limitations, and prospects in recombinant phytase biotechnology.

RESULTS

Phytase

Sources of Phytase

The primary microbial sources of phytase include *Aspergillus niger, Bacillus subtilis, Escherichia coli*, and *Klebsiella pneumoniae* (Gocheva *et al*., 2023). These organisms are widely utilized in industrial processes due to their ability to ferment and produce large quantities of phytase efficiently (Jatuwong *et*

al., 2023). Advancements in genetic engineering have been applied to these microbes to enhance enzyme production, thermal and pH stability, and overall catalytic efficiency. As a result, these genetically modified strains are extensively used for large-scale phytase production in sectors such as agriculture, animal nutrition, and environmental management (Sharma & Satyanarayana, 2013).

The commercially significant phytase-producing microorganisms and plant sources are included in Table 1, along with their corresponding EC numbers. Due to their high enzyme output and stability under industrial processing settings, *Escherichia coli, Bacillus subtilis*, and *Aspergillus niger* are some of the most commonly utilized sources of phytase (Kumar & Sinha, 2018; Liu *et al*., 2022). Despite being less prevalent, plant-based phytases have drawn attention due to their possible use in biofortification and animal feed augmentation techniques (Liu *et al*., 2022).

Table 1. Commercially important phytase-producing organisms.

Microbial Sources	Plant Sources	EC Number	Refences
Escherichia coli	*Tomato roots*	EC 3.1.3.8	(Kumar & Sinha, 2018; Liu *et al*., 2022)
Bacillus subtilis	*Typha latifolia* pollen	EC 3.1.3.26	(Mittal *et al.*, 2013; Liu *et al*., 2022)
Klebsiella terrigena	*Barley*	EC 3.1.3.26	(Kumar & Sinha, 2018; Liu *et al*., 2022)
Klebsiella pneumoniae	*Maize seedling*	EC 3.1.3.8	(Mittal *et al.*, 2013; Liu *et al*., 2022)
Citrobacter braakii	*Wheat bran*	EC 3.1.3.8	(Mittal *et al.*, 2013; Liu *et al*., 2022)
Lactobacillus sanfranciscensis	*Aspergillus niger*	EC 3.1.3.8	(Kumar & Sinha, 2018; Liu *et al*., 2022)
Aspergillus ficuum	*Aspergillus fumigatus*	EC 3.1.3.8	(Kumar & Sinha, 2018)
Pichia anomala	*Candida krusei*	EC 3.1.3.26	(Kumar & Sinha, 2018)
Saccharomyces cerevisiae	-	EC 3.1.3.8	(Kumar & Sinha, 2018)

Classification of Phytase

Phytases are classified based on their structural and catalytic properties, which influence their stability, substrate specificity, and suitability for industrial use. The major classes include: Histidine Acid Phosphatases (HAPs), predominantly found in bacteria, fungi, and plants. HAPs contain a conserved histidine residue crucial for their catalytic activity. They function effectively in acidic conditions, making them widely used in commercial applications, especially in food and feed industries (Bouajila *et al.,* 2020). β-Propeller Phytases (BPPs), mainly derived from bacterial species, are characterized by a β-propeller fold that provides broad pH tolerance and high thermal stability. Their ability to function in neutral to alkaline environments makes them especially valuable in animal feed formulations (Singh *et al.,* 2018). Purple Acid Phosphatases (PAPs) are mostly found in plants and some fungi. They exhibit unique substrate selectivity and pH stability and play an important role in plant phosphorus metabolism. However, they are less commonly used in commercial settings (Bhadouria & Giri, 2022). Although the primary function of Protein Tyrosine Phosphatases (PTPs) is not phytate degradation, some PTPs from microorganisms have shown potential for biotechnological applications. They possess a distinct catalytic mechanism and are under investigation for specialized uses (Singh *et al.,* 2018; Cangussu *et al.,* 2018).

Phytase Production Platforms

Phytase production is carried out using two primary approaches: wild-type production and recombinant production systems. Each method has distinct advantages and limitations, depending on the intended application (Bhavsar & Khire, 2014)

Production of Wild-Type Phytase

Phytase-producing bacteria are necessary for wild-type production. Due to its ease of use and affordability, this technique is frequently employed in large-scale fermentation. *Aspergillus niger* and other fungal strains are among the most widely employed species for the manufacture of phytase (Nagar *et al.,* 2021). Since it replicates the natural growing conditions of these fungi, solid-state fermentation (SSF) is the recommended technique for producing wild-type phytase (Santos, 2011). This method is

made both economically and environmentally feasible by using agricultural byproducts as substrates, such as soybean meal, rice bran, and wheat bran. However, the yield, thermostability, and specific activity of wild-type manufacturing are limited, frequently requiring further processing or enzyme purification (Katileviciute *et al.*, 2019).

Recombinant Phytase Production

The production of phytase has been transformed by recombinant DNA technology, which makes it possible to introduce phytase genes into host microorganisms, including *Saccharomyces cerevisiae, Pichia pastoris*, and *Escherichia coli*. This method offers greater catalytic efficiency, increased thermostability, increased enzyme yields, and resistance to proteolytic degradation (Kaur *et al.,* 2010). Some major benefits of producing recombinant phytase have been found. Optimised enzyme properties, improving pH and thermal stability made possible by genetic alterations, increase the applicability of the enzyme in a wider range of industrial settings (Rigoldi *et al.,* 2018). Compared to wild-type strains, recombinant strains can be designed for higher enzyme expression, which results in higher yields (Saxena, 2015). Recombinant systems offer improved control over the development and synthesis of enzymes, guaranteeing constant activity and quality (Huang *et al*., 2012). Modern advancements, such as codon optimization, the use of strong promoters, and cell surface display systems, have further improved recombinant phytase production (Han *et al*., 2018). The cell surface display strategy is particularly advantageous, as it allows phytase enzymes to be anchored on microbial cell membranes, facilitating direct enzyme application without the need for extensive purification (Pragya *et al*., 2023). Table 2 presents a comparative overview of recombinant phytases produced in recent years, highlighting their source organisms, host strains, expression vectors, optimal biochemical parameters, and industrial applications. The enzymes were expressed in various microbial systems such as *E. coli*, *Pichia pastoris*, *Kluyveromyces lactis*, and *P. griseoroseum*, using well-established vectors such as pET-28a (+), pPICZαA, and pYES2. These recombinant phytases exhibit diverse optimal temperatures (ranging from 50 to 60 °C) and pH levels, with specific activities varying significantly depending on the expression system and assay conditions. Applications primarily include animal feed supplementation, particularly in poultry and aquaculture, due to improved thermal stability and protease resistance. While the data provide valuable insight into enzyme performance, it should be noted that differences in assay substrates and definitions of unit activity may affect direct comparison across studies (Ribeiro *et al.,* 2015; Ranjan & Satyanarayana, 2016).

Table 2. Recombinant phytases produced in recent years: expression systems, biochemical properties, and industrial applications (data compiled from published studies).

Source Organism	Host Strain	Expression Vector	Optimum Temp (°C)	Optimum pH	Specific Activity	Km (mM)	Key Applications	EC Number	Reference
Dendroctonus frontalis	*E. coli*	pET-28a(+)	52.5	3.9	4135 U mg^{-1}	0.262	Animal feed additive	EC 3.1.3.8	(Tan *et al*., 2016)
A. niger NII08121	*Kluyveromyces lactis* GG799	pKLAC2	55	2.5 & 5.5	198 U mg^{-1}	N/A	Protease-resistant phytase for industrial use	EC 3.1.3.8	(Ushasree *et al*., 2014)
Aspergillus niger	*Pichia pastoris* GS115	pPIC9K	60	5.5	N/A	.148	Feed supplement with thermal stability	EC 3.1.3.8	(Hesampour *et al.,* 2015)
A. niger NII08121	*E. coli*	pET-21b	50	6.5	18 U mg^{-1}	N/A	Improved purification and protein yield	EC 3.1.3.8	(Vasude, Salim & Pandey, 2011)
Penicillium chrysogenum CCT 1273	*P. griseoroseum*	pYES2	50	5.1	2.86 ± 0.4 U μg^{-1}	N/A	Animal nutrition	EC 3.1.3.8	(Ribeiro, Queiroz & Araújo, 2015)
Sporotrichum thermophile	*Pichia pastoris* X-33	pPICZαA	60	5.0	480 ± 23 U mL^{-1}	0.147	Poultry and aquaculture feed additive	EC 3.1.3.8	(Ranjan & Satyanarayana, 2016)

*N/A indicates that the corresponding parameter was not reported in the original study.

Cell Surface Display System

An inventive method for creating recombinant phytase is the cell surface display system, which immobilises the enzyme on the surface of the host cell. By guiding the protein to the cell wall via a genetic cassette included in an expression vector, this method improves stability and streamlines downstream processing. Strong promoters such as GAL1 and GAL10 (Hossain *et al*., 2020), which stimulate high protein expression, and anchor proteins such as Sed1, Ccw12, Cwp1, and Cwp2 in yeast, which maintain the stability and integrity of the cell wall (Geetha *et al.,* 2019), are crucial parts of this system. Furthermore, effective protein immobilization is made possible by glycosylphosphatidylinositol (GPI) anchors, such as GCW61 in *Pichia pastoris*, which raises phytase activity to 6413.5 U g^{-1} (Müller, 2011). This technique is useful for both industrial and environmental applications since it not only increases stability and processing convenience but also provides environmental advantages, including improved ethanol production in Saccharomyces cerevisiae and effective phosphorus reduction (Kumari & Bansal, 2022). Different anchor proteins and genetic constructs have been used to successfully apply the cell surface display system across a range of expression hosts, as shown in Table 3.

Table 3. Surface display systems for recombinant phytase expression in various hosts.

Expression Host	Vector	Promoter	Anchor Protein	Phytase Activity	Reference
Candida amalonaticus CGMCC 1696	pPICZaA	AOX1	Gcw61p	6413.5 U g^{-1}	(Hossain *et al.,* 2020)
E. coli JM109	pMGK-AG	PGK1	α-agglutinin (C-terminal)	6.4 U g^{-1} (wet biomass)	(Li *et al.,* 2014)
Aspergillus niger	pPICZaA	AOX1	α-agglutinin (3'-half)	300 U g^{-1} (dry weight)	(Chen *et al.,* 2016)
Bacillus subtilis	Native OxdD motif	OxdD	OxdD	5.7×10^3 U g^{-1} (spore dry weight)	(Harnpicharnchai *et al.,* 2010)
	Codon-optimised *phyA* gene	CotG	CotG	91.62 U per 10^8 spores	(Potot *et al.,* 2010)

Various expression hosts and surface display systems have been employed to enhance phytase activity and stability for industrial applications. Hosts such as *Candida amalonaticus, E. coli, Aspergillus niger*, and *Bacillus subtilis* utilize vectors with specific promoters (e.g., AOX1, PGK1, CotG) and anchor proteins such as α-agglutinin, Gcw61p, or OxdD to facilitate efficient surface display (Hossain *et al.,* 2020; Li *et al.,* 2014; Chen *et al.,* 2016; Harnpicharnchai *et al.,* 2010; Potot *et al.,* 2010). Among them, *C. amalonaticus* and *B. subtilis* systems show notably high phytase activities, making them promising platforms for cost-effective phytase production in feed and environmental sectors.

Economic Implications and Industrial Applications

In industrial applications, recombinant phytases provide substantial financial advantages, particularly in the areas of environmental control and animal feed. For instance, supplementation of poultry feed with recombinant *Aspergillus niger* phytase has been shown to reduce inorganic phosphate supplementation by up to 30%, while simultaneously lowering phosphorus excretion into the environment (Tan *et al.,* 2016; El-Hack *et al*, 2018; Venkataraman *et al*., 2024; Bhavsar & Khire, 2014). Enzymes with increased stability and activity can be engineered to reduce phytate in feed and enhance nutrient absorption more effectively. For instance, supplementation of broiler feed with recombinant *Aspergillus niger* phytase increased phosphorus and calcium digestibility by 15–25%, improving growth performance and reducing phosphate excretion (Handa *et al.,* 2020). Additionally, by lowering the requirement for phosphate supplementation and minimizing environmental phosphorus pollution, recombinant phytases help to make animal rearing more sustainable (Kumar *et al.,* 2015; Gocheva *et al*., 2024). In order to enhance the nutritional value of foods or as possible treatment agents for phosphate-related illnesses, recombinant phytases are also being investigated for usage in the food and pharmaceutical sectors (Shunmugam, 2014; El-Hack *et al*, 2018).

DISCUSSION

There are distinct advantages and disadvantages to producing phytase from various microbiological sources and expression hosts, which are important for industrial applications. To move beyond descriptive reporting, a comparative evaluation of the major recombinant phytase expression platforms is necessary to identify systems with the highest industrial relevance. Comparative evaluation of recombinant phytase expression systems indicates that yeast-based platforms, particularly *Pichia pastoris* and *Saccharomyces cerevisiae*, provide high expression efficiency, appropriate post-translational modifications, and scalability suitable for industrial production (Bhavsar & Khire, 2014).

Bacterial hosts such as *Bacillus subtilis* further enhance industrial feasibility through efficient secretion and cell surface display, significantly reducing downstream processing costs. In contrast, filamentous fungi remain commercially dominant in feed industries due to their robustness in large-scale fermentation, despite comparatively limited genetic flexibility (Ranjan & Satyanarayana, 2016; Kaur *et al*., 2022). It is commonly known that *Aspergillus* species, especially *A. niger*, are very adaptable and easily genetically modified. For example, high yield levels were obtained by *A. niger NII 08121* produced in *Kluyveromyces lactis* GG799 (Tan *et al.,* 2016). At 826.33 U mL^{-1}, another strain, *A. niger 563*, produced a notably higher amount of phytase than its wild-type equivalent (Salaet *et al*., 2021). Expression systems based on yeast have also shown potential. For instance, employing yeast cell surface display technology, *Pichia pastoris* KM71, which expresses *A. niger* phytase, showed high specific activity (300 Ug^{-1} cell dry weight) (Müller, 2011). In a similar vein, *A. japonicus C03* showed beneficial glycosylation patterns and significant phytase activity (Geetha *et al*., 2019).

Bacillus subtilis has proven beneficial in bacterial systems because of its efficient downstream processing and ease of purification. Comparative studies show that the surface display systems of *B. subtilis* and *S. cerevisiae* both exhibit noticeably higher amounts of phytase synthesis. Furthermore, increased phosphorus digestibility has been seen in hosts such as *Lactococcus lactis* that express *E. coli* phytase. The animal feed business has also benefited from fungi such as *Penicillium chrysogenum CCT 1273* and *P. griseoroseum* (Ribeiro *et al.,* 2015). One significant development that has made purification simpler, improved thermal stability possible, and made it economically viable for commercial usage is the immobilization of phytase on the cell surface. Although these advantages have drawn attention to surface display technologies, other methods, such as intracellular and extracellular expression systems, also increase the efficiency of phytase synthesis. Despite these advantages, these systems suffer from lower overall yield, restricted enzyme flexibility, and limited substrate accessibility due to anchoring constraints (Ribeiro *et al.,* 2015).

Despite the advantages of recombinant phytase expression systems, several limitations remain. Bacterial hosts, such as *E. coli* and *Bacillus subtilis*, may face challenges in proper folding and post-translational modifications, which can reduce enzyme stability and activity (Huang *et al.,* 2012; Ranjan & Satyanarayana, 2016). Yeast-based systems, including *Pichia pastoris* and *Saccharomyces cerevisiae*, generally provide higher yields and suitable secretion but can introduce undesired glycosylation patterns and impose metabolic stress on the host, limiting overall expression efficiency (Hossain *et al*., 2020; Geetha *et al*., 2019). Cell surface display approaches simplify downstream processing and allow direct enzyme application; however, enzyme accessibility may be restricted, and substrate interaction can be suboptimal due to anchoring constraints (Potot *et al*., 2010; Müller, 2011). Acknowledging these drawbacks is essential for selecting and optimizing host systems for industrial-scale phytase production.

CONCLUSION

The industrial significance of current developments in phytase production platforms is compiled in this study. Optimizing a number of factors, such as host strain selection, substrate cost and availability, and recombinant synthesis ease, is essential for industrial-scale production. Furthermore, attaining high-yield production depends on phytase expression (Xie, 2020). Intracellular and extracellular expression technologies have shown significant success in addition to surface display techniques. Strong expression

capabilities are provided by yeast-based platforms such as *P. pastoris* and *S. cerevisiae*, but simpler downstream processing is offered by bacterial systems such as *B. subtilis* and *E. coli*. Furthermore, the commercial production of phytase, especially for use in animal feed, still depends on fungal sources (Xie, 2020). Commercial phytase production for animal feed still relies primarily on fungal sources such as *Aspergillus niger* and *Penicillium* species due to their high extracellular enzyme yield and industrial suitability (Abd El-Hack *et al*., 2018; Bhavsar & Khire, 2014). Ongoing advancements in expression hosts and biotechnological methods are crucial due to the growing need for high-yield, economical, and thermally stable phytase (Kaur *et al.,* 2022). Future studies should concentrate on incorporating cutting-edge genetic engineering techniques, refining fermentation tactics, and investigating new host systems in order to enhance phytase production (Siddique *et al.,* 2022). In order to meet changing market demands, industrial phytase production can become more sustainable and efficient by tackling these issues. Although current studies highlight the advantages of various recombinant phytase production systems, more comparative data and industrial case studies are needed to draw stronger, evidence-based conclusions. Future research should focus on generating comprehensive experimental and application-based examples to reinforce these findings.

Abbreviations: In this review, the following abbreviations are used: SSF, solid-state fermentation; HAP, histidine acid phosphatase; BPP, β-propeller phytase; PAP, purple acid phosphatase; PTP, protein tyrosine phosphatase; RA, research assistant; EC, enzyme commission number; GPI, glycosylphosphatidylinositol; Km, Michaelis-Menten constant; U, unit of enzyme activity; AOX1, alcohol oxidase 1 promoter; PGK1, phosphoglycerate kinase 1 promoter; CotG, Bacillus subtilis coat protein G; pET, pET expression vector series; pPIC, Pichia pastoris expression vector; pKLAC, Kluyveromyces lactis expression vector; and pYES, yeast expression vector.

ACKNOWLEDGEMENT

The authors are thankful to the Ministry of Education, Government of Bangladesh, and Khulna University Research and Innovation Center, Bangladesh, for their support in carrying out this review work.

REFERENCES

Abd El-Hack, M.E., Alagawany, M., Arif, M., Emam, M., Saeed, M., Arain, M.A. & Elnesr, S.S. 2018. The uses of microbial phytase as a feed additive in poultry nutrition – a review. *Annals of Animal Science*, 18(3): 639–658. https://doi.org/10.2478/aoas-2018-0019

Bhadouria, J. & Giri, J. 2022. Purple acid phosphatases: roles in phosphate utilization and new emerging functions. *Plant Cell Reports*, 41(1): 33–51.

Bhavsar, K. & Khire, J.M. 2014. Current research and future perspectives of phytase bioprocessing. *RSC Advances*, 4(51): 26677–26691.

Bouajila, A., Ammar, H., Chahine, M., Khouja, M., Hamdi, Z., Khechini, J. & López, S. 2020. Changes in phytase activity, phosphorus and phytate contents during grain germination of barley (*Hordeum vulgare* L.) cultivars. *Agroforestry Systems*, 94: 1151–1159.

Bhavsar, K. & Khire, J.M. 2014. Current research and future perspectives of phytase bioprocessing. *RSC Advances*, 4**,** 26677–26691. https://doi.org/10.1039/C4RA03445G

Cangussu, A.S.R., Aires Almeida, D., Aguiar, R.W.S., Bordignon-Junior, S.E., Viana, K.F., Barbosa, L.C.B. & Lima, W.J.N. 2018. Characterization of the catalytic structure of plant phytase, protein tyrosine phosphatase-such as phytase, and histidine acid phytases and their biotechnological applications. *Enzyme Research*, 2018: 8240698.

Chen, X., Xiao, Y., Shen, W., Zhou, X., Li, J. & Chen, J. 2016. Display of phytase on the cell surface of *Saccharomyces cerevisiae* to degrade phytate phosphorus and improve bioethanol production. *Applied Microbiology and Biotechnology*, 100: 2449–2458. https://doi.org/10.1007/s00253-015-7170-4

Geetha, S., Joshi, J.B., Kumar, K.K., Arul, L., Kokiladevi, E., Balasubramanian, P. & Sudhakar, D. 2019. Genetic transformation of tropical maize (*Zea mays* L.) inbred line with a phytase gene from *Aspergillus niger*. *3 Biotech*, 9: 208. https://doi.org/10.1007/s13205-019-1731-7

Gocheva, Y., Engibarov, S., Lazarkevich, I. & Eneva, R. 2023. Phytases—Types, sources, and factors affecting their activity. *Acta Microbiologica Bulgarica*, 39(3): 249–263.

Gocheva, Y., Stoyancheva, G., Miteva-Staleva, J., Abrashev, R., Dishliyska, V. & Yovchevska, L. 2024. Fungal phytases as useful tools in agricultural practices. *Agronomy*, 14(12): 3029. https://doi.org/10.3390/agronomy14123029

Han, L., Zhao, Y., Cui, S. & Liang, B. 2018. Redesigning of microbial cell surface and its application to whole-cell biocatalysis and biosensors. *Applied Biochemistry and Biotechnology*, 185: 396–418.

Handa, V., Sharma, D., Kaur, A. & Arya, S.K. 2020. Biotechnological applications of microbial phytase and phytic acid in food and feed industries. *Biocatalysis and Agricultural Biotechnology*, 25: 101600.

Harnpicharnchai, P., Sornlake, W., Tang, K., Eurwilaichitr, L. & Tanapongpipat, S. 2010. Cell-surface phytase on *Pichia pastoris* cell wall offers great potential as a feed supplement. *FEMS Microbiology Letters*, 302(1): 8–14. https://doi.org/10.1111/j.1574-6968.2009.01811

Hesampour, A., Siadat, S.E.R., Malboobi, M.A., Mohammadi, M. & Khosravi-Darani, K. 2015. Enhancement of thermostability and kinetic efficiency of *Aspergillus niger* PhyA phytase by site-directed mutagenesis. *Applied Biochemistry and Biotechnology*, 175: 2528–2541. https://doi.org/10.1007/s12010-014-1440-y

Hossain, S.A., Rahman, S.R., Ahmed, T. & Mandal, C. 2020. An overview of yeast cell wall proteins and their contribution in yeast display system. *Asian Journal of Medical and Biological Research*, 5(4): 246–257. https://doi.org/10.3329/ajmbr.v5i4.45261

Hossain, S.A., Mandal, C., Ahmed, T. & Rahman, S.R. 2020. A review on constructed genetic cassettes in yeast for recombinant protein production. *Borneo Science*, 41(1).

Huang, C.J., Lin, H. & Yang, X. 2012. Industrial production of recombinant therapeutics in *Escherichia coli* and its recent advancements. *Journal of Industrial Microbiology and Biotechnology*, 39(3): 383–399.

Jatuwong, K., Suwannarach, N., Kumla, J., Penkhrue, W., Kakumyan, P. & Lumyong, S. 2020. Bioprocess for production, characteristics, and biotechnological applications of fungal phytases. *Frontiers in Microbiology*, 11: 188.

Katileviciute, A., Plakys, G., Budreviciute, A., Onder, K., Damiati, S. & Kodzius, R. 2019. A sight to wheat bran: High value-added products. *Biomolecules*, 9(12): 887.

Kaur, P., Singh, B., Böer, E., Straube, N., Piontek, M., Satyanarayana, T. & Kunze, G. 2010. Pphy—a cell-bound phytase from the yeast *Pichia anomala*: molecular cloning of the gene *PPHY* and characterization of the recombinant enzyme. *Journal of Biotechnology*, 149(1–2): 8–15.

Kaur, P., Vohra, A. & Satyanarayana, T. 2022. Developments in fungal phytase research: characteristics and multifarious applications. In: *Progress in Mycology: Biology and Biotechnological Applications*. Singapore: Springer Nature Singapore: 73–109.

Kumar, V. & Sinha, A.K. 2018. General aspects of phytases. In: *Enzymes in Human and Animal Nutrition*. Academic Press: 53–72.

Kaur, P., Vohra, A. & Satyanarayana, T. 2022. Developments in fungal phytase research: characteristics and multifarious applications. In *Progress in Mycology: Biology and Biotechnological Applications*. Springer Nature, Singapore.

Kumar, V., Singh, D., Sangwan, P. & Gill, P.K. 2015. Management of environmental phosphorus pollution using phytases: current challenges and future prospects. In: *Applied Environmental Biotechnology: Present Scenario and Future Trends*: 97–114.

Liu, X., Han, R., Cao, Y., Turner, B.L. & Ma, L.Q. 2022. Enhancing phytate availability in soils and phytate-P acquisition by plants: a review. *Environmental Science & Technology*, 56(13): 9196–9219.

Mittal, A., Gupta, V., Singh, G., Yadav, A. & Aggarwal, N.K. 2013. Phytase: a boom in food industry. *Octa Journal of Biosciences*, 1(2).

Müller, G. 2011. Novel applications for glycosylphosphatidylinositol-anchored proteins in pharmaceutical and industrial biotechnology. *Molecular Membrane Biology*, 28(3): 187–205.

Nagar, A., Kamble, A. & Singh, H. 2021. Preliminary screening, isolation and identification of microbial phytase producers from soil. *Environmental and Experimental Biology*, 19(1): 11–22.

Outchkourov, N. & Petkov, S. 2019. Phytases for feed applications. In: *Industrial Enzyme Applications*: 255–285.

Potot, S., Serra, C.R., Henriques, A.O. & Schyns, G. 2010. Display of recombinant proteins on *Bacillus subtilis* spores, using a coat-associated enzyme as the carrier. *Applied and Environmental Microbiology*, 76(17): 5926–5933. https://doi.org/10.1128/AEM.01103-10

Pragya, Sharma, K.K., Kumar, A., Singh, D., Kumar, V. & Singh, B. 2023. Immobilized phytases: an overview of different strategies, support material, and their applications in improving food and feed nutrition. *Critical Reviews in Food Science and Nutrition*, 63(22): 5465–5487.

Ranjan, B. & Satyanarayana, T. 2016. Recombinant HAP phytase of the thermophilic mold *Sporotrichum thermophile*: expression of the codon-optimised phytase gene in *Pichia pastoris* and applications. *Molecular Biotechnology*, 58: 137–147. https://doi.org/10.1007/s12033-015-9909-7

Ravindran, V. 2013. Feed enzymes: the science, practice, and metabolic realities. *Journal of Applied Poultry Research*, 22(3): 628–636.

Rebello, S., Jose, L., Sindhu, R. & Aneesh, E.M. 2017. Molecular advancements in the development of thermostable phytases. *Applied Microbiology and Biotechnology*, 101: 2677–2689.

Ribeiro Corrêa, T.L., de Queiroz, M.V. & de Araújo, E.F. 2015. Cloning, recombinant expression and characterization of a new phytase from *Penicillium chrysogenum*. *Microbiological Research*, 170: 205–212. https://doi.org/10.1016/j.micres.2014.06.005

Ranjan, B. & Satyanarayana, T. 2016. Recombinant HAP phytase of the thermophilic mold *Sporotrichum thermophile*: expression in *Pichia pastoris* and applications. *Molecular Biotechnology*, 58**,** 137–147. https://doi.org/10.1007/s12033-015-9909-7

Rigoldi, F., Donini, S., Redaelli, A., Parisini, E. & Gautieri, A. 2018. Engineering of thermostable enzymes for industrial applications. *APL Bioengineering*, 2(1).

Salaet, I., Marques, R., Yance-Chávez, T., Macías-Vidal, J., Giménez-Zaragoza, D. & Aligué, R. 2021. Novel long-term phytase from *Serratia odorifera*: cloning, expression, and characterization. *ACS Food Science & Technology*, 1(4): 689–697. https://doi.org/10.1021/acsfoodscitech.0c00074

Salim, R., Nehvi, I.B., Mir, R.A., Tyagi, A., Ali, S. & Bhat, O.M. 2023. A review on anti-nutritional factors: unraveling the natural gateways to human health. *Frontiers in Nutrition*, 10: 1215873.

Santos, T. 2011. *Optimisation of phytase production by Aspergillus niger using solid state fermentation*. Doctoral Dissertation, National University of Ireland, Maynooth, Ireland.

Saxena, S. 2015. Strategies of strain improvement of industrial microbes: classical and recombinant DNA technology. In: *Applied Microbiology*. New Delhi: Springer India: 155–171.

Sharma, A. & Satyanarayana, T. 2013. Microbial acid-stable α-amylases: characteristics, genetic engineering and applications. *Process Biochemistry*, 48(2): 201–211.

Siddique, A., Tayyaba, T., Imran, M. & Rahman, A. 2022. Biotechnology applications in precision food. In: *Biotechnology in Healthcare*. Academic Press: 197–222.

Singh, B., Pragya, Tiwari, S.K., Singh, D., Kumar, S. & Malik, V. 2024. Production of fungal phytases in solid state fermentation and potential biotechnological applications. *World Journal of Microbiology and Biotechnology*, 40(1): 22.

Tan, H., Wu, X., Xie, L., Huang, Z., Peng, W. & Gan, B. 2016. Identification and characterization of a mesophilic phytase highly resilient to high temperatures from a fungus-garden associated metagenome. *Applied Microbiology and Biotechnology*, 100: 2225–2241. https://doi.org/10.1007/s00253-015-7097-9

Ushasree, M.V., Vidya, J. & Pandey, A. 2014. Extracellular expression of a thermostable phytase (*phyA*) in *Kluyveromyces lactis*. *Process Biochemistry*, 49: 1440–1447. https://doi.org/10.1016/j.procbio.2014.05.010

Vasudevan, U.M., Salim, S.H.B. & Pandey, A. 2011. A comparative analysis of recombinant expression and solubility screening of two phytases in *Escherichia coli*. *Food Technology and Biotechnology*, 49(3): 304.

Venkataraman, S., Karthikanath, P.R., Gokul, C.S., Adhithya, M., Vaishnavi, V.K. & Rajendran, D.S. 2024. Recent advances in phytase thermostability engineering towards potential application in the food and feed sectors. *Food Science and Biotechnology*, 33: 1–18.

Xie, Z. 2020. *Engineering and optimization of phosphate-responsive Pichia pastoris yeast for phytate hydrolysis*. Doctoral Dissertation, The Chinese University of Hong Kong, Hong Kong.

Zhou, Y., Anoopkumar, A.N., Tarafdar, A., Madhavan, A., Binoop, M. & Lakshmi, N.M. 2022. Microbial engineering for the production and application of phytases to the treatment of toxic pollutants: a review. *Environmental Pollution*, 308: 119703.

RESEARCH ARTICLE

BORNEO SCIENCE
THE JOURNAL OF SCIENCE & TECHNOLOGY

Journal homepage: https://jurcon.ums.edu.my/ojums/index.php/borneo-science

CHEMICAL PROPERTIES AND SURFACE MORPHOLOGY OF ENR/PVC FILLED CELLULOSE GRAFTED PMMA MEMBRANE

Mohd Razali Shamsuddin* **and Muhammad Rashidi Rosli**

Preparatory Centre for Science and Technology, Universiti Malaysia Sabah,
88400 Kota Kinabalu, Sabah, Malaysia.

***Correspondence:**
razalishamsuddin@ums.edu.my

Received: 16 April2025
Revised: 19 December 2025
Accepted: 24 December 2025
Published online:
30 December 2025

Doi:
10.51200/bsj.v46i2.6333

Keywords:
Cellulose; ENR/PVC; Membrane; PMMA; Morphology

ABSTRACT. *The ENR/PVC thin film has great potential as a membrane due to its ideal owing to unique characteristics such as freestanding, high-pressure resistance, and durability over time, but low porosity. This research aims to investigate inside into chemical and morphological properties of the developed composite epoxidized natural rubber with polyvinyl chloride-filled cellulose grafted polymethyl methacrylate (ENR/PVC/cellulose-g-PMMA) membrane. Solution blending of 60:40 wt. % ENR/PVC 10 % w/v of filler was mixed homogeneously for 24 h, stirring in THF solution. The membranes were cast onto a glass plate, and the phase inversion technique was used to prepare ENR/PVC/Cell-g-PMMA membranes. The characterization of chemical properties was carried out by Fourier Transform İnfrared Spectroscopy (FTIR) to determine functional groups related to bond breaking and the formation of new bonds of the species during grafting copolymerization and membrane fabrication. Variable Pressure Scanning Electron Microscopy (VPSEM) was conducted to determine surface morphology and textural properties of fillers and membranes. Furthermore, it contributes to porosity and the formation of pores on the membrane. FTIR spectrum shows that absorption peaks around the range 1735-1725 cm^{-1} of the carbonyl ester -C=O functional group have been detected and prove the success of the grafting method between cellulose and PMMA. The rough surface of fibers, formation of open pores, and interspace structure between ENR/PVC matrix and filler affirmed the addition of cell-g-PMMA fillers caused by film-filler and filler-filler interfaces interaction, as shown by the VPSEM micrograph. In summary, the chemical properties and morphological analysis give useful information on the effectiveness of potential ENR/PVC/Cell-g-PMMA membranes in developing standalone, highly pressure-resistant, porous, and elastic membranes.*

INTRODUCTION

Membranes are used extensively in a variety of industries, including water purification, petrochemical refining, pharmaceutical manufacture, mining, building, and space exploration (Norfarhana *et al.,* 2022). They are divided into organic (polymeric) and inorganic (ceramic, metallic, and zeolite) forms depending on their component ingredients. Organic membranes are made from synthetic or natural polymers such as polytetrafluoroethylene (PTFE), polyamide-imide (PAI), polyvinylidene difluoride (PVDF), polyether sulfone (PES), and polyacrylonitrile (PAN) (Arman Alim & Othaman, 2018; Norfarhana *et al.,* 2022). Several factors, including the composition of the feed solution, the operating environment, the features of the application, and the need for separation, influence the choice of these polymers. Compared to organic membranesstability andmbranes are easier to clean after fouling, offer

greater chemical and thermal stability, and are less susceptible to microbiological deterioration. Nonetheless, the reason for their initial greater costs is the exact thickness specifications required to withstand different pressure drops (Castro-Muñoz, 2020).

To tackle these issues, new polymers with enhanced mechanical and pressure-tolerant qualities have been created, inorganic fillers or nanoparticles have been added to boost strength, freestanding membranes have been made via phase inversion or electrospinning, and mixed matrix membranes (MMMs)—a blend of organic and inorganic components—have been employed (Castro-Muñoz, 2020). Nevertheless, there are often trade-offs between cost, complexity, and performance due to these improvements. Resolving these obstacles is essential to progressing the field, especially in pressure-resistant, robust, and standalone organic membrane advancement, which is still an active area of membrane science and technology research (Farahbakhsh *et al.,* 2021).

A composite membrane with several advantages has been created by combining epoxidized natural rubber (ENR) and polyvinyl chloride (PVC). This composite's hybrid structure of plastic and rubber makes it possible to create a freestanding single-layer membrane that does not require support material. This membrane differs from other composites due to the strength and flexibility of rubber and the porous nature of PVC plastic (Norfarhana *et al.,* 2022). The porosity of PVC and the strength and flexibility of rubber work together to enhance the overall functionality of the ENR/PVC composite membrane. While the PVC plastic contributes porosity—which is necessary for filtration applications—the rubber component provides flexibility and durability (Ismail *et al.,* 2015).

Nevertheless, treating wastewater with a high oil content can be less successful when using the ENR/PVC composite alone. Methyl methacrylate (MMA) can be grafted onto cellulose to enhance membrane performance in water-oil filtration (Shamsuddin *et al.,* 2013). This alteration boosts the membrane's hydrophobicity and creates sufficient porosity for effective water and oil separation. This research aims to understand the chemical and morphological properties of ENR/PVC/Cell-g-PMMA membrane to develop an effective membrane for oil-water separation. Inside chemical properties analysis, FTIR was used to determine how the functional group affects bond breaking and formation of new bonds in the graft copolymerization reaction of modified cellulose. Furthermore, this study focuses on identifying the relationship between surface morphology and pore formation during the fabrication of membranes. This characteristic is very important to boost the membrane's hydrophobicity and porosity, resulting in a more effective membrane for water-oil separation applications.

MATERIALS AND METHODS

Materials from several sources are used in the production of ENR/PVC thin films with cell-g-PMMA filler. Epoxidized natural rubber with 50 % epoxidation level (ENR50) was supplied by Guthrie Polymer Ltd., Thailand. High molecular weight polyvinyl chloride (PVC 97000), tetrahydrofuran (THF), and methyl methacrylate (monomer) were purchased from Sigma Aldrich, Germany. As previously documented, the Technical Association of the Pulp and Paper Industry (TAPPI) method was used to extract cellulose from pineapple leaves. Following the protocol previously described in the literature, this extracted cellulose is then functionalized with PMMA by graph-copolymerization (Figure 1A) (Shamsuddin *et al.,* 2013).

Development of ENR/PVC Thin Films

The thin film manufacturing process consists of two main stages: matrix preparation and thin film molding. The ENR/PVC matrix was prepared using a solution mixing process. Epoxidized natural rubber (ENR) was dissolved in THF to produce a homogenous solution. 6 g of ENR was soaked overnight in 80 mL of THF, agitated until homogeneous, then mixed with 4 g of powdered polyvinyl chloride. The mass ratio of ENR to PVC was 60:40, whereas the ratio of matrix to THF solvent was 1:8 (Ismail *et al.,* 2020).

Phase reversal and solution moulding were used to generate the ENR/PVC/Cell-g-PMMA thin film. 10% Cell-g-PMMA fillers were introduced to a homogenous ENR/PVC matrix solution during the solution moulding process to examine their effects on the thin film properties. To make sure the fillers were dispersed equally, the mixture was stirred. After that, the solution was poured onto a glass surface and smoothed with a 0.035 mm-thick casting knife.

Reversing a liquid phase into a solid state is known as phase reversal. To remove the THF solvent and enable the creation of the ENR/PVC/Cell-g-PMMA thin film, the leveled solution was rapidly evaporated and then immersed in distilled water. Before being removed from the glass plate and allowed to dry at room temperature until sufficiently mature for additional analysis, the membrane was allowed to finish phase reversal for about ten minutes (Mod *et al.,* 2019).

Characterization of Filler and ENR/PVC Thin Films

A Perkin Elmer Fourier Transform Infrared Spectroscope Spectrum 400 FTIR/FT-NIR equipped with a Spotlight 400 Imaging System was used to examine the interaction between the filler and the membrane matrix. The functional groups showing how the filler interacts with the matrix were found using this technique. Using a Leo 1450 VP model Scanning Electron Microscope (SEM) running at 15 kV, the morphology, texture, and interaction of the thin films with filler were investigated. The preparation of the samples involved putting them on conductive adhesive tape, gold sputter-coating, and VPSEM observation. All the characterization methods were followed by Shamsuddin *et al.* (2013).

RESULTS AND DISCUSSION

Chemical Interaction and Grafting Mechanisms

The chemical interaction of filler and matrix was analyzed by using peak intensities of certain functional groups in the sample. Figure 1A shows the FTIR spectrum of Cell, Cell-g-PMMA, ENR/PVC metrics, and ENR/PVC/Cell-g-PMMA. The absorption peak between 3300 - 3400 cm^{-1} refers to the vibrational stretching of hydroxyl groups, -OH, and hydrogen bonds that exist between cellulose molecules (Rosa et *al.* 2010), as well as the water absorption peak (Mohd *et al.,* 2021). While the absorption peak around 1650-1630 cm^{-1} refers to the stretching of the –OH group from cellulose (Sheltami *et al.,* 2012). Note that the -OH intensity of cell-g-PMMA was slightly decreased compared to cellulose due to the transformation of the -OH stretching bond into the ester carbonyl group.

The grafting process of cellulose and PMMA was successful due to the formation and transformation of a few functional groups. The peak 1736 cm^{-1} refers to the stretching vibration of ester carbonyl, C=O bond, belonging to PMMA that grafted onto the cellulose backbone (Sheltami *et al.,* 2012). The formation of the aldehyde (HC=O) functional group was detected by the stretching vibration of the CH bonding at 2776 cm^{-1}. Transformation of the C-C bond into HC=O and C-OH initiated by Ce (IV), preferably at the C_2-C_3 glycol unit by graft polymerization, occurred during the initiation and propagation step as described in Figure 1B.

The absorption spectral features observed within the wavenumber range of 3000-2000 cm^{-1} across all membrane spectra were indicative of CH stretching vibrations. Specifically, the peak at 1450 cm^{-1} corresponded to CH bending modes within the thin film, as reported by Nor *et al.* (2013). Additionally, the asymmetric and symmetric stretching vibrations of the CO functional group are characterized by an absorption peak at 1254 cm^{-1} and a range between 1110-1000 cm^{-1}, respectively. The presence of epoxy rings, C-O-C, and C-Cl bonds in ENR/PVC compounds was signified by absorption peaks at 876 cm^{-1} and 699 cm^{-1}, as suggested by Ismail *et al.* (2015), Nor *et al.* (2016) and Jon *et al.* (2017).

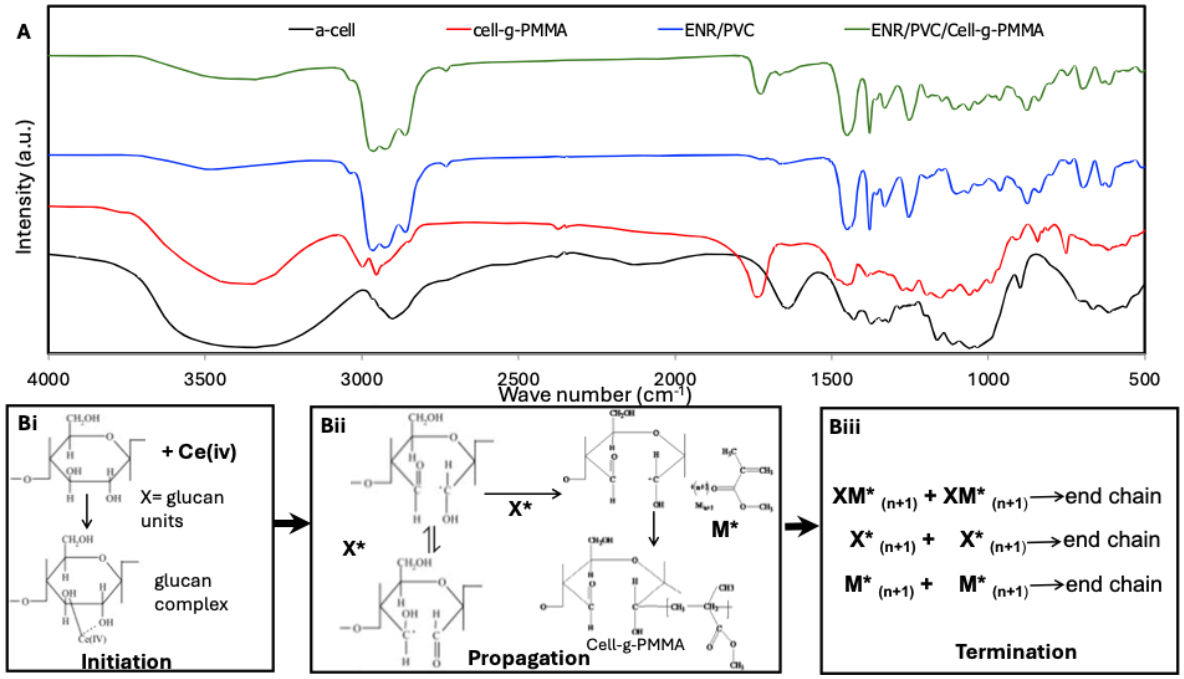

Figure 1. A) FTIR spectra; and B) Grafting of cellulose and PMMA.

Surface Morphology and Textural Properties

Surface morphology and pore production on the fillers and membrane were assessed by analyzing the morphological and textural features. The resulting micrographs were employed as well to investigate the effects of grafting alterations and the interactions between the filler and the membrane. Figure 2i shows the top surface morphology of the cellulose filler without any modification under 5000× magnification. Clearly, a smooth surface fiber was obtained with a fiber diameter of around 4.5 µm. Alteration by grafting polymerization of PMMA onto the cellulose backbone drastically changes the surface morphology of the fibers. The rough surface with a flaky texture was obtained in Figure 2ii with an increasing diameter of the fibers around 10 µm. These were due to grafting PMMA coated on top of the fibers' surface to give extra diameter to the modified fibers.

Membrane fabrication of ENR/PVC/Cell-g-PMMA prepared by solution casting and phase inversion method was exhibited in Figure 2iii, representing the surface area of the membrane at a magnification of 1000×. A previous study by Nor *et al.* (2016), Jon *et al.* (2017), and Norfarhana *et al.* (2017) found that the surface micrograph of the ENR/PVC membrane reveals a smooth, phase-stable, and uniform morphology with no observable pore formation on either the surface or cross-section. This indicates that the ENR/PVC blend achieves phase compatibility without requiring additional synchronization to ensure homogeneity. However, the incorporation of cell-g-PMMA filler into the ENR/PVC matrix induces notable alterations in both the surface morphology and the cross-sectional structure of the membrane. Following the introduction of cell-g-PMMA filler, the membrane surface exhibited the formation of fine pores, which transitioned the previously smooth and uniform surface of the ENR/PVC to a more textured appearance. Although the membrane surface became slightly irregular, the cross-sectional view did not reveal any translucent pores. Additionally, the cross-sectional analysis (Figure 2iv) of the membrane revealed the formation of pores between the filler and the membrane, as well as between individual filler particles. The interactions at the interface between the membrane and the filler, as well as among the filler particles themselves, contributed significantly to the increased development of these pores within the membrane.

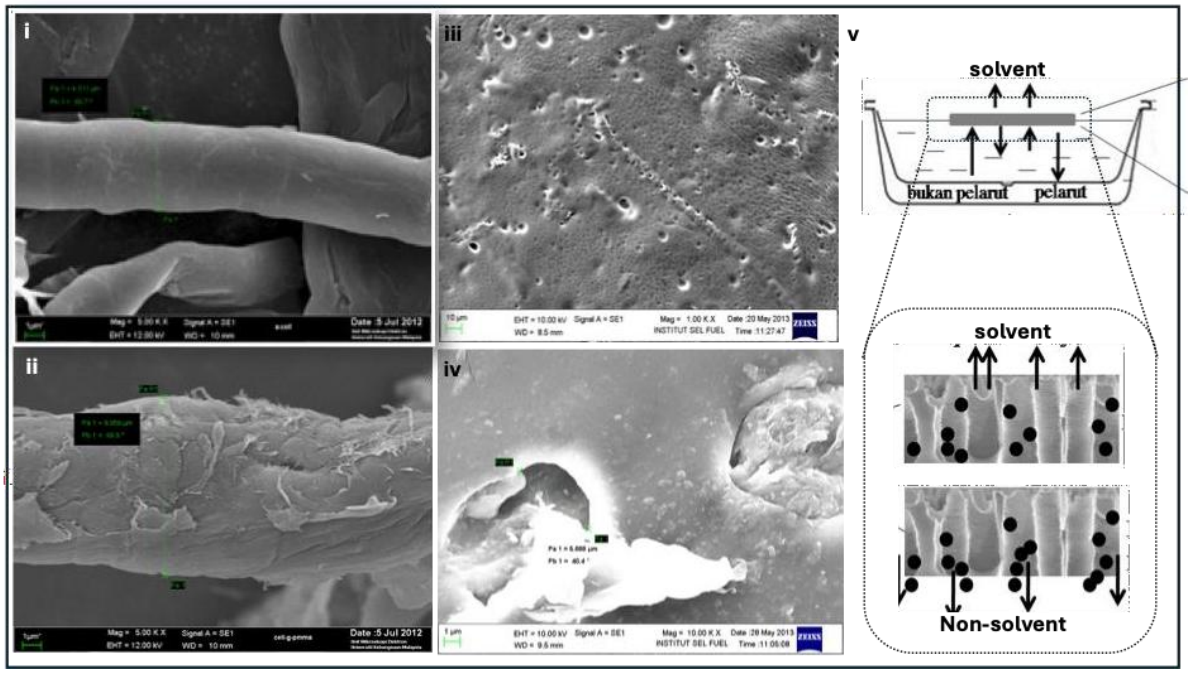

Figure 2. VPSEM micrograph and phase inversion method.

DISCUSSION

Grafting Mechanisms

Graft copolymerization of cellulose involves the synthesis of synthetic polymer branches (grafts) that impart specific characteristics to the cellulose while preserving its inherent properties. Through this modification process, new functional attributes are introduced to the cellulose, enhancing its performance without compromising its original features. The graft polymerization reaction between cellulose and methyl methacrylate monomer, which yields Cell-g-PMMA, is initiated by cerium ammonium nitrate (CAN). The proposed schematic of the three-step grafting reaction process—initiation, propagation, and termination—is depicted in Figure 1B. The mechanisms were inspired by Kumar *et al.* (2011).

For methyl methacrylate to graft polymerize onto cellulose, nitric acid is an essential ingredient. Cerium ions react with nitric acid in aqueous solutions as shown by the following equations:

$$Ce^{4+} + H_2O \rightarrow Ce\ (OH)_3{}^{3+} + H^+ \quad (1)$$

$$2Ce(OH)_3{}^{3+} \rightarrow Ce\text{-}O\text{-}Ce^{6+} + H_2O \quad (2)$$

In aqueous solutions, cerium ions can exist in the forms of Ce^{4+}, $Ce\ (OH)_3{}^{3+}$, and $Ce\text{-}O\text{-}Ce^{6+}$. These species' presence depends on the concentration of nitric acid used in the reaction. The ions Ce^{4+} and $Ce\ (OH)_3{}^{3+}$ exhibit smaller sizes and are more effective in forming complexes with cellulose compared to $Ce\text{-}O\text{-}Ce^{6+}$ (Arthur *et al.,* 1966; Hermans, 1962; Kumar *et al.,* 2011). Cerium ions are also involved in the oxidation process during the termination of monomer chains, as illustrated by the following equation (Arthur *et al.,* 1966; Kumar *et al.,* 2011; Nada *et al.,* 1989):

$$Ce^{4+} + M_n{}^* \rightarrow Ce^{3+} + H^+ \quad (3)$$

Nitric acid was used to dissolve CAN and create Ce^{4+} ions during the initiation stage. A Ce^{4+}-cellulose coordination complex was then formed because of these Ce^{4+} ions attacking the hydroxyl (OH) groups on the C_2 and C_3 carbons of cellulose (Hermans, 1962). The bonding in this compound is weak and unstable. Ce^{4+} ions are used in the oxidation process of different alcohols and substrates with

hydroxyl groups when perchloric and nitric acids are present (Hermans, 1962; Kedzior *et al.,* 2016; Wohlhauser *et al.,* 2020). Subsequent investigation indicates that the hydroxyl group at C_6 and the glycol C_2-C_3 locations are the main locations where free radicals originate (Hermans, 1962; Nada *et al.,* 1989). The diol group oxidizes six times faster at the glycol C_2-C_3 than it does at the hydroxyl C_6, according to a study on the relative oxidation rates of the two groups. This shows that the glycol C_2-C_3 locations exhibit the most $[Ce]^{4+}$ oxidation, with very little reaction taking place at the main hydroxyl group C_6 (Boujemaoui *et al.* 2019).

The complex then reduces to Ce^{3+} ions, which causes free radicals to be produced at the C_2 or C_3 locations of the glucan repeat units. This starts the propagation stage (Arthur *et al.,* 1966; Nada *et al.,* 1989). The graft polymerization process is then started when the free radicals react with the vinyl monomers that are in the reaction mixture. These free radicals target the double bonds ($-C=CH_3$) in the methyl methacrylate monomer, leading to the formation of new bonds. Free radical transfer also occurs within the methyl methacrylate chain, resulting in the formation of polymethyl methacrylate. The free radical attack continues, facilitating chain extension until the polymerization reaches the chain termination phase. Chain termination is achieved when the free radicals interact with each other, producing a neutral polymer.

FTIR spectrum of cellulose and Cell-g-PMMA proves that the bond breaking and new bond formation during the propagation step occurred. Decreasing intensity of the OH functional group of PMMA compared to cellulose shows the formation of Ce^{4+}-cellulose coordination complex, which attacks the OH functional group mainly at the C_2 and C_3 positions. Furthermore, the formation of an aldehyde functional group (HC=O) during the bond breaking of the C_2-C_3 position and the existence of the ester carbonyl group, C=O, from PMMA grafted on the cellulose backbone.

Relationship Between Textural Properties and Pore Formation

The pore formation in ENR/PVC/Cell-g-PMMA membrane can be attributed to three principal mechanisms. Firstly, pore formation occurs during the phase inversion process involved in membrane production. During this phase, solvent evaporation from the membrane surface, coupled with the substitution of part of the solvent by water (a non-solvent), leads to pore creation (Lalia *et al.,* 2013). Post-drying, the residual water vaporizes, resulting in the formation of fine pores. Figure 2v illustrates this phase inversion mechanism, highlighting solvent evaporation and non-solvent replacement as critical factors in pore generation. As solvent evaporation and water substitution proceed, the mixture undergoes a transition to a solid phase during aging, leading to the formation of pores as the remaining water evaporates (Mod *et al.,* 2019).

The second mechanism involves the interfacial interactions between the filler and the polymer matrix. Effective filler-polymer interactions ensure that the filler particles are uniformly coated with the ENR/PVC mixture. Conversely, poor interactions create gaps between the filler and the matrix, which manifest as functional pores within the thin film. Micrographs (Figure 2) provided proof of this phenomenon, showing that insufficient interaction between the cellulose filler and the ENR/PVC matrix resulted in pores that were unevenly distributed and sized (Shamsuddin *et al.,* 2013). The third process concerns the interactions between the filler particles in the matrix. Particles agglomerate when filler concentration rises, forming filler clusters. These clusters are close to one another, which causes spaces between them to form pores (Nor *et al.,* 2016). Increased filler content makes these agglomerations more likely, which increases the pore size of the membrane and its porosity.

CONCLUSION

Critical information about the mechanisms of graft copolymerization and pore formation is provided by the surface morphology and chemical properties of the filler (cell-g-PMMA) and the ENR/PVC/Cell-g-PMMA membrane. The ester carbonyl (C=O) group of PMMA and the formation of aldehyde (HC=O) functional groups, indicated by the stretching vibration of CH bonds at 2776 cm^{-1} and an absorption

peak at 1736 cm^{-1}, respectively, were detected by FTIR spectroscopy as proof of the successful grafting of PMMA onto the cellulose backbone. VPSEM showed that grafting PMMA onto cellulose resulted in rough, flaky surface roughness and an increase in fiber diameter from about 4.5 μm to 10 μm. The addition of cell-g-PMMA filler to the ENR/PVC matrix caused the membrane's surface to become more textured as tiny pores began to form. Pores were found within and between filler particles as well as between the filler and the membrane matrix, according to cross-sectional examination. The improved pore development within the membrane was largely caused by interactions at the interfaces between the filler, the membrane, and the filler particles. All things considered, the grafting of PMMA onto cellulose and its incorporation into the ENR/PVC membrane changed the chemical composition and surface morphology, leading to a rise in porosity.

ACKNOWLEDGEMENT

This research was funded by a grant from Skim Penyelidikan Lantikan Baru, Universiti Malaysia Sabah (SLB 2252).

REFERENCES

Arman Alim, A.A. & Othaman, R. 2018. Epoxidized natural rubber/polyvinyl chloride/microcrystalline cellulose (ENR/PVC/MCC) composite membrane for palm oil mill effluent (POME) treatment. *Sains Malaysiana*, 47(7): 1517–1525. https://doi.org/10.17576/jsm-2018-4707-20.

Arthur, J.C., Baugh, P.J. & Hinojosa, O. 1966. ESR study of reactions of cellulose initiated by the ceric ion method. *Journal of Applied Polymer Science*, 10(10): 1591–1606. https://doi.org/10.1002/app.1966.070101015.

Boujemaoui, A., Ansari, F. & Berglund, L.A. 2019. Nanostructural effects in high cellulose content thermoplastic nanocomposites with a covalently grafted cellulose-poly(methyl methacrylate) interface. *Biomacromolecules*, 20(2): 598–607. https://doi.org/10.1021/acs.biomac.8b00701.

Castro-Muñoz, R. 2020. The role of new inorganic materials in composite membranes for water disinfection. *Membranes*, 10(5). https://doi.org/10.3390/membranes10050101

Farahbakhsh, J., Vatanpour, V., Khoshnam, M. & Zargar, M. 2021. Recent advancements in the application of new monomers and membrane modification techniques for the fabrication of thin film composite membranes: A review. *Reactive and Functional Polymers*, 166: 105015. https://doi.org/10.1016/j.reactfunctpolym.2021.105015

Ismail, N.F.H., Abdullah, I., Daik, R., Ahmad, I., Jamil, S., Lazim, M. A. M. & Othaman, R. 2015. Effect of radiation on properties of ENR/PVC/SiO_2 membrane. *AIP Conference Proceedings*, 1678. https://doi.org/10.1063/1.4931308

Ismail, N.F.H., Chai, T. M., Daik, R. & Othaman, R. 2020. Epoxidised natural rubber (ENR)/polyvinyl chloride (PVC)/silica (SiO_2) membrane for treating palm oil mill effluents (POME). *Plastics, Rubber and Composites*, 49(3): 134–140. https://doi.org/10.1080/14658011.2020.1718323

Hermans, J.J. 1962. Chemical mechanisms in the grafting of cellulose. *Pure and Applied Chemistry*, 5(12): 147–164.

Jon, N., Abdullah, N. A. & Othaman, R. 2017. Effects of silica composition on gas permeability of ENR/PVC membrane. *Journal of Fundamental and Applied Science*, 9(6S): 632–641. https://doi.org/10.4314/jfas.v9i6s

Kedzior, S.A., Graham, L., Moorlag, C., Dooley, B.M. & Cranston, E.D. 2016. Poly(methyl methacrylate)-grafted cellulose nanocrystals: One-step synthesis, nanocomposite preparation, and characterization. *Canadian Journal of Chemical Engineering*, 94(5): 811–822. https://doi.org/10.1002/cjce.22456

Kumar, V., Naithani, S. & Pandey, D. 2011. Optimization of reaction conditions for grafting of α-cellulose isolated from *Lantana camara* with acrylamide. *Carbohydrate Polymers*, 86(2): 760–768. https://doi.org/10.1016/j.carbpol.2011.05.019

Lalia, B.S., Kochkodan, V., Hashaikeh, R. & Hilal, N. 2013. A review on membrane fabrication: Structure, properties and performance relationship. *Desalination*, 326: 77–95. https://doi.org/10.1016/j.desal.2013.06.016

Mod, N., Hannan Anuar, F. & Othaman, R. 2019. Solution casting epoxidized natural rubber/poly(vinylidene fluoride) membrane for palm oil effluent treatment. *Malaysian Journal of Analytical Sciences*, 23: 725–735. https://doi.org/10.17576/mjas-2019-2304-19

Mohd, N.H., Kargazadeh, H., Miyamoto, M., Uemiya, S., Sharer, N., Baharum, A., Lee Peng, T., Ahmad, I., Yarmo, M. A. & Othaman, R. 2021. Aminosilanes grafted nanocrystalline cellulose from oil palm empty fruit bunch aerogel for carbon dioxide capture. *Journal of Materials Research and Technology*, 13: 2287–2296. https://doi.org/https://doi.org/10.1016/j.jmrt.2021.06.018

Nada, A.M.A., El-Kalyoubi, S.F. & El-Roweiny, I.A. 1989. Methylmethacrylate grafting onto cotton stalk pulp. *Polymer-Plastics Technology and Engineering*, 28(4): 439–451. https://doi.org/10.1080/03602558908048607

Nor, F. M., Abdullah, I. & Othaman, R. 2013. Gas permeability of ENR/PVC membrane with the addition of inorganic fillers. *AIP Conference Proceedings*, 1571, 911–917. https://doi.org/10.1063/1.4858770

Nor, F.M., Karim, N.H.A., Abdullah, I. & Othaman, R. 2016. Permeability of carbon dioxide and nitrogen gases through SiO_2 and MgO incorporated ENR/PVC membranes. *Journal of Elastomers and Plastics*, 48(6): 483–498. https://doi.org/10.1177/0095244315580459

Norfarhana, A.S., Ilyas, R.A., Ngadi, N., Sharma, S., Sayed, M.M., El-Shafay, A.S., & Nordin, A.H. 2022. Natural fiber-reinforced thermoplastic ENR/PVC composites as potential membrane technology in industrial wastewater treatment: a review. *Polymers*, 14(12).

Norfarhana A.S., Jon, N., Abdullah, I., Samad, N.A., Shah, A., Lazim, M. & Othaman, R. 2017. Preparation of ENR/PVC/RH composite membrane for water permeation application extraction of bioactive compounds from plant bioresources view project composite membrane view project preparation of ENR/PVC/RH composite membrane for water permeation application. *Advanced Journal of Technical and Vocational Education*, 1(1): 20–30.

Shamsuddin, M. R., Abdullah, I. & Othaman, R. 2013. Celluloses filled ENR/PVC membranes for palm oil mill effluent (POME) treatment. *AIP Conference Proceedings*, 1571, 897–903.

Shamsuddin, M.R., Fauzee, S.N., Anuar, F.H., Abdullah, I. & Othaman, R. 2013. Modification of cellulose by polymethyl methacrylate grafting for membrane applications. *Jurnal Teknologi (Sciences & Engineering)*, 2(65): 47–53.

Sheltami, R.M., Abdullah, I., Ahmad, I., Dufresne, A. & Kargarzadeh, H. 2012. Extraction of cellulose nanocrystals from mengkuang leaves (*Pandanus tectorius*). *Carbohydrate Polymers*, 88(2): 772–779.

Wohlhauser, S., Kuhnt, T., Meesorn, W., Montero De Espinosa, L., Zoppe, J. O. & Weder, C. 2020. One-component nanocomposites based on polymer-grafted cellulose nanocrystals. *Macromolecules*, 53(3): 821–834. https://doi.org/10.1021/acs.macromol.9b01612

RESEARCH ARTICLE

BORNEO SCIENCE
THE JOURNAL OF SCIENCE & TECHNOLOGY

Journal homepage: https://jurcon.ums.edu.my/ojums/index.php/borneo-science

SUSTAINABLE THE IMPACT OF INDOOR AIR QUALITY ON OCCUPANCY STRESS LEVEL IN WARSHIP: SYSTEMATIC LITERATURE REVIEW

Muhammad Hisham Abdul Halim*, Asmat Ismail, and Siti Rasidah MD Sakip

Faculty of Built Environment, UiTM Seri Iskandar Perak, Malaysia.

***Correspondence:**
hisham4877@gmail.com

Received: 2 September 2025
Revised: 24 December 2025
Accepted: 24 December 2025
Published online: 31 December 2025

Doi:
10.51200/bsj.v46i2.6775

Keywords:
Indoor Air Quality; Systematic Literature Review; Occupancy Stress Level; Self-Efficacy
.

ABSTRACT. *Indoor air quality (IAQ) plays a critical role in influencing the health, comfort, and psychological performance of individuals operating in enclosed and confine space such as warships. However, research regarding the impact of IAQ on occupancy stress levels in warships remains challenging due to the limited number of studies. Therefore, this study aims to conduct a systematic literature review on the impact of IAQ on stress levels among warship crews. The methodology is based on a systematic literature review that employs the Preferred Reporting Items for Systematic Reviews and Meta-Analyses (PRISMA). A comprehensive search was conducted across Scopus, Google Scholar, Web of Science, ProQuest, and ScienceDirect databases, covering literature published between 2019 and 2025. The review process includes three main methodological steps: identification, screening, and eligibility, followed by the PRISMA checklist. Three key themes were found: (a) IAQ– physical parameter and indoor air contaminant, (b) Self-efficacy– vicarious experience and performance outcomes, and (c) Stress – response and trigger. A factor analysis confirmed the validity of the thematic structure and reinforced the interconnection between environmental conditions and psychological outcomes. The findings provide valuable knowledge gaps for future studies. This review supports Environmental, Social, and Governance (ESG) principles by advocating for sustainable and health-centric practices in the maritime environment.*

INTRODUCTION

Indoor air quality (IAQ) has increasingly been recognized as a critical component of human health, cognitive function, and psychological well-being, especially in enclosed environments such as warships. Naval vessels, by design, operate in confined and isolated conditions with limited ventilation, recycled air systems, and shared living quarters, factors that amplify the potential exposure to airborne pollutants (Al-Mamun *et al.,* 2022).

In such settings, IAQ not only affects physical health but may also act as an environmental stressor that contributes to elevated psychological stress levels among naval personnel (Chen, 2023). Military operations often subject crew members to long-term confinement, strict routines, and high-stakes missions. These operational demands, when combined with poor IAQ, may heighten stress responses, impair decision-making, and reduce occupational performance (Yusof, 2021). While existing literature has addressed the influence of IAQ in residential, educational, and healthcare settings (Khan, 2022; Zhang, 2020), studies specific to warship environments remain limited. This gap is concerning, as warships present unique environmental stressors that are not directly comparable to land-based

facilities. which is known as re-suspension. When this happens, the compound or pollutant that is trapped in the sediment will be remobilized (Lick, 2009).

Furthermore, the psychological resilience and well-being of naval personnel have strategic implications, affecting both individual mental health and overall operational readiness. Proactively managing environmental stressors, including air quality, is essential in supporting mission effectiveness and reducing long-term occupational health risks (Lim, 2021). To address these concerns, this study presents a systematic literature review (SLR) aimed at evaluating the relationship between IAQ and stress levels in warship settings. This review follows the Preferred Reporting Items for Systematic Reviews and Meta-Analyses (PRISMA) 2020 framework (Page, 2021) to ensure a transparent and replicable methodology. The search strategy focused on peer-reviewed literature published between 2019 and 2025 across multiple databases, including Scopus, Web of Science, Google Scholar, ScienceDirect, and ProQuest. The findings of this review not only highlight key IAQ indicators and psychological outcomes but also contribute to the development of a conceptual framework grounded in Social Cognitive Theory to explore mediating factors such as self-efficacy. Ultimately, this study supports sustainable naval operations and aligns with Environmental, Social, and Governance (ESG) goals by advocating for improved air quality monitoring and stress mitigation strategies in maritime defense environments.

METHODS

This study employed an SLR methodology to identify and synthesize existing research on the relationship between IAQ and occupancy stress levels in warship environments. The review process adhered to the PRISMA 2020 guidelines (Page, 2021), ensuring transparency, replicability, and methodological rigor.

Systematic Search Strategy

A comprehensive search was conducted across multiple databases, including Scopus, ScienceDirect, ProQuest, Web of Science (WoS), and Google Scholar, to retrieve relevant peer-reviewed and grey literature published between 2019 and 2025. The selection of these databases was based on their multidisciplinary coverage and credibility, in line with best practices for systematic reviews (Haddaway, 2015; Kounadi, 2020).

The literature search combined elements of both traditional and systematic review approaches to identify knowledge gaps in the current body of research. Boolean operators (e.g., AND, OR), truncation, and phrase searching were used to formulate the search strings. The primary keywords included “indoor air quality,” “warship,” “crew stress,” and “self-efficacy,” along with their related synonyms (e.g., "indoor air contaminant," "vicarious experience," "performance outcome"). Table 1 details the complete keyword mapping and Boolean combinations used.

This hybrid search method was critical for capturing a broad yet focused pool of literature while minimizing bias. There is no specific tool to reduce the risk of bias in this study. Following the identification stage, studies were screened and assessed for eligibility based on predefined inclusion and exclusion criteria. These criteria included language (English only), publication date (2019–2025), peer-reviewed status, and relevance to the themes of IAQ, stress, and naval or maritime environments.

Table 1. Selected Database Used for the Search String

Database	String
Scopus	TITLE-ABS-KEY ((“warship” OR “indoor air quality” OR “maritime” OR “indoor air contaminant” OR “physical parameter”) AND (“crew stress” OR “stress triggered” OR “stress response” OR “stress confined space”) AND (“self-efficacy naval” OR “vicarious experience” OR “performance outcome”))
Science Direct	((“warship” OR “indoor air quality” OR “maritime” OR “indoor air contaminant” OR “physical parameter”) AND (“crew stress” OR “stress triggered” OR “stress response” OR “stress confined space”) AND (“self-efficacy naval” OR “vicarious experience” OR “performance outcome”))
Google Scholar	allintitle: ((“warship” OR “indoor air quality” OR “maritime” OR “indoor air contaminant” OR “physical parameter”) AND (“crew stress” OR “stress triggered” OR “stress response” OR “stress confine space”) AND (“self-efficacy naval” OR “vicarious experience” OR “performance outcome”))
ProQuest	((“warship” OR “indoor air quality” OR “maritime” OR “indoor air contaminant” OR “physical parameter”) AND (“crew stress” OR “stress triggered” OR “stress response” OR “stress confined space”) AND (“self-efficacy naval” OR “vicarious experience” OR “performance outcome”))
WoS	TS= ((“warship” OR “indoor air quality” OR “maritime” OR “indoor air contaminant” OR “physical parameter”) AND (“crew stress” OR “stress triggered” OR “stress response” OR “stress confined space”) AND (“self-efficacy naval” OR “vicarious experience” OR “performance outcome”))

PRISMA Flow Diagram

The PRISMA flow diagram was employed to visually present the literature selection process (Page, 2021). The diagram illustrates the systematic flow of articles through four distinct phases: identification, screening, eligibility, and inclusion. This visual tool enhances methodological transparency and provides readers with a clear overview of how studies were selected and filtered for inclusion in the review.

1) Identification Phase: This phase involved searching databases and repositories using tailored search strings. A total of 3,774 records were retrieved during this initial search stage. Synonym expansion and keyword refinement were conducted to increase search accuracy (Mohamed, 2020).

2) Screening Phase: Duplicate records were removed, and titles and abstracts were reviewed to exclude irrelevant studies. Articles published before 2019 were also excluded at this stage to maintain relevance.

3) Eligibility Phase: Full-text articles were assessed against the inclusion criteria. Studies unrelated to warship environments or those lacking empirical IAQ or stress measurements were excluded. Specific reasons for exclusion were documented to ensure transparency.

4) Included Phase: A total of 37 studies met the eligibility criteria and were included in the final synthesis. These studies were reviewed in detail and incorporated into the conceptual framework. To ensure the validity and reliability of the review process, a quality appraisal of all included studies was conducted. Studies were assessed based on clarity of research design, relevance to the review objectives, and methodological soundness. The use of multiple databases, keyword expansion, and systematic filtering helped minimize selection bias (Kounadi, 2020).

PRISMA Checklist

The PRISMA 2020 Checklist was used as a reporting framework to guide the development of the review (Page, 2021). The checklist comprises 27 items covering key sections of the review, including the title,

abstract, introduction, methods, results, discussion, and funding. Each item ensures comprehensive reporting to facilitate transparency, reproducibility, and evidence-based synthesis.

1) Title and Abstract: Clearly identify the study as a systematic review and summarize the review scope, methods, and key findings.

2) Introduction: Clearly state the review's rationale, objectives, and research questions.

3) Methods: Report the eligibility criteria, data sources, selection process, and search strategy.

4) Results: Provide detailed outcomes of the selection process, study characteristics, and synthesized findings using narrative and tabular formats.

5) Discussion: Address major findings, limitations, and implications for future research and practice.

6) Funding: Disclose any funding sources and potential conflicts of interest.

By adhering to the PRISMA framework, this study enhances the transparency and rigor of the systematic review process, ensuring that the findings contribute meaningfully to the literature on IAQ and psychological well-being in warship environments.

RESULTS AND DISCUSSIONS

This systematic review analyzed 37 selected studies to explore the relationship between IAQ, self-efficacy, and crew stress aboard warships. Using the PRISMA method, studies were screened, evaluated, and categorized into key themes and sub-themes. A validated factor analysis confirmed three core components: IAQ, self-efficacy, and stress. The findings guided the development of a conceptual framework grounded in Social Cognitive Theory, emphasizing the mediating role of self-efficacy in linking environmental conditions to psychological outcomes among naval personnel.

PRISMA Flow Diagram Result

The PRISMA flow diagram, summarized in Figure 1, outlines the four key phases: identification, screening, eligibility, and inclusion. During the Identification Phase, a total of 3,774 records were retrieved from major academic databases: Scopus (n = 161), ScienceDirect (n = 629), Google Scholar (n = 429), ProQuest (n = 1,843), and Web of Science (n = 712). After removing 924 duplicate records, 2,850 records remained for screening.

In the Screening Phase, all 2,850 records were assessed based on titles and abstracts. A total of 2,710 records were excluded for irrelevance, and 140 full-text articles were selected for detailed evaluation. However, seven articles could not be retrieved, leaving 133 full-text articles for eligibility assessment, including population involving seafarers, IAQ element, persistent stress scales, and any related to self-efficacy.

During the Eligibility Phase, these 133 articles were reviewed in detail. The following were excluded: (a) Studies not conducted in ship or maritime settings (n = 60), (b) Articles targeting non-naval populations (n = 24), (c) Studies employing non-quantitative methodologies (n = 12).

This process resulted in 37 studies that met the full inclusion criteria and were included in the final review. This rigorous multi-step approach enhances the validity and reproducibility of the review, consistent with PRISMA's objectives of improving reporting transparency in systematic reviews (Liberati, 2020; Page, 2021).

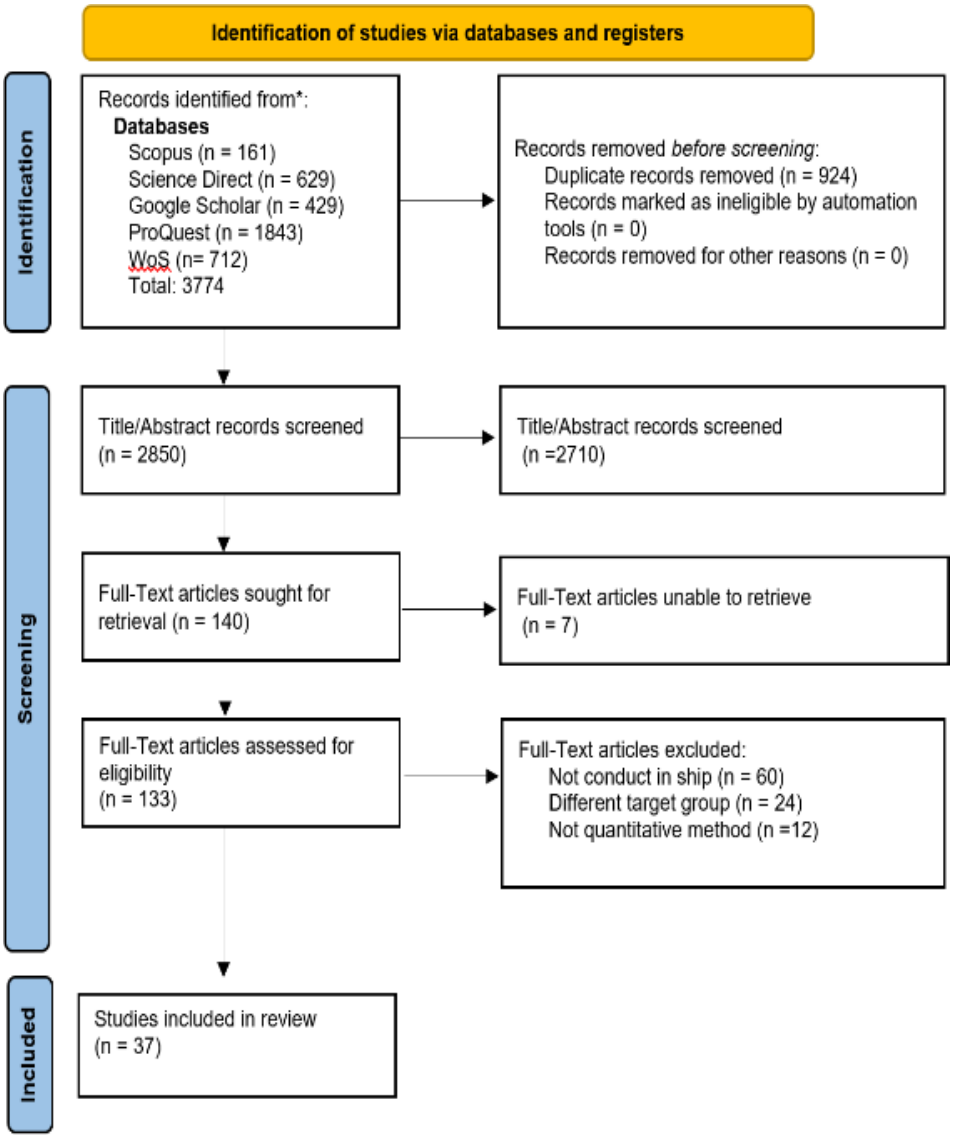

Figure 1. PRISMA flow diagram.

PRISMA Check List Result

The 37 studies paper included in this systematic review were assessed using the PRISMA 2020 Checklist, which is listed in Table 1 encompasses five major domains: title, abstract and introduction; methods; results; discussion; and other relevant information. This evaluation aimed to determine the extent to which each study adhered to the recommended standards for transparent and rigorous reporting in systematic reviews.

Table 1. Table for the summary of the 27 PRISMA checklist.

Group	Item No.	Keyword Checklist Item	Reported (n)	Percentage (%)
Title, Abstract & Introduction	1	Title as literature review	20	54.05%
	2	Structured abstract	22	59.46%
	3	Rationale for review	34	91.89%
	4	Stated objectives (PICOS)	30	81.08%
Methods	5	Eligibility criteria	24	64.86%
	6	Info sources used	18	48.64%
	7	Search strategy	27	72.97%
	8	Selection process	21	56.76%
	11	Risk of bias assessment	20	54.05%
Results	16a	Study selection (e.g., PRISMA flow)	15	40.54%
	16b	Excluded studies with reason	20	54.05%
	17	Study characteristics	18	48.64%
	18	Bias results per study	6	16.21%
	19	Individual study results	29	78.38%
Discussion	23a	Interpretation of findings	14	37.84%
	23b	Evidence limitations	8	21.62%
	23c	Review process limitations	29	78.38%
	23d	Practice/research implications	28	75.68%
Other Information	24a	Review registration info	9	24.32%
	24b	Protocol access	8	21.62%
	24c	Amendments to protocol	21	56.76%
	25	Support/funding info	11	29.73%
	26	Competing interests	8	21.62%
	27	Data/material availability	4	10.81%

Title, Abstract, and Introduction

The analysis revealed that 54.05% (n = 20) of the studies explicitly included both the terms "indoor air quality" and "stress" in their titles, while the remainder omitted one or both keywords. A total of 59.45% (n = 22) of the abstracts were found to be well-structured and clearly outlined the research methodologies, reflecting good adherence to reporting guidelines. Moreover, 81.08% (n = 30) of the studies articulated their research questions using the PICOS framework, an essential component in systematic review design that covers population, intervention, comparison, outcomes, and study design. Importantly, 91.89% (n = 34) of the studies provided a strong rationale and justification for conducting the review, demonstrating an understanding of the research problem's relevance and significance.

Methods

In the methods section, 56.75% (n = 21) of the studies presented clear inclusion and exclusion criteria for study selection, while 48.64% (n = 18) identified the specific databases, registers, and sources used to collect information. A total of 72.97% (n = 27) of the papers provided a detailed description of the search strategy used for each database, including keywords and Boolean logic, enhancing the transparency and reproducibility of the literature search process. However, only 56.75% (n = 21) reported a controlled selection process that included detailed eligibility screening. Consideration of study bias was identified in 54.05% (n = 20) of the papers, indicating room for improvement in the methodological quality appraisal across the reviewed literature.

Results

Regarding the results domain, only 40.54% (n = 15) of the studies included a clearly presented flow diagram to visually depict the literature screening and selection process, despite its importance in communicating systematic review procedures. Surprisingly, just 50.05% (n = 2) of the studies provided a complete justification for study inclusion or exclusion decisions, with appropriate citations and reasoning. Approximately 48.64% (n = 18) of the studies reported detailed characteristics of the included studies, such as sample sizes, study designs, or follow-up periods. Alarmingly, risk of bias assessments were conducted in only 16.21% (n = 6) of the studies, reflecting a significant methodological limitation. Nevertheless, a high proportion of the studies, 78.47% (n = 29), presented summary statistics and effect estimates for each outcome, thereby enhancing the interpretability and comparability of results across studies.

Discussion

Within the discussion section, 37.84% (n = 14) of the studies provided a comprehensive interpretation of their findings in the context of existing literature. Only 21.62% (n = 8) acknowledged limitations in the body of evidence included in their reviews. Despite this, 78.37% (n = 29) of the studies discussed the limitations of the review process itself, such as potential search bias, inclusion bias, or methodological weaknesses. Furthermore, 75.67% (n = 28) of the papers thoughtfully considered the implications of their findings for practice, policy, or future research, indicating an effort to link research evidence with practical application and decision-making contexts.

Other Information

In terms of other information, 56.75% (n = 21) of the studies documented amendments made to their protocol or research registration records, if applicable. Only 24.32% (n = 9) referenced any form of review registration, including details such as registration platform or number, while the rest either omitted or did not register their systematic review. In relation to transparency, 29.73% (n = 11) of the papers acknowledged financial or non-financial support received, and 21.62% (n = 8) disclosed any potential conflicts of interest among the authors. Finally, only 10.81% (n = 4) of the studies reported the availability of supplementary materials such as data extraction forms, datasets, or analysis codes, thereby limiting reproducibility and transparency.

Included Paper for Theme Selection

A total of 37 papers were selected for theme extraction, as outlined in Table 2. These papers were identified through the PRISMA systematic review process and represent the final pool of eligible studies. Each paper was systematically analyzed and categorized according to its focus on the three central themes of this review: IAQ, Self-Efficacy, and Crew Stress. Within these main themes, a series of sub-themes were also identified to provide more nuanced insights.

For IAQ, the sub-themes include IAQ Contaminants (such as VOCs, CO_2, and $PM_{2.5}$) and Physical Parameters (temperature, humidity, and ventilation). For Self-Efficacy, the sub-themes encompass Vicarious Experience (VE) and Performance Outcomes (PO), while Crew Stress is further examined through Stress Triggers (ST) and Stress Responses (SR). This thematic classification not only facilitates an organized synthesis of the literature but also contributes to the development of a conceptual framework linking IAQ, self-efficacy, and stress among naval personnel.

Table 2. Summary of included paper for theme selection.

No	Author	Factors Contributing to IAQ					Mediating Factor		Factor in Stress	
		IAQ Contaminant			Physical Parameter		VE	PO	ST	SR
		CO_2	CO	Temp	RH	WS				
1.	Boxer, P. (1990)	*	*	*	*	*		*		
2.	Abdul-Wahab, S.A., En, S., Elkamel, A., Ahmadi, & Yetilmezsoy, K. (2015).	*	*	*	*	*		*		
3.	Org, S. (2015)	*						*		
4.	Śmiełowska, M. & Zabiegała, B. (2017).	*	*	*	*	*		*		
5.	Wame (2019)	*	*	*	*	*		*		
6.	Xu, X. & Ou, S. (2019)		*	*	*	*		*		
7.	Kelly, F.J. & Fussell, J.C. (2019)						*	*		
8.	Mujan, Anđelk, Munćan, Kljajić, & Ružić (2019)	*	*	*	*	*		*		
9.	Khanna, Chatterjee, Goyal, Pisharody, Patra. & Sharma (2019)						*	*	*	*
10.	D., G.L. (2019)						*	*	*	*
11.	Bluyssen, P.M. (2019)	*	*	*	*	*		*		
12.	Petrowski, Bastianon, Bührer, & Brähler, (2019)	*	*	*	*	*		*	*	*
13.	David P.W. & Pawel W. (2019)						*	*	*	*
14.	Langer, Österman, Strandberg, Moldanová. & Fridén, H. (2020)	*	*	*	*	*		*		
15.	Roskams, M. & Haynes, B.P. (2020)	*	*	*	*	*		*		
16.	Saini, J., Dutta, M. & Marques, G. (2020)	*	*	*	*	*		*		
17.	Tham, Thompson, Landeg, Murray, K.A. & Waite, T. (2020).	*	*	*	*	*		*		
18.	Gawade, A., Sanap, A., Baviskar, V.S., Jahnige, R., Zhang, Q. & Zhu, T. (2020).	*	*	*	*	*		*		
19.	Kim S, & Lee. (2020)	*	*	*	*	*		*		
20.	Pinault, Thomson, Christidis. & Colman, I. (2020).	*	*	*	*	*		*	*	*
21.	Sutherland & Cooper (2020)							*	*	*
22.	Lazarus, R.S. & Folkman, S. (2020)						*	*	*	*
23.	Bellizzi, Panu Napodano, Pichierri. & Muthu, (2021)	*	*	*	*	*		*		
24.	Glaser *et al.* (2021)							*		
25.	Jo, D. & Koh, C. (2021).	*	*	*	*	*		*		
26.	Jensen, H. & Oldenburg, M. (2021)						*	*	*	*
27.	Paleologos, Selim. & Mohamed, A.O. (2021)	*	*	*	*	*		*		
28.	Metreveli, Y. (2021)	*	*	*		*				
29.	Thach, T.Q., Mahirah, D. & Sauter, C. (2022)	*	*	*		*		*	*	*
30.	Maryam Zahaba *et al.* (2022)	*	*	*		*		*		
31.	Dąbrowiecki, Z. (2022)	*	*	*		*		*		
32.	Du, B. (2022)			*				*		
33.	Qiu, X. & Danesh-Yazdi, M. (2022).			*						
34.	Weisskopf, M. (2022)			*				*		
35.	Kumar, Rana, Sharma. & Kumar (2022)	*	*	*						
36.	Schalm, Carro, Jacobs, Lazarov. & Stranger (2023)			*	*	*				
37.	Gilardi, L., Marconcini, M., Metz-Marconcini, A., Esch, T. & Erbertseder, T. (2023)	*	*	*				*	*	*

Theme Selection

The theme selection process identified three main variables, which are IAQ as the Independent Variable (IV), Self-Efficacy as the Mediating Variable (MV), and Crew Stress as the Dependent Variable (DV). Each theme is supported by relevant sub-themes: IAQ Contaminant and Physical Parameter under IAQ; Vicarious Experience and Performance Outcome under Self-Efficacy; and Stress Triggers and Stress Responses under Crew Stress.

These themes and sub-themes, derived from the SLR, are summarized in Table 3. To ensure the validity of these constructs, a factor analysis was conducted, confirming the grouping of items and reinforcing the study's variables.

Table 3. Theme considered a variable.

Theme	Sub Theme	Type of Variable
Indoor Air Quality (IAQ)	IAQ Contaminant	Independent Variable (IV)
	Physical Parameter	
Self-Efficacy	Vicarious Experience	Mediating Variable (MV)
	Performance Outcome	
Crew Stress	Stress Triggers	Dependent Variable (DV)
	Stress Responses	

Factor Analysis

To validate the selection of themes derived from the SLR, a factor analysis was conducted to identify the underlying structure among the observed variables. This statistical method is particularly useful when dealing with a large set of interrelated variables, as it reduces dimensionality by grouping variables that exhibit similar patterns of responses. In this study, factor analysis was used to confirm whether the survey items could be meaningfully categorized into the three proposed components: IAQ, Self-Efficacy, and Crew Stress Levels.

The analysis was performed using Principal Component Analysis (PCA) with Varimax rotation, a technique that facilitates clearer interpretation by maximizing the variance of loadings across factors. As suggested by Hair *et al.* (2010), the threshold for acceptable factor loading depends on the sample size. Given that the sample size for this study was fewer than 200 respondents, a minimum factor loading of 0.50 was applied to ensure that only variables with moderate to strong contributions to each component were retained for interpretation (Hair *et al.,* 2010). The results of the factor analysis, summarized in Table 4, identified three principal components, aligning with the thematic constructs identified in the literature.

Component 1: Indoor Air Quality (IAQ)

This component includes items related to indoor air contaminants and physical parameters. Factor loadings ranged from 0.510 to 0.743, with Item A4 (0.743) and Item A7 (0.643) demonstrating the highest loadings. These items are strong indicators of air quality conditions aboard warships and reinforce the validity of IAQ as a distinct construct.

Component 2: Self-Efficacy

This factor captures items associated with vicarious experience and performance outcomes, with loadings between 0.543 and 0.767. Item C5 (0.767) exhibited the strongest contribution to this factor, indicating its central role in measuring perceived self-efficacy among crew members in operational settings.

Component 3: Crew Stress Levels

The third component represents stress-related dimensions, including both stress triggers and stress responses. Loadings for this component ranged from 0.527 to 0.698, with Item F2 (0.698) having the highest factor loading, highlighting its importance in capturing the psychological stress experienced by naval personnel.

Table 4. Factor analysis table.

Construct	Dimension	Items	Component 1	2	3
IAQ	Indoor Air Contaminant	A1	.619	.176	-.214
		A2	.528	.031	-.435
		A3	.575	.107	-.167
		A4	.743	-.027	-.005
		A5	.607	-.078	.098
		A6	.571	-.143	.006
		A7	.643	-.031	.082
	Physical Parameter	B1	.603	-.117	-.247
		B2	.510	-.060	-.140
		B3	.506	-.184	-.109
		B4	.617	-.079	-.313
		B5	.547	-.076	-.106
		B6	.509	-.188	-.042
Self Efficacy	Vicarious Experience	C1	-.165	.544	.036
		C2	-.197	.694	-.316
		C3	-.207	.656	.338
		C4	-.440	.590	.302
		C5	-.214	.767	.071
	Performance Outcome	D1	-.449	.543	.339
		D2	-.161	.619	.195
		D3	-.177	.544	.098
		D4	-.036	.606	.103
		D5	-.052	.573	.225
Stress Level	Stress Response	E1	-.043	.546	.514
		E2	.130	.177	.658
		E3	-.120	.190	.593
		E4	-.473	.074	.594
		E5	-.325	.267	.684
		E6	.238	-.411	.650
	Stress Triggered	F1	.326	-.437	.551
		F2	.488	-.405	.698
		F3	-.340	-.410	.527
		F4	-.267	-.325	.618
		F5	-.447	-.415	.654

Extraction Method: Principal Component Analysis
a. 3 components extracted.

Collectively, these three components accounted for a substantial proportion of the total variance, confirming that the identified variables effectively represent distinct but interrelated constructs within the study. Notably, Component 1 (IAQ) explained the largest share of the variance, followed by Self-Efficacy and Crew Stress Levels. The outcome of the factor analysis supports the theoretical framework of the study and validates the categorization of the items into the three core themes. This empirical confirmation provides a solid foundation for further statistical analysis and reinforces the relevance of IAQ, self-efficacy, and stress as critical dimensions in understanding the well-being and performance of crew members aboard warships.

CONCLUSION

This SLR has provided a comprehensive and structured examination of the relationship between IAQ and occupancy stress levels within the confined environment, which is warships. This systematic literature review has explored the relationship between IAQ and occupancy stress levels in warship environments, revealing three core themes: IAQ, self-efficacy, and crew stress. Using the PRISMA approach and supported by factor analysis, the study confirmed that IAQ significantly impacts crew well-being. The significance of this study lies in its contribution to bridging a critical gap in maritime and military research. By focusing specifically on naval environments, this review sheds light on the effects of poor air quality in confined space ventilation systems, prolonged occupancy, and operational stressors typical of naval life at sea. Furthermore, the study contributes to a novel interdisciplinary connection that integrates environmental science, occupational psychology, and naval operations, offering valuable insights for researchers, naval architects, and defense health policymakers. In doing so, it aligns with broader ESG objectives by advocating for health-centric, sustainable practices within the defense sector.

Based on the findings, several key recommendations are proposed. From an operational standpoint, it is imperative that naval organizations invest in routine monitoring and assessment of IAQ aboard ships, employing advanced filtration systems and real-time sensors to detect contaminants. Additionally, ship design and retrofitting initiatives should incorporate IAQ-enhancing engineering solutions, including improved ventilation systems and environmental feedback systems. From a research perspective, there is a need for more empirical, field-based studies that directly measure IAQ and psychological outcomes aboard warships. Moreover, future research should integrate ESG metrics, emphasizing not only environmental compliance but also crew welfare and health centric of defense resources. In conclusion, this study contributes to a deeper understanding of the environmental determinants of stress in naval settings and provides a foundation for evidence-based interventions. Enhancing IAQ is a strategic move that affects mission readiness, mental health, and the sustainability of naval operations.

REFERENCES

Ajzen, I. 1975. Attitudes, personality, and behavior. Open University Press.

Al-Mamun, A., Rahman, S. M. & Hasan, M.K. 2022. Indoor air quality and psychological effects on naval personnel: A review. *Environmental Monitoring and Assessment*, 194(6): 408. https://doi.org/10.1007/s10661-022-10050-3

Bandura, A. 1986. *Social foundations of thought and action: A social cognitive theory*. Prentice-Hall.

Chen, Y., Lin, Z. & Zhang, Y. 2023. The impact of shipboard air quality on stress biomarkers among seafarers. *Journal of Occupational Health*, 65(1): e12345. https://doi.org/10.1002/1348-9585.12345

Hair, J.F., Black, W.C., Babin, B.J. & Anderson, R.E. 2010. *Multivariate data analysis.* 7th Ed. Pearson.

Haddaway, N.R., Woodcock, P., Macura, B. & Collins, A. 2015. Making literature reviews more reliable through application of lessons from systematic reviews. *Conservation Biology*, 29(6): 1596–1605. https://doi.org/10.1111/cobi.12541

Khan, A., Abbas, M. & Zhang, Y. 2022. Impact of indoor air quality in school settings on cognitive performance. *Environmental Research,* 208: 112568.

Kounadi, O., Lampoltshammer, T.J., Groff, E., Sitko, I. & Leitner, M. 2020. Systematic literature review: Literature reviews in GIScience. *International Journal of Geographical Information Science*, 34(1): 1–22. https://doi.org/10.1080/13658816.2019.1612846

Liberati, A., Altman, D.G., Tetzlaff, J., Mulrow, C., Gøtzsche, P.C., Ioannidis, J.P., Clarke, M., Devereaux, P. J., Kleijnen, J. & Moher, D. 2020. The PRISMA statement for reporting systematic reviews and meta-analyses of studies that evaluate health care interventions: Explanation and elaboration. *PLoS Medicine,* 6(7): e1000100. https://doi.org/10.1371/journal.pmed.1000100

Lim, W.Y., Liew, T.M. & Ng, W.J. 2021. Psychological stress among seafarers during long-term deployment: A systematic review. *Occupational Medicine*, 71(2): 82–90. https://doi.org/10.1093/occmed/kqab002

Maslow, A.H. 1943. A theory of human motivation. *Psychological Review*, 50(4): 370–396. https://doi.org/10.1037/h0054346

Mohamed, N.M., Salleh, M.N.M. & Wahab, N.I.A. 2020. Synonym expansion technique in systematic reviews: Enhancing search comprehensiveness. *Journal of Information and Communication Technology*, 19(3): 457–473. https://doi.org/10.32890/jict2020.19.3.6

Page, M.J., McKenzie, J.E., Bossuyt, P.M., Boutron, I., Hoffmann, T.C., Mulrow, C.D. & Moher, D. 2021. The PRISMA 2020 statement: An updated guideline for reporting systematic reviews. *The BMJ*, 372(71). https://doi.org/10.1136/bmj.n71

Saini, J., Dutta, M. & Marques, G. 2020. Indoor air quality monitoring systems based on Internet of Things: A systematic review. *Environmental Science and Pollution Research*, 27(6): 6746–6760. https://doi.org/10.1007/s11356-019-07515-4

Strunk, W., Jr. & White, E.B. 2000. *The elements of style*. 4th Ed. Longman.

Thach, T.Q., Mahirah, D. & Sauter, C. 2022. Stressor interaction effects from confined air quality on naval personnel. *International Maritime Health*, 73(2): 115–122. https://doi.org/10.5603/IMH.2022.0020

Van der Geer, J., Hanraads, J.A.J. & Lupton, R.A. 2010. The art of writing a scientific article. *Journal of Scientific Communications,* 163: 51–59. https://doi.org/10.1016/j.Sc.2010.00372

Van der Geer, J., Hanraads, J.A.J. & Lupton, R.A. 2018. The art of writing a scientific article. Heliyon, 19: e00205. https://doi.org/10.1016/j.heliyon.2018.e00205

Weisskopf, M.G. 2022. Military shipboard exposures and mental health: A developing concern. Military Medicine, 187(7–8): e1003–e1009. https://doi.org/10.1093/milmed/usac032

Yusof, M.Z.M., Roslan, N.A. & Jamil, N. 2021. Occupational stressors aboard Royal Malaysian Navy vessels: An exploratory study. *Asian Journal of Behavioural Studies,* 6(2): 39–53. https://doi.org/10.21834/ajbes.v6i2.303

Zhang, Y., Chen, Y. & Deng, Y. 2020. Indoor environmental quality and occupants' health in residential buildings: A systematic literature review. Building and Environment, 180: 106964. https://doi.org/10.1016/j.buildenv.2020.106964

RESEARCH ARTICLE

BORNEO SCIENCE
THE JOURNAL OF SCIENCE & TECHNOLOGY

Journal homepage: https://jurcon.ums.edu.my/ojums/index.php/borneo-science

BEYOND ANTIBIOTICS: PROBIOTICS, PREBIOTICS, AND SYNBIOTICS IN CATFISH (*Clarias gariepinus*) AQUACULTURE FOR THE CONTROL OF *Aeromonas hydrophila* IN MALAYSIA– A REVIEW

Arlene Debbie Lingoh[1], Sui Sien Leong[*1,2], Kamil Latif[1], Yih Nin Lee[3] and Shahrul Razid Sarbini[4]

[1] Department of Animal Sciences and Fishery, Faculty of Agricultural and Forestry Sciences, Universiti Putra Malaysia Sarawak, 97008 Bintulu, Sarawak, Malaysia.
[2] Research Laboratory of Probiotics and Cancer Therapeutics (CANRES 2), UPM-MAKNA Cancer Research Laboratory (CANRES), Institute of Bioscience, Universiti Putra Malaysia, 43400 UPM Serdang, Selangor, Malaysia.
[3] Faculty of Engineering and Sciences, Curtin University, CDT 250, 98009 Miri, Sarawak, Malaysia
[4] Department of Crop Sciences, Faculty of Agricultural and Forestry Sciences, Universiti Putra Malaysia Sarawak, 97008 Bintulu, Sarawak, Malaysia.

[*]**Correspondence:**
leongsuisien@upm.edu.my

Received: 23 February 2025
Revised: 1 March 2025
Accepted: 29 December 2025
Published online: 31 December 2025

Doi :
10.51200/bsj.v46i2.6783

Keywords:
Antibiotics alternative; Aquaculture; Probiotics; Prebiotics; Synbiotics.

ABSTRACT. *Aquaculture remains the fastest-growing sector in global food production, providing a vital source of protein and supporting economic development. In Malaysia, freshwater aquaculture, particularly the farming of Clarias gariepinus, is central to food security, yet the intensification of production has heightened disease risks, feed inefficiencies, and vulnerability to bacterial pathogens such as Aeromonas hydrophila. Conventional use of antibiotics has proven unsustainable due to antimicrobial resistance and environmental concerns, driving the need for alternative management strategies. Functional feed additives, including probiotics, prebiotics, and synbiotics, have emerged as eco-friendly approaches to enhance growth performance, feed utilization, immune competence, and pathogen resistance. This review aims to critically evaluate recent progress (2015–2025) in the use of probiotics, prebiotics, and synbiotics in freshwater aquaculture, with a particular focus on catfish farming in Malaysia. It highlights their types, mechanisms of action, comparative effects on fish growth and immune modulation, and their role in disease resistance against A. hydrophila. By synthesizing current evidence, the review identifies both the opportunities and research gaps associated with these functional feed additives. The findings underscore their potential as sustainable alternatives to antibiotics, supporting healthier and more resilient aquaculture systems.*

INTRODUCTION

Aquaculture continues to be one of the most rapidly expanding sectors within global food production, driven by the increasing demand for sustainable and affordable sources of high-quality animal protein (Food and Agriculture Organization, 2022). Worldwide, aquaculture has surpassed capture fisheries in providing fish for human consumption, and its role in supporting food and nutritional security is expected to grow further in the coming decades (Naylor *et al*., 2021). In Malaysia, freshwater aquaculture is a vital component of the national food system, contributing to both economic

development and rural livelihoods, with total harvests exceeding 40,000 tons annually in recent years (Department of Fisheries Malaysia, 2021). Catfish aquaculture constitutes a significant segment of Malaysia's freshwater aquaculture sector and plays an important role in supporting domestic fish supply. In Malaysia, catfish production represents an important segment of the freshwater aquaculture sector, with annual outputs reaching tens of thousands of tonnes in recent years. Commercial farming is largely dominated by African catfish (*Clarias gariepinus*) and its hybrids with local species, reflecting their rapid growth, tolerance to intensive culture conditions, and strong market demand (Department of Fisheries Malaysia, 2021). In addition to these farmed species, several other catfish taxa are present in Malaysia, including Asian walking catfish (*Clarias batrachus*), striped catfish (*Pangasianodon hypophthalmus*), river catfish (*Mystus* spp.), bagrid catfish (*Hemibagrus* spp.), silurid catfish (*Ompok* spp.), and the giant sheatfish (*Wallago leerii*), which are primarily associated with capture fisheries or produced at smaller aquaculture scales.

Despite this progress, the intensification of aquaculture in Malaysia has also given rise to several constraints, including inconsistent growth performance, inefficient feed utilization, and recurrent disease outbreaks. Among the pathogens of concern, *Aeromonas hydrophila* has been identified as a major cause of high mortality and economic losses in catfish culture (Ridzuan *et al*., 2022). Episodes of motile *Aeromonas septicaemia* have affected cultured species such as tilapia (*Oreochromis* spp.) and African catfish (*Clarias gariepinus*), leading to acute mortality, haemorrhagic lesions, fin erosion, and septicaemia, especially under intensive farming conditions (Omeje & Kolndadacha, 2024). Several outbreaks documented in ponds and cage culture systems have been linked to environmental stressors, including elevated water temperature, poor water quality, and high stocking density, which facilitate opportunistic *Aeromonas* infections. These disease events have resulted in substantial stock losses and increased reliance on antimicrobial treatments, underscoring the continuing challenge posed by *Aeromonas* infections to freshwater fish health management in Malaysia. Basri *et al*. (2020) stated that cultured tilapia have been affected by co-infections involving Tilapia Lake Virus (TiLV) together with *Aeromonas hydrophila* and *Streptococcus agalactiae*, resulting in mortality rates of up to around 70 % on affected farms in Selangor in early 2020, highlighting the threat of viral and bacterial synergy in intensive systems. The reliance on antibiotics for disease control has further triggered concerns regarding antimicrobial resistance and environmental risks, highlighting the need for safer and more sustainable solutions (Leong *et al*., 2013; Lingoh *et al*., 2020). To address these challenges, hybridization strategies have been applied to enhance growth, feed efficiency, and resilience of aquaculture species. Hybrid catfish, for example, exhibit heterosis effects that improve survival and adaptability (Wang *et al*., 2022). However, hybridization alone may not be sufficient to overcome disease-related and nutritional limitations, which has prompted increasing attention toward the use of functional feed additives.

In this context, probiotics, prebiotics, and their combination as synbiotics have been extensively studied as alternatives to antibiotics and chemotherapeutics in aquaculture nutrition and health management (Leong *et al*., 2023). Probiotics, defined as live beneficial microorganisms, support gut microbiota balance, enhance digestion, and modulate immune responses (Lingoh *et al*., 2025). Prebiotics, commonly non-digestible oligosaccharides, selectively promote the proliferation of beneficial microbes, contributing to intestinal health and nutrient absorption (Rawi *et al*., 2020). Synbiotics integrate both components, providing synergistic effects that translate into improved growth, feed utilization, immune stimulation, and resistance to infectious diseases (Khanjani *et al*., 2024).

Recent studies from 2015 to 2025 consistently report positive effects of these additives on fish or shrimp growth performance, feed conversion efficiency, and health status (Hosseini *et al*., 2024). Importantly, they have also demonstrated protective roles against opportunistic pathogens such as *A. hydrophila*, one of the most problematic bacteria in Malaysian freshwater aquaculture. By stimulating mucosal barriers, enhancing immune responses, and reducing pathogen colonization, these additives offer a promising approach to improve the sustainability and productivity of aquaculture systems (Leong *et al*., 2023).

Therefore, the present review aims to consolidate current knowledge on the use of probiotics, prebiotics, and synbiotics in aquaculture, with a special focus on Malaysian freshwater catfish production. Specifically, it discusses global aquaculture trends, the development and challenges of Malaysian aquaculture, and the roles of probiotics, prebiotics, and synbiotics in improving growth performance, feed utilization, immune system function, and resistance against *A. hydrophila*. By integrating recent evidence, this review provides insights into the potential of these functional supplements as sustainable alternatives to antibiotics in Malaysian aquaculture.

MATERIALS AND METHODS

Literature Search

A structured literature search was carried out to identify studies and reviews addressing the use of probiotics, prebiotics, and synbiotics as alternative supplements in aquaculture. Relevant publications were retrieved from major scientific databases, including PubMed, Web of Science, Scopus, and Google Scholar. The initial screening yielded approximately 100 articles. Search terms applied included "probiotics," "prebiotics," "aquaculture," "fish immune system," "pathogen," and "lactic acid bacteria." To ensure the review reflected current knowledge, only studies published in the past ten years were considered. Furthermore, the selection was limited to English-language articles to maintain uniformity in analysis.

Inclusion and Exclusion

During the initial screening, 40 articles were excluded due to a lack of relevance. A further 60 publications were later removed after applying the selection criteria, which excluded studies limited to feed formulation supplements or those without empirical evidence and mechanistic insights. This stringent screening approach ensured that only the most relevant and informative studies were included, allowing for a focused synthesis of current trends and recent advances in the field.

Analysis of the Database

The gathered literature was carefully reviewed to capture emerging patterns and developments in aquaculture research. This process included analysing recent progress, such as the identification of novel probiotic and prebiotic strains as well as advances in their application strategies. A comparative evaluation was undertaken to examine the effectiveness of probiotics, prebiotics, and symbiotics on fish growth performance, drawing on reported outcomes across various species and culture environments. Differences in efficacy under distinct conditions were considered to provide a broader perspective. In addition, the methodological quality of the studies was assessed to gauge the reliability and validity of the evidence presented.

RESULTS AND DISCUSSIONS

Global Trends in Malaysian Aquaculture

Global aquaculture has experienced remarkable growth over the past decade, underlining its importance in meeting the increasing global demand for animal protein. Farmed finfish production alone reached approximately 57.5 million tonnes in 2020, generating an estimated USD 146.1 billion in value (Food and Agriculture Organization, 2022). Despite the challenges posed by the COVID-19 pandemic, including disruptions to supply chains and market access, the aquaculture sector continued to expand, demonstrating resilience and its integral role in sustainable food systems. This steady trajectory highlights aquaculture's capacity not only to supplement declining capture fisheries but also to contribute to global food and nutritional security. However, the intensification of aquaculture practices has been accompanied by significant challenges. Antibiotic resistance is the most alarming scenario in

aquaculture because it not only reduces treatment efficacy against common pathogens such as *Aeromonas hydrophila* but also leads to recurrent outbreaks, economic losses, and the potential transfer of resistant genes from aquatic environments to human and animal health systems. High stocking densities and rapid system expansion have resulted in greater susceptibility to infectious diseases, particularly bacterial pathogens, which continue to cause heavy production losses (Walker & Winton, 2010). In addition, feed remains the highest operational cost, with rising prices of fishmeal and soybean meal exerting pressure on production sustainability (Naylor *et al*., 2021). Environmental concerns, such as nutrient loading and effluent discharge, further exacerbate the ecological footprint of the industry (Li *et al*., 2023). These issues underscore the urgent need for alternative, environmentally sound approaches that balance productivity with sustainability.

One promising avenue is the application of functional feed additives, including probiotics, prebiotics, and synbiotics. These biotic supplements have been widely studied for their potential to enhance growth performance, feed efficiency, gut health, and immune responses in aquaculture species while reducing dependence on antibiotics (Khairul *et al*., 2024). In Malaysia, aquaculture forms a cornerstone of the agri-food sector, supporting both economic development and national food security. The industry is broadly divided into three production categories: brackish-water aquaculture (dominated by shrimp and marine finfish), freshwater aquaculture (notably catfish and tilapia), and seaweed farming. Among these, freshwater aquaculture has shown consistent growth, reflecting strong domestic demand for affordable protein sources and continued government support through policies, subsidies, and research initiatives (Garlock *et al*., 2024). According to the Department of Fisheries Malaysia (2021), aquaculture production increased by 4.3% in volume and 10.1% in value between 2020 and 2021, even as inland capture fisheries experienced a 4% decline. This trend emphasizes the growing reliance on aquaculture to meet Malaysia's protein requirements and reduce pressure on natural fish stocks. Within freshwater aquaculture, catfish (*Clarias* spp.) occupy a dominant position. Production of catfish exceeded 417,000 metric tonnes in 2021, making it one of the most widely cultured freshwater species in the country (Department of Fisheries Malaysia, 2021).

Freshwater Aquaculture: Catfish

The African catfish (*Clarias gariepinus*) (Figure 1), first introduced to Malaysia in the late 1980s, has become a cornerstone species in the country's aquaculture sector. Its popularity stems from its rapid growth, tolerance to low water quality, adaptability to high-density culture systems, and strong consumer demand (Manyise *et al*., 2024). These traits make it particularly attractive for small- and medium-scale farmers, who rely on catfish farming as a cost-effective source of livelihood and a steady supplier of affordable animal protein. Production levels of *C. gariepinus* have consistently ranked among the highest in Malaysia's freshwater aquaculture. According to the Department of Fisheries Malaysia (2021), catfish production exceeded 417,000 metric tonnes in 2021, representing a significant proportion of total freshwater fish output. The species has also been prioritized under national food security initiatives due to its high market acceptance and relatively low production costs (Manyise *et al*., 2024).

Figure 1. African catfish (*Clarias gariepinus*).

Despite these advantages, the intensification of catfish farming presents notable challenges. Disease outbreaks, particularly motile *Aeromonas septicaemia* caused by *Aeromonas hydrophila*, remain a persistent constraint, often leading to high mortality rates and economic losses (Semwal *et al*., 2023). In addition, escalating feed costs, which account for up to 60–70% of production expenses, pose a threat to farm profitability (Pawlak & Kołodziejczak, 2020). Environmental concerns, such as effluent discharge and water quality deterioration in densely farmed areas, further complicate sustainable production. Addressing these challenges will require integrated management approaches, including functional feed additives, improved biosecurity, and selective breeding programs tailored to Malaysian aquaculture conditions.

Probiotics

Probiotics, derived from the Greek words' pro ("for") and bios ("life"), are defined as live microorganisms that confer health benefits to the host when administered in adequate amounts (Khairul *et al*., 2024). They have gained increasing recognition in aquaculture as sustainable alternatives to antibiotics and chemotherapeutics, largely driven by growing concerns over antimicrobial resistance, treatment costs, and the ecological impacts of conventional disease management (Lingoh *et al*., 2025). Probiotics in aquaculture are not only regarded as microbial feed additives that modulate the gut microbiota but also as functional components capable of improving host physiology and environmental quality (Hoseinifar *et al*., 2018; El-Saadony *et al*., 2021).

The beneficial effects of probiotics arise from multiple mechanisms of action. First, they competitively exclude pathogens by occupying adhesion sites on the intestinal epithelium and competing for available nutrients, thereby reducing pathogen colonization (Hoseinifar *et al*., 2018). Second, many probiotic strains secrete antimicrobial metabolites such as organic acids, hydrogen peroxide, and bacteriocins that directly inhibit pathogenic bacteria (El-Saadony *et al*., 2021). Third, probiotics promote gut microbiota balance, enhancing microbial diversity and resilience, which in turn reduces dysbiosis and improves digestive efficiency (Leong *et al*., 2023). Probiotic-derived enzymes, including amylases, proteases, and lipases, further facilitate nutrient assimilation and feed utilization, supporting growth performance (Tabassum *et al*., 2021). At the immunological level, probiotics enhance host defense by stimulating lysozyme activity, phagocytosis, cytokine production, and antimicrobial peptide expression, thus improving resistance against pathogens and environmental stressors (Wang *et al*., 2024). Collectively, these mechanisms explain why probiotics are increasingly viewed as critical tools in sustainable aquaculture.

Among the diverse microbial candidates, lactic acid bacteria (LAB) are the most widely studied due to their proven safety and effectiveness in terrestrial and aquatic systems. Enterococcus spp. has emerged as a promising probiotic group in freshwater aquaculture. These bacteria colonize the gastrointestinal tract, produce bacteriocins, and stimulate immune responses (Lingoh *et al*., 2020).

Prebiotics

Prebiotics are generally defined as indigestible compounds that withstand gastric acidity, undergo fermentation by intestinal microbiota, and selectively stimulate the growth and activity of beneficial microorganisms, thereby enhancing host health (Davani-Davari *et al*., 2019; Rawi *et al*., 2020). They are typically composed of long-chain complex carbohydrates that provide energy for probiotics or resident gut microbes, ultimately supporting host well-being. Most prebiotics are derived from plant-based sources (Mohammadi *et al*., 2020), with additional contributions from edible mushrooms (Balakrishnan *et al*., 2021), to a lesser extent, animal-derived dairy products, and fruit waste (Abdul Rahim *et al*., 2022). Natural sources of prebiotics include vegetables, fruits, legumes, seaweeds, microalgae, and animal milk (Ahmadifar *et al*., 2019; Van Doan *et al*., 2020). Beyond serving as a nutrient supply, prebiotics exert multiple biological functions: they prevent pathogen adhesion to intestinal epithelial cells, act as decoy receptors to block pathogen colonization, modulate immune system activity, and regulate inflammatory responses (Mohammadi *et al*., 2021).

Unlike probiotics, which introduce live microorganisms, prebiotics act as fermentable substrates that enhance the activity of resident or co-administered microbiota, contributing to gut stability and resilience in intensively farmed fish. Prebiotics are employed in aquaculture to stimulate the growth and metabolic activity of beneficial gut microbes, thereby supporting overall host health (Sanders *et al*., 2019; Rohani *et al*., 2021). Commonly applied prebiotics include β-glucans, inulin, arabinoxylan oligosaccharides (AXOS), mannan oligosaccharides (MOS), galactooligosaccharides (GOS), fructooligosaccharides (FOS), and other related oligosaccharides. Fermentation of prebiotics generates short-chain fatty acids (SCFAs), including acetate, propionate, and butyrate, which lower gut pH to suppress pathogens, provide energy for intestinal cells, and regulate immune functions (Wang *et al*., 2021). Prebiotics have been shown to improve growth performance (Li *et al*., 2019), enhance feed utilization (Shoaei *et al*., 2015), stimulate immune responses (Li *et al*., 2020), and strengthen disease resistance in aquaculture species (Abdel-Latif *et al*., 2022). Their use is therefore considered a valuable strategy to boost aquaculture productivity. Nevertheless, the effectiveness of prebiotics is highly dependent on host-specific gut microbiota interactions (Gibson *et al*., 2017), as not all prebiotics are universally effective in promoting beneficial microbial growth.

Synbiotic

Symbiotic, the combined use of probiotics and prebiotics, is increasingly applied in aquaculture to enhance growth, immunity, and disease resistance. The updated definition by Swanson *et al*. (2020) emphasizes symbiotic as "a mixture comprising live microorganisms and substrate(s) selectively utilized by host microorganisms that confers a health benefit on the host." Synbiotics are generally classified into two categories: complementary and synergistic. Complementary synbiotics combine probiotics and prebiotics that act independently but together contribute to host health, while synergistic synbiotics are specifically formulated so that the prebiotic selectively enhances the growth and activity of the co-administered probiotic, thereby amplifying their combined benefits. The majority of synbiotics available commercially, as well as those tested in clinical applications, fall under the complementary type. These typically combine probiotics such as *Lactobacillus* spp. and *Bifidobacterium* spp. with prebiotics like fructooligosaccharides (FOS), galactooligosaccharides (GOS), and inulin-type fructans (ITFs) (Smolinska *et al*., 2025). In recent years, complementary synbiotics have been widely investigated for managing metabolic and health-related conditions, including obesity, hypertension, gastrointestinal dysfunction, and immune disorders (Lee *et al*., 2024). However, because complementary synbiotics act independently, their effectiveness often depends on the host's existing gut microbiota composition. This variability highlights the need for more personalized approaches when applying such products. By contrast, synergistic synbiotics are designed to overcome these limitations by pairing probiotics with specific prebiotics that selectively enhance their activity. This targeted interaction may yield consistent benefits even in individuals who do not respond well to complementary formulations.

Application in *Clarias gariepinus*

Experimental studies have demonstrated the efficacy of probiotic supplementation across different catfish species. Dietary inclusion of *Enterococcus faecalis* has been shown to enhance growth performance, feed conversion efficiency, and innate immune indicators such as lysozyme activity in African catfish (*Clarias gariepinus*) (Allameh *et al*., 2017; Lingoh *et al*., 2025). Similarly, *Enterococcus hirae* supplementation improved immune-related gene expression and increased disease resistance in hybrid catfish (*C. gariepinus* × *C. macrocephalus*) (Hamid *et al*., 2021). Collectively, these findings indicate that species-specific and ecologically compatible probiotics—particularly *Enterococcus* strains can contribute meaningfully to addressing key constraints in Malaysian catfish farming, including suboptimal feed utilization and recurrent *Aeromonas hydrophila* infections.

Prebiotics further support intestinal health by reinforcing gut barrier integrity through enhanced mucin secretion, upregulation of tight junction proteins, and preservation of villus architecture, thereby limiting pathogen translocation and intestinal inflammation (Smolinska *et al*., 2025). These structural improvements are often accompanied by increased digestive enzyme activity and more efficient nutrient absorption, ultimately translating into improved growth performance and feed efficiency (Lingoh *et al*.,

2025). In catfish aquaculture, several studies have demonstrated the functional benefits of prebiotic supplementation. For instance, dietary inulin has been reported to enhance growth performance, haematological parameters, and lysozyme activity in *C. gariepinus* (Kattakdad *et al*., 2025). Likewise, mannan-oligosaccharide (MOS) supplementation has been shown to improve gut histomorphology, digestive enzyme activity, and nutrient utilization in hybrid *Clarias* species, thereby supporting both health status and productivity under intensive culture conditions. Together, these findings highlight the potential of prebiotics as effective functional feed additives for improving growth, immunity, and disease resistance in freshwater catfish.

Synbiotics, which combine probiotics and prebiotics, are increasingly valued in catfish aquaculture because of their synergistic effects on gut function and host physiology, often exceeding the benefits observed when either component is applied alone. Their primary mode of action involves modulation of the intestinal microbiota, whereby prebiotics serve as selective substrates that enhance probiotic survival, colonization, and metabolic activity. This interaction promotes the production of beneficial metabolites, including bacteriocins, organic acids, and short-chain fatty acids (SCFAs), which suppress pathogenic bacteria and contribute to intestinal homeostasis (Khanjani *et al*., 2024). In addition to microbial regulation, synbiotics improve intestinal morphology by increasing villus height, goblet cell density, and mucosal thickness, thereby strengthening epithelial barrier function and facilitating more efficient nutrient absorption (Mohammed *et al*., 2022). A comparative overview of probiotics, prebiotics, and synbiotics in aquaculture nutrition, including their mechanisms of action, is summarized in Figure 2.

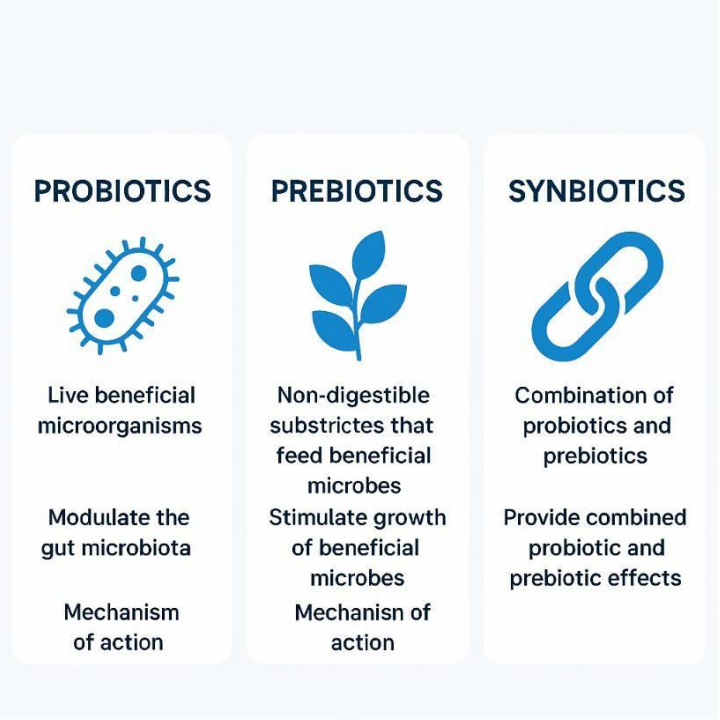

Figure 2. Comparison of probiotics, prebiotics, and synbiotics in aquaculture nutrition. The infographic illustrates their definitions, primary roles, and mechanisms of action.

At the immunological level, synbiotics stimulate key components of non-specific defense, including lysozyme activity, phagocytic capacity, complement activation, and respiratory burst responses. SCFAs generated during prebiotic fermentation further modulate cytokine expression and promote anti-inflammatory pathways, reinforcing mucosal and systemic immunity (Ghosh, 2025). In freshwater catfish, particularly *Clarias gariepinus* and hybrid *Clarias* species, synbiotic supplementation has consistently been associated with improved growth performance, enhanced feed efficiency, elevated innate immune parameters, and reduced mortality following bacterial challenge with *Aeromonas hydrophila* (Mohammed *et al*., 2022). Collectively, these findings underscore the strong

potential of synbiotics as a sustainable nutritional strategy to enhance health, disease resistance, and productivity in intensive catfish aquaculture systems.

Which Is Better: Probiotics, Prebiotics, or Synbiotics?

The choice between probiotics, prebiotics, and synbiotics in catfish aquaculture depends largely on production objectives, health challenges, and economic considerations. Probiotics have been widely adopted due to their direct effects on pathogen inhibition, gut microbiota modulation, and immune stimulation. Their ability to produce antimicrobial compounds such as bacteriocins and organic acids makes them highly effective for disease control in systems prone to bacterial outbreaks (El-Saadony *et al*., 2021; Leong *et al*., 2025). However, their success depends on strain selection and the ability of the bacteria to colonize the gut under variable farming conditions.

Prebiotics, on the other hand, are cost-effective and stable feed additives that selectively stimulate beneficial microbial populations. They improve gut fermentation processes, SCFA production, and nutrient assimilation, indirectly enhancing host immunity and growth (Wang *et al*., 2021). Yet, their effectiveness can be host-specific, as not all prebiotics universally support the same gut microbiota composition across species or environments (Gibson *et al*., 2017). Synbiotics represent a combined approach, integrating the direct antimicrobial and immunomodulatory functions of probiotics with the selective stimulatory effects of prebiotics. This synergy enhances probiotic colonization, boosts immune responses, and strengthens gut barrier integrity. Evidence from catfish trials consistently shows that synbiotics deliver superior outcomes in terms of growth performance, feed efficiency, and resistance to pathogens such as *Aeromonas hydrophila* compared to probiotics or prebiotics alone (Khanjani *et al*., 2024). Thus, probiotics and prebiotics individually provide clear benefits to gut health and immunity; their effectiveness may be limited by strain survival, colonization efficiency, or substrate availability when applied alone. Synbiotics overcome these constraints by combining complementary microorganisms and fermentable substrates, thereby enhancing probiotic persistence, metabolic activity, and functional efficacy within the host intestine (Khanjani *et al*., 2024). Experimental evidence in aquaculture demonstrates that synbiotic formulations more consistently improve growth performance, feed efficiency, immune responses, and disease resistance than single-component supplements (Mohammed *et al*., 2022; Ghosh, 2025). This synergistic interaction supports the view that synbiotics represent a more robust and reliable nutritional strategy for sustainable fish health management compared with probiotics or prebiotics used independently. Overall, synbiotics are often considered the most effective strategy for intensive catfish farming, particularly in regions like Malaysia, where disease outbreaks and antibiotic resistance remain major challenges.

CONCLUSION

Probiotics, prebiotics, and synbiotics each contribute meaningfully to the advancement of sustainable freshwater aquaculture, particularly in catfish production, through complementary mechanisms that support gut health and host immunity. While probiotics exert direct antimicrobial and immunomodulatory benefits and prebiotics act as stable, cost-effective substrates that shape beneficial microbial communities, their individual efficacy can be constrained when applied in isolation. In contrast, synbiotics integrate both components to achieve synergistic effects, consistently resulting in superior growth performance, improved nutrient utilization, enhanced immune competence, and greater resistance to pathogens such as *Aeromonas hydrophila*. In the context of increasing antimicrobial resistance and mounting pressure to reduce antibiotic dependence, synbiotics emerge as a strategically superior and environmentally responsible feed-based intervention for intensive catfish aquaculture. Future research should prioritize the rational design of strain–substrate combinations tailored to host species, culture systems, and regional conditions, alongside mechanistic and field-scale validation to support their wider adoption in sustainable aquaculture practices.

ACKNOWLEDGEMENT

The cooperation of the supporting laboratory staff is appreciated. The first author appreciated the financial support from the Grant IPS, Universiti Putra Malaysia (GP-IPS/2024/9789900).

REFERENCES

Abdel-Latif, H.M.R., Yilmaz, E., Dawood, M.A.O., Ringø, E., Ahmadifar, E. & Yilmaz, S. 2022. Shrimp vibriosis and possible control measures using probiotics, postbiotics, prebiotics, and synbiotics: A review. *Aquaculture*, 551: 737951. https://doi.org/10.1016/j.aquaculture.2022.737951.

Abdul Rahim, E.F., Leong, S.S., Sarbini, S.R., Latif, K. & Malahubban, M. 2022. Banana (*Musa acuminata*), Orange (*Citrus reticulata*), and Watermelon (*Citrullus lanatus*) peels as prebiotic. *Borneo Journal of Resource Science and Technology*, 12(1): 81-94. https:doi.org/10.33736/bjrst.4528.2022.

Allameh, S.K., Noaman, V. & Nahavandi, R. 2017. Effects of probiotic bacteria on fish performance. *Advanced Techniques in Clinical Microbiology*, 1: 11.

Ahmadifar, E., Sheikhzadeh, N., Roshanaei, K., Dargahi, N. & Faggio, C. 2019. Can dietary ginger (*Zingiber officinale*) alter biochemical and immunological parameters and gene expression related to growth, immunity and antioxidant system in zebrafish (*Danio rerio*)? *Aquaculture*, 507: 341-348. https://doi.org/10.1016/j.aquaculture.2019.04.049.

Balakrishnan, K., Dhanasekaran, D., Krishnaraj, V., Anbukumaran, A., Ramasamy, T. & Manickam, M. 2021. Edible mushrooms: A promising bioresource for prebiotics. *Advances in Probiotics*, 81-97. https://doi.org/10.1016/b978-0-12-822909-5.00005-8.

Basri, L., Nor, R.M., Salleh, A., Md Yasin, I.S., Saad, M.Z., Abd Rahaman, N.Y., Barkham, T. & Amal, M.N.A. 2020. Co-infections of Tilapia lake virus, *Aeromonas hydrophila* and *Streptococcus agalactiae* in farmed red hybrid Tilapia. *Animals (Basel)*, 10(11): 2141. https://doi.org/10.3390/ani10112141

Davani-Davari, D., Negahdaripour, M., Karimzadeh, I., Seifan, M., Mohkam, M., Masoumi, S.J., Berenjian, A. & Ghasemi, Y. 2019. Prebiotics: definition, types, sources, mechanisms, and clinical applications. *Foods*, 8(3): 92. https://doi.org/10.3390/foods8030092.

Department of Fisheries Malaysia. 2021. *Annual Fisheries Statistics 2021*. Malaysia: Department of Fisheries Malaysia.

El-Saadony, M.T., Alagawany, M., Patra, A.K., Kar, I., Tiwari, R., Dawood, M.A.O., Dhama, K. & Abdel-Latif, H.M.R. 2021. The functionality of probiotics in aquaculture: An overview. *Fish and Shellfish Immunology*, 117: 36-52. https:doi.org/10.1016/j.fsi.2021.07.007.

Food and Agriculture Organization of the United Nations. 2022. *The state of world fisheries and aquaculture-Towards blue transformation*. Rome, Italy: Food and Agriculture Organization of the United Nations: 32.

Garlock, T.M., Asche, F., Anderson, J.L., Eggert, H., Anderson, T.M., Che, B., Chávez, C.A., Chu, J., Chukwuone, N., Dey, M.M., Fitzsimmons, K., Flores, J., Guillen, J., Kumar, G., Liu, L., Llorente, I., Nguyen, L., Nielsen, R., Pincinato, R.B.M., Sudhakaran, P.O., Tibesigwa, B. & Tveteras, R. 2024. Environmental, economic, and social sustainability in aquaculture: the aquaculture performance indicators. *Nature Communication*, 15: 5274. https://doi.org/10.1038/s41467-024-49556-8.

Gibson, G.R., Hutkins, R., Sanders, M.E., Prescott, S.L., Reimer, R.A., Salminen, S.J., Scott, K., Stanton, C., Swanson, K.S., Cani, P.D., Verbeke, K. & Reid, G. 2017. Expert consensus document: The International Scientific Association for Probiotics and Prebiotics (ISAPP) consensus statement on the definition and scope of prebiotics. *Nature Reviews Gastroenterology and Hepatology*, 14(8): 491-502. https://doi.org/10.1038/nrgastro.2017.75.

Ghosh, T. 2025. Recent advances in the potential and multifaceted role of probiotics in the development of sustainable aquaculture: Its current form and future perspectives. *The Microbe*, 7: 100317. https://doi.org/10.1016/j.microb.2025.100317.

Hamid, N.H., Daud, H.M., Kayansamruaj, P., Hassim, H.A., Mohd Yusoff, M.S., Abu Bakar, S.N. & Srisapoome, P. 2021. Short- and long-term probiotic effects of *Enterococcus hirae* isolated from fermented vegetable wastes on the growth, immune responses, and disease resistance of hybrid catfish (*Clarias gariepinus* × *Clarias macrocephalus*). *Fish and Shellfish Immunology*, 114: 1-19. https://doi.org/10.1016/j.fsi.2021.04.012.

Hoseinifar, S.H., Sun, Y.Z., Wang, A. & Zhou, Z. 2018. Probiotics as means of diseases control in aquaculture, a review of current knowledge and future perspectives. *Frontiers in Microbiology*, 9: 2429. https://doi.org/10.3389/fmicb.2018.02429.

Hosseini, S.S., Sudaagar, M., Zakariaee, H., Paknejad, H., Baruah, K. & Norouzitalab, P. 2024. Evaluation of the synbiotic effects of *Saccharomyces cerevisiae* and mushroom extract on the growth performance, digestive enzyme activity, and immune status of zebrafish *Danio rerio*. *BMC Microbiology*, 24(1): 331. https:doi.org/10.1186/s12866-024-03459-2.

Kattakdad, S., Phungam, N., Pongket, U., Muangmala, W., Udduang, S., Aripin, S.A. & Yuangsoi, B. 2025. Microencapsulated inulin as a prebiotic: Enhancing growth, digestive enzyme activity, and immune response in striped catfish (*Pangasianodon hypophthalmus*). *Aquaculture Reports*, 43: 102986. https://doi.org/10.1016/j.aqrep.2025.102986.

Khairul, S.R., Leong, S.S., Korel, F., Lingoh, A.D. & Toh, S.C. 2024. Systematic review of emerging trends in soil-based probiotics. *Malaysian Journal of Soil Science*, 28: 401-413.

Khanjani, M.H., Mozanzadeh, M.T., Gisbert, E. & Hoseinifar, S.H. 2024. Probiotics, prebiotics, and synbiotics in shrimp aquaculture: Their effects on growth performance, immune responses, and gut microbiome. *Aquaculture Reports*, 38: 102362. https://doi.org/10.1016/j.aqrep.2024.102362.

Lee, S., Choi, S.-P., Choi, H.-J., Jeong, H. & Park, Y.-S. 2024. A comprehensive review of synbiotics: an emerging paradigm in health promotion and disease management. *World Journal of Microbiology and Biotechnology*, 40(9). https://doi.org/10.1007/s11274-024-04085-w.

Leong S.S., Korel, F., Lingoh, A.D., Sarbini, S.R., Toh, S.C., Abit, L.Y. & Wong, S.C. 2023. Current probiotics application for aquaculture feed: A review. *Borneo Science Journal*, 44(2). https://doi.org/10.51200/bsj.v44i2.

Leong, S.S., Samuel, L., Ling, T.Y., Chia, H.C. & Lim, C.K. 2013. Isolation and characterization of antibiotic-resistant bacteria from swiftlet feces in swiftlet farmhouses in Sarawak, Malaysia. *Microbiology Indonesia Journal*, 7(4): 137-143.

Li, J., Li, X., Liu, H., Gao, L., Wang, W., Wang, Z., Zhou, T. & Wang, Q. 2023. Climate change impacts on wastewater infrastructure: A systematic review and typological adaptation strategy. *Water Research*, 242: 120282. https://doi.org/10.1016/j.watres.2023.120282.

Li, Y., Yuan, W., Zhang, Y., Liu, H. & Dai, X. 2020. Single or combined effects of dietary arabinoxylan-oligosaccharide and inulin on growth performance, gut microbiota, and immune response in Pacific white shrimp *Litopenaeus vannamei*. *Journal of Oceanology and Limnology*, 39(2): 741-754. https://doi.org/10.1007/s00343-020-9083-z.

Li, Z., Tran, N. T., Ji, P., Sun, Z., Wen, X. & Li, S. 2019. Effects of prebiotic mixtures on growth performance, intestinal microbiota and immune response in juvenile chu's croaker, *Nibea coibor*. *Fish and Shellfish Immunology*, 89: 564-573. https://doi.org/10.1016/j.fsi.2019.04.025.

Lingoh, A.D., Latif, K., Lee, Y.N., Abit, L.Y., Sarbini, S.R., Vincent Mojilis, M.I., Shamsul Azhar, F. M., Khairul, S.R. & Leong, S.S. 2025. Enrichment of artemia with synbiotic and its effects on growth nutrient utilization survival and gut microbial communities of larval hybrid catfish (*Clarias microstomus* × *Clarias gariepinus*). *Aquaculture Nutrition*, 2025: 6616288. https://doi.org/10.1155/anu/6616288

Lingoh, A.D., Leong, S.S. & Sarbini, S.R. 2020. Detection of lactic acid bacteria (LAB) from local chicken breed gut as probiotic agent in livestock. *Pakistan Journal of Nutrition*, 19: 197-203.

Manyise, T., Basiita, R.K., Mwema, C.M., Oyesola, O., Siriwardena, S., Fregene, B., Cole, S.M., Dompreh, E.B., Lam, R.D., Lozano, D.L., Rossignoli, C.M. & Benzie, J.A.H. 2024. Farmer perspectives on desired catfish attributes in aquaculture systems in Nigeria. An exploratory focus group study. *Aquaculture*, 588: 740911. https://doi.org/10.1016/j.aquaculture.2024.740911.

Mohammadi, G., Rafiee, G., El Basuini, M.F., Abdel-Latif, H.M.R. & Dawood, M.A. O. 2020. The growth performance, antioxidant capacity, immunological responses, and the resistance against *Aeromonas hydrophila* in Nile tilapia (*Oreochromis niloticus*) fed Pistacia vera hulls derived polysaccharide. *Fish and Shellfish Immunology*, 106: 36-43. https://doi.org/10.1016/j.fsi.2020.07.064.

Mohammed, A., Hu, J., Murugesan, R. & Cheng, H.-W. 2022. Effects of a synbiotic as an antibiotic alternative on behavior, production performance, cecal microbial ecology, and jejunal histomorphology of broiler chickens under heat stress. *PLOS ONE*, 17(9): e0274179. https://doi.org/10.1371/journal.pone.0274179.

Naylor, R.L., Kishore, A., Sumaila, U.R., Issifu, I., Hunter, B.P., Belton, B., Bush, S.R., Cao, L., Gelcich, S., Gephart, J.A., Golden, C.D., Jonell, M., Koehn, J.Z., Little, D.C., Thilsted, S.H., Troell, M. & Zhang, W. 2021. Blue food demand across geographic and temporal scales. *Nature Communications,* 12: 5413. https://doi.org/10.1038/s41467-021-25516-4.

Omeje, V.O. & Kolndadacha, O.D. 2024. *Motile aeromonas septicaemia infection in African catfish (Clarias gariepinus, Burchell, 1822): A review*. United Kingdom: CABI Reviews. https://doi.org/10.1079/cabireviews.2024.0010

Pawlak, K. & Kołodziejczak, M. 2020. The role of agriculture in ensuring food security in developing countries: considerations in the context of the problem of sustainable food production. *Sustainability*, 12(13): 5488. https://doi.org/10.3390/su12135488.

Rawi, M.H., Zaman, S.A., Pa'ee, K.F., Leong, S.S. & Sarbini, S.R. 2020. Prebiotics metabolism by gut-isolated probiotics. *Food Science and Technology*, 57: 2786-2799. https://doi.org/10.1007/s13197-020-04244-5

Ridzuan, M.S.M., Abdullah, A., Ramly, R., Mansor, N.N., Ramli, N. & Firdaus-Nawi, M. 2022. Current status and advances of fish vaccines in Malaysia. *Veterinary World*, 15(2): 465-482. https://doi.org/10.14202/vetworld.2022.465-482.

Rohani, M.F., Islam, S.M., Hossain, M.K., Ferdous, Z., Siddik, M. AB., Nuruzzaman, M., Padeniya, U., Brown, C. & Shahjahan, M. 2022. Probiotics, prebiotics and synbiotics improved the functionality of aquafeed: Upgrading growth, reproduction, immunity and disease resistance in fish. *Fish and Shellfish Immunology*, 120: 569-589. https://doi.org/10.1016/j.fsi.2021.12.037.

Sanders, M.E., Merenstein, D.J., Reid, G., Gibson, G.R. & Rastall, R.A. 2019. Probiotics and prebiotics in intestinal health and disease: from biology to the clinic. *Nature Reviews Gastroenterology and Hepatology*, 16(10): 605-616. https://doi.org/10.1038/s41575-019-0173-3.

Semwal, A., Kumar, A. & Kumar, N. 2023. A review on pathogenicity of *Aeromonas hydrophila* and their mitigation through medicinal herbs in aquaculture. *Heliyon*, 9(3): e14088. https://doi.org/10.1016/j.heliyon.2023.e14088.

Shoaei, R., Akrami, R., Ghobadi, S. & Razeghi Mansour, M. 2015. Effect of dietary of prebiotic mannan oligosaccharide and β-1, 3 glucan on growth performance, survival, body composition and serum lysozyme activity in Rainbow trout (*Oncorhynchus mykiss*) fingerling. *Journal of Marine Biology*, 7 (2): 45-56.

Smolinska, S., Popescu, F.-D. & Zemelka-Wiacek, M. 2025. A Review of the influence of prebiotics, probiotics, synbiotics, and postbiotics on the human gut microbiome and intestinal integrity. *Journal of Clinical Medicine*, 14(11): 3673. https://doi.org/10.3390/jcm14113673.

Swanson, K.S., Gibson, G.R., Hutkins, R., Reimer, R.A., Reid, G., Verbeke, K., Scott, K.P., Holscher, H.D., Azad, M.B., Delzenne, N.M. & Sanders, M.E. 2020. The International Scientific Association for Probiotics and Prebiotics (ISAPP) consensus statement on the definition and scope of synbiotics. *Nature Reviews Gastroenterology & Hepatology*, 17(11): 687-701. https://doi.org/10.1038/s41575-020-0344-2.

Tabassum, T., Sofi Uddin Mahamud, A.G.M., Acharjee, T.K., Hassan, R., Akter Snigdha, T., Islam, T., Alam, R., Khoiam, Md. U., Akter, F., Azad, Md. R., Al Mahamud, Md. A., Ahmed, G.U. & Rahman, T. 2021. Probiotic supplementations improve growth, water quality, hematology, gut microbiota and intestinal morphology of Nile tilapia. *Aquaculture Reports*, 21: 100972. https://doi.org/10.1016/j.aqrep.2021.100972.

Van Doan, H., Hoseinifar, S.H., Ringø, E., Ángeles Esteban, M., Dadar, M., Dawood, M.A.O. & Faggio, C. 2019. Host-associated probiotics: A key factor in sustainable aquaculture. *Reviews in Fisheries Science and Aquaculture*, 28(1): 16-42. https://doi.org/10.1080/23308249.2019.1643288.

Wang, H., Bruce, T.J., Su, B., Li, S., Dunham, R.A. & Wang, X. 2022. Environment-dependent heterosis and transgressive gene expression in reciprocal hybrids between the Channel Catfish *Ictalurus punctatus* and the Blue Catfish *Ictalurus furcatus*. *Biology (Basel)*, 11(1): 117. https://doi.org/10.3390/biology11010117.

Walker, P.J. & Winton, J.R. 2010. Emerging viral diseases of fish and shrimp. *Veterinary Research*, 41(6): 51. https://doi.org/10.1051/vetres/2010022.

.

RESEARCH ARTICLE

BORNEO SCIENCE
THE JOURNAL OF SCIENCE & TECHNOLOGY

Journal homepage: https://jurcon.ums.edu.my/ojums/index.php/borneo-science

A SOR METHOD UTILIZING REDLICH-KISTER FINITE DIFFERENCE FOR TWO POINT BOUNDARY VALUE PROBLEMS

Mohd Norfadli Suardi [1,*] and Jumat Sulaiman [2]

[1] Preparatory Centre for Science and Technology, Universiti Malaysia Sabah, Jln UMS 88400, Kota Kinabalu, Sabah, Malaysia.
[2] Research Management Centre, Universiti Malaysia Sabah, Jln UMS 88400, Kota Kinabalu, Sabah, Malaysia.

[*]Correspondence:
mohdnorfadlisuardi@ums.edu.my

Received: 10 April 2025
Revised: 30 December 2025
Accepted: 30 December 2025
Published online: 31 December 2025

Doi:
10.51200/bsj.v46i2.6313

Keywords:
Boundary problem; Redlich-Kister finite difference; SOR iteration; Two point boundary value problems

ABSTRACT. *This study presents a numerical method using a second-order Redlich-Kister Finite Difference (RKFD) discretization scheme to approximate the two-point boundary value problems (TPBVPs). The approach creates a linear system for the given problem by using the first two derivatives to create the RKFD approximation equation. Two iterative approaches are used to solve the linear system: Gauss-Seidel (GS) and Successive Over-Relaxation (SOR). Two model examples that assess each approach according to its number of iterations, execution time, and maximum norm over five different mesh sizes indicate the effectiveness of these proposed iterative methods. The results show that the SOR method outperforms the GS methods in providing an extremely accurate approximation of the known exact solution.*

INTRODUCTION

In recent years, there has been increasing interest in creating, applying, and studying numerical methods for boundary value problems due to the difficulties in deriving analytical solutions (Aarao *et al*., 2010). One such equation, the two-point boundary value problem, has widespread applications in science, engineering, and physics research areas (Gupta, 2012; Wang & Guo, 2008). Many researchers have devoted their efforts to designing accurate numerical solutions for TPBVPs and recognize the difficulties associated with obtaining them. Previous studies have explored various numerical techniques to address the TPBVPs. Mohsen and El-Gamel (2008) used the Galerkin and collocation methods to numerically simulate this problem, while Liu *et al*. (2011) proposed a polynomial spline implementation as a numerical solution. Furthermore, researchers have investigated a B-spline method (Caglar & Caglar, 2009) to tackle the diffusion problem. Additionally, the literature provides a range of other numerical solutions for TPBVPs (Al-Towaiq, 2023; Pandey, 2023; Rashidinia & Sharifi, 2015; Wang, 2023; Zhanlav *et al*., 2024), which can be applied to the study of TPBVPs.

Based on the method mentioned in the previous paragraph, we propose a new approach called the RKFD method to solve the boundary value problem. This method is based on the Redlich-Kister (RK) function, which is widely used in physics and chemistry to obtain solutions but has been less

commonly utilised in other fields (Babu *et al*., 2019; Gayathri *et al*., 2019; Komninos & Rogdakis, 2020). Over time, its application has been extended to solve numerical analysis problems. The background of this method in numerical analysis started with the study (Hasan *et al*., 2010), in which the piecewise RK polynomial model has been used, focusing on the construction of first- and third-order models and on analysing the relationship between Gauss-Seidel iteration and mesh sizes. The findings indicated that the third Redlich-Kister model offers good accuracy compared to the first model.

Following this research, subsequent research has gone deeper into the application of RK functions to numerical analysis fields. For example, in Suardi and Sulaiman (2021b), the authors suggested the use of RK polynomials to solve a one-dimensional boundary value problem. Furthermore, Suardi & Sulaiman (2021a, 2022) proposed RKFD, which combines the RK polynomial and finite difference methods to solve a problem of two-point boundary value problems. The use of the RKFD approximation equation generates the system of the RKFD equation, which will be solved by iterative methods, which is the SOR method, as a linear solver. In literature, Young (1970) explored the various SOR methods for solving linear equation systems of $Au = b$ and discovered that the SOR methods with optimal relaxation parameters produce small radio waves. In addition, Sampoorna and Bueno (2010) tested the partial atomic redistribution problems by using the Gauss-Seidel method and the SOR, and they then found that the SOR method could solve the problem in a short time. This is supported by Radzuan *et al*. (2018), who mentioned that the SOR method can accelerate the convergence of linear equation solutions using optimal relaxation parameters. Inspired by all those studies, the paper aims to develop numerical solutions for problems involving TPBVPs in Equation 1.

$$\frac{d^2U}{dx^2} + Z(x)\frac{dU}{dx} + G(x)U(x) = r(x) \tag{1}$$

With the Dirichlet conditions

$$U(0) = \varphi_0, U(\phi) = \varphi_1.$$

RKFD APPROXIMATION EQUATION

Before the numerical process begins for Equation 1, the two newly established RKFD approximation equations must be constructed, as described in the preceding section. To construct these approximation equations, a discretisation process based on the Redlich–Kister (RK) function is required. Defining the general formula of the RK function is in Equation 2.

$$U_n(x) = \sum_{k=0}^{n} a_k \cdot T_k(x) \tag{2}$$

where $a_k, k = 0,1,2,\dots,n$ are the unknown parameters.

Before calculating the unknown parameters in equation 2, the distribution of the mesh sizes utilised is depicted in Figure 1. The size of the mesh shown in Figure 1 provides an understanding of the formulation of the first three Redlich-Kister (RK) functions, as depicted in Figure 2.

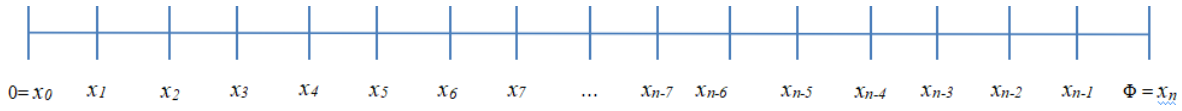

Figure 1. Distribution of mesh sizes considered.

Figure 2. The path for T_0, T_1, and T_2.

Applying the concept of Figure 2 to Equation 2 can mean that the second-order RK approximation function is expressed in Equation 3.

$$U(x) = a_0T_0(x) + a_1T_1(x) + a_2T_2(x) \tag{3}$$

Where the first three RK functions are defined as

$$T_0(x) = 1, \quad T_1(x) = x, \quad T_2(x) = x(1-x).$$

Then, the grid network shown in Figure 1 is set up as a reference domain for equation 3 by applying the node points, $x_c = x_0 + ch, c = 0,1,2,\dots,n$ and defining the uniform step size as $h = \frac{\varphi-0}{n}, n = 2^p, p \geq 1$. This process is used to solve the following linear system and obtain unknown parameters in equation 3.

$$\begin{bmatrix} U_{c-1} \\ U_c \\ U_{c+1} \end{bmatrix} = \begin{bmatrix} T_0(x_{c-1}) & T_1(x_{c-1}) & T_2(x_{c-1}) \\ T_0(x_c) & T_1(x_c) & T_2(x_c) \\ T_0(x_{c+1}) & T_1(x_{c+1}) & T_2(x_{c+1}) \end{bmatrix} \begin{bmatrix} a_0 \\ a_1 \\ a_2 \end{bmatrix}, \tag{4}$$

where $U(x_c) = U_c$. After that, Equation 4 is solved using the matrix approach to derive the formulas for the three unknown parameters in Equation 3. Equation 3 was used to replace all three parameters and rewrite them as Equation 5.

$$U(x) = N_0(x)U_{c-1} + N_1(x)U_c + N_2(x)U_{c+1} \tag{5}$$

where the RKFD shape functions, $N_k(x), k = 0,1,2$ can be defined as Equation 6.

$$\left.\begin{aligned} N_0(x) &= (x^2 - 2xhc - xh + h^2c^2 + h^2c)/(2h^2) \\ N_1(x) &= (2xhc - x^2 - h^2c^2 + h^2)/(h^2) \\ N_2(x) &= (x^2 - 2xhc + xh + h^2c^2 - h^2c)/(2h^2) \end{aligned}\right\} \tag{6}$$

By evaluating the first and second derivatives concept on Equation (6), the RKFD approximation function is expressed as Equation 7.

$$\left.\begin{aligned} \frac{dU}{dx}\Big|_c &= N_0'(x_c)U_{c-1} + N_1'(x_c)U_c + N_2'(x_c)U_{c+1} \\ \frac{d^2U}{dx^2}\Big|_c &= N_0''(x_c)U_{c-1} + N_1''(x_c)U_c + N_2''(x_c)U_{c+1} \end{aligned}\right\} \tag{7}$$

where $U(x_c) = U_c, c = 0,1,2,\dots,n$ accorded as the approximation solution of the function U(x). The expression generated by equation 7 highlights the two newly established RKFD discretisation methods, which correspond to the primary objective of this work. These approaches have been designed for constructing the RKFD approximation equation to solve the suggested problem (1). By substituting equation 7 into the given problem and applying the second-order central difference techniques for discretising in time, a second-order RKFD approximation, Equation 8, could be constructed as follows for the TPBVP

$$\alpha_cU_{c-1} + \beta_cU_c + \gamma_{c+1}U_{c+1} = R_c, \tag{8}$$

where

$$\alpha_c = N_{0}''(x_c) + ZN_{0}'(x_c), \beta_c = N_{1}''(x_c) + ZN_{1}'(x_c) + G_c, \gamma_c = N_{2}''(x_c) + ZN_{2}'(x_c)$$

Next, the RKFD linear systems can then be built in matrix form using the RKFD approximation equation 8 as follows:

$$W \cdot \underline{U} = \underline{R} \tag{9}$$

DERIVATION OF SOR ITERATIVE METHOD

From the previous section, the generated large-scale and sparse linear systems (9) emerge as a result of the completed RKFD discretisation scheme process. Based on many research studies (Hackbusch, 1994; Saad, 2003; Young, 2014), it is recommended to use iterative methods to solve this linear system since it involves a large scale within the coefficient matrix. To solve equation 9 in this study, the SOR iterative approach has been regarded as a linear solution. Studies on the application and effectiveness of the SOR method, which is an enhancement of the GS method, have been conducted by Kalambi (2008) and Youssef (2012). When applying the SOR approach, which is impacted by the weighted parameter's value determination, the range should be $1 \leq \omega \leq 2$. However, when the weighted parameter is taken as equal to one, $\omega = 1$the SOR method will change into the GS method (Equation 10) (Kalambi, 2008).

$$(F + J + L) \cdot \underline{U} = \underline{R}, \tag{10}$$

where J, F and L are diagonal matrix, triangular lower and upper matrices. Through manipulation of equation 10, the representation of the SOR method in the form of a point iteration form is presented in Equation11.

$$\underline{U}^{(q+1)} = (1 - \omega)\underline{U}^{(q)} + \omega(J + F)^{-1}(\underline{R} - L\underline{U}^{(q)}) \tag{11}$$

where $\underline{U}^{(q+1)}$ referring to the value of $U(x)$ at the $(q + 1)^{th}$ iteration.

NUMERICAL PROBLEM AND DISCUSSION

In the previous discussion, the RKFD approximation equation was derived, and the numerical experiment was conducted to solve problem (1) using the SOR method. To determine the applicability of the suggested method, two examples were tested with different mesh sizes, $n = 256,512,1024,2048,4096$. Additionally, numerical comparisons were done in terms of the number of iterations (Iter), execution time (Time), and maximum norm. Following that, a tolerance error, $\varepsilon = 10^{-10}$ is always used for all examples that are taken into consideration.

Example 1
The TPBVPs (1) as (Caglar *et al*., 2006)

$$\frac{d^2U}{dx^2} - \frac{dU}{dx} = -e^{(x-1)^{-1}} \tag{12}$$

and the analytical solution of problem (12) is $U(x) = x(1 - e^{(x-1)})$.

Example 2
The TPBVPs (1) with as (Ramadan *et al*., 2007)

$$\frac{d^2U}{dx^2} - U(x) = -1 \tag{13}$$

and the analytical solution of problem (13) is $U(x) = \cos(x) + \frac{1-\cos(1)}{\sin(1)}\sin(x) - 1$.

As predicted in Table 1, the numerical result indicates that the SOR method with the RKFD approximation equation outperforms the GS method, the benchmark method in this study, in terms of iteration and time. The SOR method can generate fewer iterations and converge more quickly across all examples tested. For instance, in Table 1, 769 iterations are required by the SOR method and 0.73 seconds to converge Example 1 at a 256 mesh size, while the GS method required 82043 iterations and 22.54 seconds. The advantage of the SOR method becomes more pronounced as the mesh size increases, as seen in the results for n = 4096, where the SOR method required 10244 iterations and 10.51 seconds, compared to the GS method, which required 11811519 iterations and 2359.09 seconds. The numerical results for solving problems exhibit a similar pattern, with the SOR method demonstrating improved performance over the GS method, as reported in Example 2. These findings are consistent with the literature (Suardi & Sulaiman, 2022), which indicates that the SOR method can enhance the applicability of the GS method for solving TPBVPs. In terms of accuracy, both the SOR and GS methods showed excellent agreement with their respective exact solutions.

Table 1. Numerical results for examples 1 and 2.

n	Method	Example 1			Example 2		
		Iter	Time	MaxNorm	Iter	Time	MaxNorm
256	GS	82043	22.54	4.0343e-07	89973	19.88	5.4091e-07
	SOR	769	0.73	2.4519e-07	769	0.39	2.0467e-07
512	GS	292276	35.51	2.5291e-06	318924	60.80	2.9059e-06
	SOR	1526	1.57	6.7390e-08	1537	0.88	4.3126e-08
1024	GS	1025489	117.83	1.0346e-05	1111808	256.86	1.1810e-05
	SOR	2946	3.46	1.9947e-08	3057	1.81	1.5554e-08
2048	GS	3527433	409.02	4.1443e-05	3791677	1260.25	4.7285e-05
	SOR	5792	6.64	1.7364e-08	5733	3.44	2.5779e-08
4096	GS	11811519	2359.09	1.6579e-04	12544476	2681.69	1.8915e-04
	SOR	10244	10.51	9.3638e-08	10660	5.71	1.0453e-07

CONCLUSION

The GS and SOR methods are looked at in this paper as two iterative ways to get the numerical solution of two new RKFD approximation equations for solving TPBVPs. Firstly, the problem was discretised to form the RKFD approximation equation. The resulting linear system was then solved using the considered iterative methods. To validate the applicability of the iterative methods, two examples were tested, and the numerical results revealed that the SOR method produces the lowest number of iterations and is faster than the GS method. This conclusion was drawn from the analysis of the comparison of both methods presented in Table 1, which demonstrates the superior performance of the SOR method compared to the GS method.

ACKNOWLEDGEMENT

The authors would like to express sincere gratitude to Universiti Malaysia Sabah for funding this research under the UMSGreat research grant for postgraduate students: GUG0494-1/2020.

REFERENCES

Aarao, J., Bradshaw-Hajek, B.H., Miklavcic, S.J. & Ward, D.A. 2010. The extended- domain–eigenfunction method for solving elliptic boundary value problems with annular domains. *Journal of Physics A: Mathematical and Theoretical*, 43(18): 185202.

Al-Towaiq, A. 2023. Useful ideas on the numerical techniques used for the solution of the two-point boundary value problems of ordinary differential equations. *Journal of Educational and Scientific Studies* (EPSTEM), 13(2): 171–175.

Babu, S., Trabelsi, R., Srinivasa Krishna, T., Ouerfelli, N. & Toumi, A. 2019. Reduced Redlich–Kister functions and interaction studies of Dehpa+ Petrofin binary mixtures at 298.15 K. *Physics and Chemistry of Liquids,* 57(4): 536–546.

Caglar, H., Caglar, N. & Elfaituri, K. 2006. B-spline interpolation compared with finite difference, finite element, and finite volume methods which applied to two-point boundary value problems. *Applied Mathematics and Computation,* 175(1): 72–79.

Caglar, N. & Caglar, H. 2009. B-spline method for solving linear system of second-order boundary value problems. *Computers & Mathematics with Applications*, 57(5): 757–762.

Gayathri, A., Venugopal, T. & Venkatramanan, K. 2019. Redlich-Kister coefficients on the analysis of physico-chemical characteristics of functional polymers. *Materials Today: Proceedings,* 17: 2083–2087.

Gupta, Y. 2012. A numerical algorithm for solution of boundary value problems with applications. *International Journal of Computer Applications*, 40(8): 48–51.

Hackbusch, W. 1994. *Iterative solution of large sparse systems of equations* (Vol. 95). Springer.

Hasan, M.K., Sulaiman, J., Ahmad, S., Othman, M. & Abdul Karim, S.A. 2010. Approximation of iteration number for Gauss-Seidel using Redlich-Kister polynomial. *American Journal of Applied Sciences,* 7: 956–962.

Kalambi, I.B. 2008. A comparison of three iterative methods for the solution of linear equations. *Journal of Applied Sciences and Environmental Management*, 12(4).

Komninos, N. P. & Rogdakis, E.D. 2020. Geometric investigation of the three-coefficient Redlich-Kister expansion global phase diagram for binary mixtures. *Fluid Phase Equilibria,* 525: 112728.

Liu, L.-B., Liu, H.-W. & Chen, Y. 2011. Polynomial spline approach for solving second-order boundary-value problems with Neumann conditions. *Applied Mathematics and Computation*, 217(16): 6872–6882.

Mohsen, A. & El-Gamel, M. 2008. On the Galerkin and collocation methods for two-point boundary value problems using sinc bases. *Computers & Mathematics with Applications,* 56(4): 930–941.

Pandey, P.K. 2023. A method for an approximate numerical solution of two-point boundary value problems: Nonstandard finite difference method on a semi-infinite domain. *International Journal of Computing Science and Mathematics,* 17(3): 220–228.

Radzuan, N.Z.F.M., Suardi, M.N. & Sulaiman, J. 2018. Explicit group SOR iterative method with quadrature scheme for solving system of Fredholm integral equations of second kind. *AIP Conference Proceedings*, 1974(1).

Ramadan, M.A., Lashien, I.F. & Zahra, W.K. 2007. Polynomial and nonpolynomial spline approaches to the numerical solution of second order boundary value problems. *Applied Mathematics and Computation,* 184(2): 476–484.

Rashidinia, J. & Sharifi, S. 2015. B-spline method for two-point boundary value problems. *International Journal of Mathematical Modelling & Computations*, 5(2 (SPRING)), 111– 125.

Saad, Y. 2003. Iterative methods for sparse linear systems. SIAM.

Sampoorna, M. & Bueno, J.T. 2010. Gauss–seidel and successive overrelaxation methods for radiative transfer with partial frequency redistribution. *The Astrophysical Journal*, 712(2): 1331.

Suardi, M.N. & Sulaiman, J. 2021a. Redlich-Kister finite difference solution for two-point boundary value problem by using MKSOR iteration. *AIP Conference Proceedings*, 2423(1).

Suardi, M.N. & Sulaiman, J. 2021b. Solution of one-dimensional boundary value problem by using Redlich-Kister Polynomial. Computational Science and Technology: 7th ICCST 2020, Pattaya, Thailand, 29–30 August, 2020, 487–500.

Suardi, M.N. & Sulaiman, J. 2022. The use of two newly established Redlich-Kister Finite differences with KSOR method in a numerical solution of one dimensional telegraph equations. *International Journal of Mathematics and Computer Science*, 17(3).

Wang, Y.-M. & Guo, B.-Y. 2008. Fourth-order compact finite difference method for fourth- order nonlinear elliptic boundary value problems. *Journal of Computational and Applied Mathematics*, 221(1): 76–97.

Wang, M. 2023. Approximate solutions of two-point boundary value problems by the weak-form integral equation method. *Journal of Applied Science and Engineering*, 26(10): 1491–1500.

Young, D.M. 1970. Convergence properties of the symmetric and unsymmetric successive overrelaxation methods and related methods. *Mathematics of Computation*, 24(112): 793– 807.

Young, D.M. 014. *Iterative solution of large linear systems*. Elsevier.

Youssef, I.K. 2012. On the successive overrelaxation method. *Journal of Mathematics and Statistics*, 8(2): 176–184.

Zhanlav, T., Ganbat, B. & Gerelt-Od, G. 2024. Higher-order finite-difference schemes for nonlinear two-point boundary value problems. *Journal of Mathematical Sciences*, 279: 929–945.

RESEARCH ARTICLE

BORNEO SCIENCE
THE JOURNAL OF SCIENCE & TECHNOLOGY

Journal homepage: https://jurcon.ums.edu.my/ojums/index.php/borneo-science

SENTIMENT ANALYSIS OF PUBLIC HEALTH SOCIAL MEDIA COMMENT USING EXPERT ANNOTATION

Daimler B. Alebaba, Suaini Sura*, Nooralisa M. Tuah, and Nona M. Mohd Nistah

Faculty of Computing and Informatics, Universiti Malaysia Sabah, Jln UMS Kota Kinabalu 88400, Sabah, Malaysia.

***Correspondence:**
su_sura@ums.edu.my

Received: 29 April 2025
Revised: 6 January 2026
Accepted: 6 January 2026
Published online: 21 January 2026

Doi:
10.51200/bsj.v46i2.6321

Keywords:
Expert annotation; Public health; Sentiment analysis; Social media; User engagement.

ABSTRACT. *Sentiment analysis has become a critical tool for organizations and researchers to understand user sentiment. However, it faces challenges such as managing noisy data, interpreting sarcasm or irony, and adapting to the evolving nature of language, especially in public health, where users often express opinions about their health conditions, healthcare experiences, and complex medical terminology on various topics. Addressing these challenges is crucial to maintaining the integrity of sentiment analysis results. Hence, this study analyzes public health social media user comments using a structured sentiment analysis framework. The framework includes dataset collection and annotation, text preprocessing, feature vectorization, and text classification. Experimental results show that the proposed model achieved an accuracy of 98% on the annotated dataset, indicating strong predictive performance within the scope of this study. The findings suggest that the framework is effective in capturing sentiment patterns in public health social media data and provides a foundation for further evaluation using comparative and benchmark-based analyses.*

INTRODUCTION

Sentiment analysis is a subfield of Natural Language Processing (NLP) and has become a vital method for organizations and researchers seeking to understand user sentiment (Aftab *et al*., 2023; Hartmann *et al*., 2023). The origins of sentiment analysis trace back to early research in 2001, when Das and Chen attempted to use evaluative texts to predict public sentiment, laying the groundwork for what would become a rapidly expanding field of study (Ogbuokiri *et al*., 2024; Venkit *et al*., 2023). Since the foundational work of Das and Chen, sentiment analysis has undergone significant advancements. Researchers began developing methods to classify the polarity of text, which involves determining whether a given piece of text expresses a positive or negative sentiment (Tan *et al*., 2023). This evolution was driven by the increasing availability of digital text data, particularly from public health social media platforms where users frequently express their opinions concerning their health condition, healthcare, and complex medical-related terminology on a variety of topics.

However, sentiment analysis faces several challenges, including managing noisy data, interpreting sarcasm or irony, and adapting to the fluidity of language (Lakshmi *et al*., 2024, 2024). These challenges could lead to misleading insights and incorrect sentiment interpretation, resulting in faulty decision-making based on inaccurate data. In the context of public health, for example, inaccurate sentiment analysis might cause misunderstandings of user concerns or needs, leading to ineffective

responses or interventions (Mohammad Amini *et al*., 2023). Furthermore, poor accuracy can reduce the reliability of predictive models, limiting their practical applications and diminishing trustworthiness in real-world scenarios (Adli *et al*., 2024; Lakshmi *et al*., 2024). Therefore, addressing challenges such as noisy data and sarcasm is essential to maintain the integrity of sentiment analysis results.

Hence, this study analyzes public health social media user comments using a structured sentiment analysis framework. The framework includes the steps of dataset collection and annotation, text preprocessing, feature vectorization, and text classification (Adli *et al*., 2024; Aftab *et al*., 2023; Md Suhaimin *et al*., 2019). Each step is designed to refine and ensure the relevance of the data, enhancing the accuracy of text classification (Venkit *et al*., 2023). The final step involves evaluating the accuracy of the classification results.

MATERIALS AND METHODS

The method of this study follows a structured sentiment analysis framework, which includes annotation by three public health experts, text preprocessing using NLP techniques, feature vectorization with Term Frequency-Inverse Document Frequency (TF-IDF), and classification using the Support Vector Machine (SVM) algorithm. Classification accuracy is evaluated using metrics such as the confusion matrix and assessed through the Area Under the Curve (AUC). The framework of this study is illustrated in Figure 1.

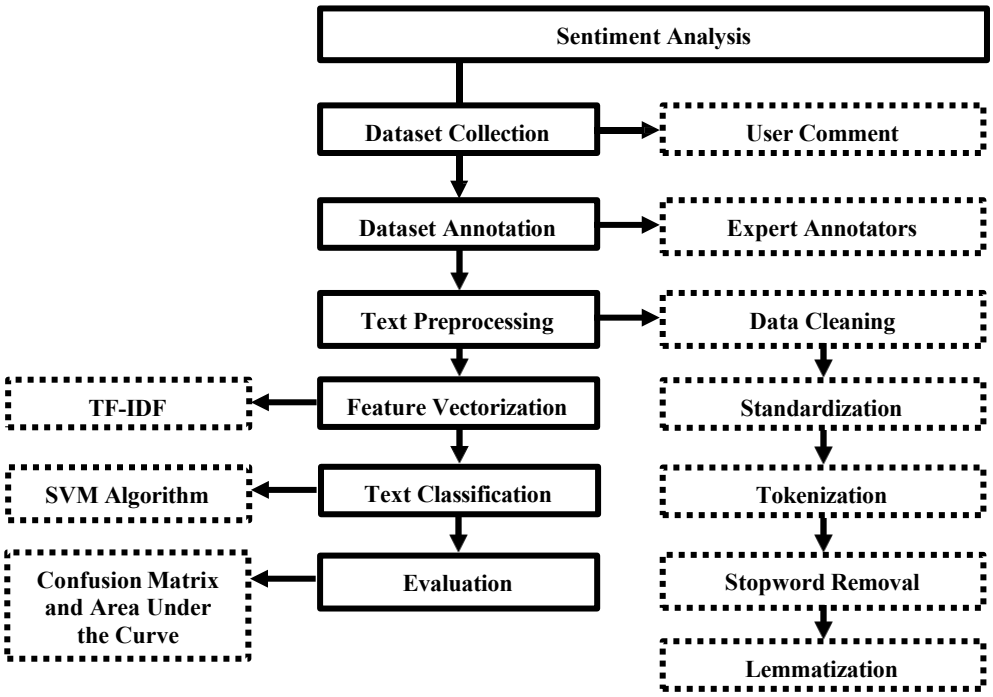

Figure 1. Structure sentiment analysis framework.

Dataset Collection

The dataset was sourced from the public health Facebook page of Hospital UMS, comprising user comments in textual data. Permission to collect this dataset was formally granted by Hospital UMS, ensuring adherence to ethical standards and data protection regulations (Mohammad Amini *et al*., 2023). The dataset spans from June 1, 2020, to September 30, 2022, and was stored in a Microsoft Excel worksheet. Given that, mixed languages, including Malay and English, appeared in the dataset. To ensure consistency, the Google Translate Sheets function was used to translate all non-English comments into English.

Dataset Annotation

Three public health experts were assigned to manually label the sentiment of each comment as either positive or negative. The first annotator is a medical officer, while the second and third annotators are dental surgery assistants. These healthcare professionals were selected for their expertise in medical terminology, health-related issues, and public health concerns. The dataset contains 368 rows and seven columns: id, comment, comment translated, annotator_1, annotator_2, annotator_3, and result. The id column represents the content ID, comment holds the original user comment, and comment_translated contains the translated version in English. The annotator_1 column reflects the sentiment labels assigned by the medical officer, while annotator_2 and annotator_3 correspond to the labels given by the two dental surgery assistants. The result column indicates the inter-annotator agreement on the sentiment polarity.

Text Preprocessing

While the collected and annotated dataset is labeled, it may still contain unnecessary elements that do not contribute to sentiment analysis tasks. Therefore, it is crucial to remove these irrelevant elements. For that, text preprocessing using NLP techniques is conducted to prepare the dataset. This preprocessing involves several stages, including data cleaning, standardization, tokenization, stopword removal, and lemmatization (Ogbuokiri *et al*., 2024). Each stage simplifies and standardizes the text, ensuring a consistent and well-structured dataset that facilitates accurate feature vectorization and text classification (Bordoloi & Biswas, 2023).

Data cleaning removes non-useful elements such as names, emojis, links, and administrative comments from the dataset. This manual process ensures that only relevant user comments are included, refining the dataset and improving the quality of the sentiment analysis. Standardization involves converting all text to lowercase, ensuring uniformity and preventing case-related discrepancies, which facilitates more accurate text classification. This stage is implemented using Python's Pandas library. Tokenization breaks the text into individual words or tokens, transforming sentences into analyzable units, which simplifies the analysis of word frequencies. Stopword removal eliminates common, non-informative words like "and," "the," or "is," as well as numbers and unnecessary punctuation. This reduces the dataset's dimensionality and focuses on words that contribute meaningful information. Lemmatization reduces words to their base or canonical forms using language-specific rules, enhancing accuracy by unifying different word forms into a single representation.

Feature Vectorization

Feature vectorization converts text data into numerical features necessary for predictions (Lakshmi *et al*., 2024; Mohammad Amini *et al*., 2023). In this study, TF-IDF vectorization was used. The dataset, comprising 368 text documents, was split into 70% for training and 30% for testing using the `train_test_split` function from Python's `sklearn.model_selection` library. This ensures random partitioning while maintaining the target variable's distribution. TF-IDF vectorization was then applied to the training set, calculating scores that reflect each term's importance within a document relative to the entire corpus.

Text Classification

Text classification was performed using the SVM algorithm from Python's sklearn.svm library. A polynomial kernel (kernel='poly') was chosen to handle non-linear separations in the data, allowing the SVM to find a flexible decision boundary. The classifier was trained on the TF-IDF vectorized training set using the fit method, which optimizes the hyperplane to maximize the margin between classes and improve classification accuracy.

Evaluation

The evaluation was conducted using the `sklearn.metrics` library in Python. A classification report was generated with the `classification_report` function, detailing performance metrics such as classification accuracy, precision, recall, F1-score, and support for each class. The confusion matrix was used to evaluate and summarize prediction results, showing counts of True Positives (TP), True Negatives (TN), False Positives (FP), and False Negatives (FN). Additionally, the classification accuracy was assessed using the AUC metric, with higher scores indicating better predictive performance. Table 1 outlines the interpretation of AUC scores.

Table 1. Area under the curve.

Score	Predictive Performance
0.90-1.00	Excellent Classification
0.80-0.90	Good Classification
0.70-0.80	Fair Classification
0.60-0.70	Poor Classification
0.50-0.60	Failure

RESULTS AND DISCUSSIONS

The evaluation begins with analyzing both the 70% training set and the 30% testing set using the confusion matrix. The confusion matrix categorizes the predicted instances into four outcomes, namely TP, TN, FP, and FN. The results are summarized in Table 2, highlighting the model's performance in terms of correct and incorrect classifications.

Table 2. Confusion matrix result.

Predicted Instance	Actual Positive	Actual Negative	Metrics
Positive	73 (TP)	1 (FP)	0.99 (precision)
Negative	7 (FN)	51 (TN)	0.00
Metrics	0.91 (recall)	0.98 (specificity)	0.94 (accuracy) and 0.95 (F1-score)

Table 2 reveals that the model has a high precision of 0.99, indicating that 99% of instances predicted as positive were indeed positive. This demonstrates the model's strong predictive performance. The recall of 0.91 suggests that the model correctly identified all actual positive instances without any missing (FN = 7), reflecting its high sensitivity to positive cases. The confusion matrix is visually represented as a heatmap in Figure 2.

The model's specificity is 0.98 due to the absence of true negative instances (TN = 51), indicating that the model did not identify any actual negative cases. This suggests the model is heavily focused on detecting positive instances, potentially at the expense of identifying negatives. Despite this, the model's overall accuracy is 0.94, meaning 94% of all predictions, whether positive or negative, were correct. The F1-score of 0.95 combines precision and recall into a single metric, reflecting a high level of accuracy in positive predictions.

The model's classification accuracy of 0.94 includes a 6% error margin, represented by FP =1. This error margin is within acceptable limits for most practical applications. Achieving absolute perfection is rare in machine learning, and a small number of errors are generally acceptable, especially when the model shows strong precision and recall (Ogbuokiri *et al*., 2024). The classification report, detailed in Table 3, provides a comprehensive breakdown of performance metrics.

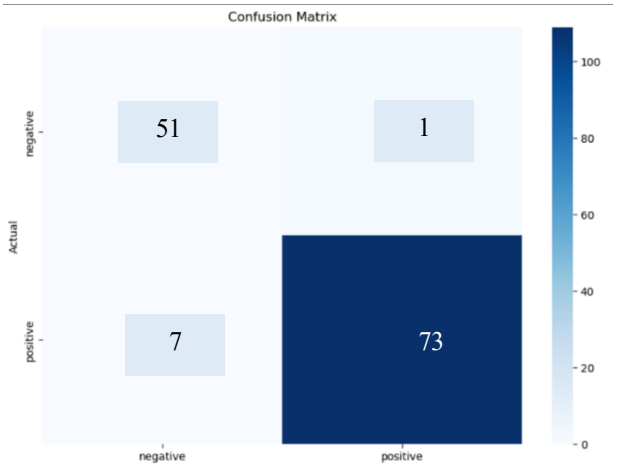

Figure 2. Confusion matrix results in a heatmap plot.

Table 3. Sentiment analysis classification report.

	Precision	Recall	F1-score	Support
Negative	0.879310	0.980769	0.927273	52.000000
Positive	0.986486	0.912500	0.948052	80.00000
Accuracy	0.939394	0.939394	0.939394	0.939394
Macro Average	0.932898	0.946635	0.937662	132.000000
Weighted Average	0.944266	0.939394	0.939866	132.000000

According to the AUC evaluation criteria outlined in Table 1, the model's classification accuracy of 0.94 falls within the 'Excellent Classification' range, which is defined as an AUC score between 0.90 and 1.00. This range is widely recognized as an industry standard for high-performing models, indicating that the model is not only accurate but operates with a level of precision and recall that exceeds the benchmarks typically required in practical applications (Lakshmi *et al*., 2024). Models within this range are capable of distinguishing between positive and negative instances with a high degree of certainty, minimizing both false positives and false negatives (Ogbuokiri *et al*., 2024).

.

CONCLUSION

This study successfully analyzed public health social media user comments using a structured sentiment analysis framework. The framework involved annotation by three public health experts, text preprocessing with NLP techniques, feature vectorization using TF-IDF, and classification with the SVM algorithm. The classification achieved 98% accuracy, demonstrating a strong predictive performance. According to the AUC evaluation criteria, the accuracy of 0.94 falls within the 'Excellent Classification' range, where this range is widely recognized as an industry standard for high-performing models, indicating that the model is not only accurate but operates with a level of precision and recall that exceeds the benchmarks typically required in practical applications. The key contribution of this study is that the framework can be used to conduct sentiment analysis in challenging areas such as handling noisy data, detecting sarcasm or irony, and adapting to the fluid nature of language. Future work will focus on comparing the SVM algorithm with Naïve Bayes, Decision Tree, and Neural Networks to explore further improvements in accuracy performance.

ACKNOWLEDGEMENT

The authors wish to express their sincere gratitude to Universiti Malaysia Sabah for the support in facilitating this study (SBK0461-2021, Skim Penyelidikan Bidang Keutamaan). Special thanks are also extended to Hospital Universiti Malaysia Sabah for their contribution to the data collection process, which was crucial for the completion of this study.

REFERENCES

Adli, N.B.Z., Ahmad, M., Ghani, N. A., Ravana, S.D. & Norman, A.A. 2024. An ensemble classification of mental health in Malaysia related to the COVID-19 pandemic using social media sentiment analysis. *KSII Transactions on Internet and Information Systems*, 18(2): 370–396. https://doi.org/10.3837/TIIS.2024.02.006

Aftab, F., Bazai, S.U., Marjan, S., Baloch, L., Aslam, S., Amphawan, A. & Neo, T.-K. 2023. A comprehensive survey on sentiment analysis techniques. *International Journal of Technology*, 14(6): 1288–1298. https://doi.org/10.14716/ijtech.v14i6.6632

Bordoloi, M. & Biswas, S.K. 2023. Sentiment analysis: A survey on design framework, applications and future scopes. *Artificial Intelligence Review*, 56(11): 12505–12560. https://doi.org/10.1007/s10462-023-10442-2

Hartmann, J., Heitmann, M., Siebert, C. & Schamp, C. 2023. More than a feeling: Accuracy and application of sentiment analysis. *International Journal of Research in Marketing*, 40(1): 75–87. https://doi.org/10.1016/j.ijresmar.2022.05.005

Lakshmi, C.S., Saxena, S. & Kumar, B.S. 2024. Sentiment analysis and classification of COVID-19 tweets using machine learning classifier. *Journal of Autonomous Intelligence*, 7(2): 1–13. https://doi.org/10.32629/jai.v7i2.801

Md Suhaimin, M.S., Ahmad Hijazi, M.H., Alfred, R. & Coenen, F. 2019. Modified framework for sarcasm detection and classification in sentiment analysis. *Indonesian Journal of Electrical Engineering and Computer Science*, 13(3): 1175. https://doi.org/10.11591/ijeecs.v13.i3.pp1175-1183

Mohammad Amini, M., Jesus, M., Fanaei Sheikholeslami, D., Alves, P., Hassanzadeh Benam, A. & Hariri, F. 2023. Artificial intelligence ethics and challenges in healthcare applications: a comprehensive review in the context of the European GDPR Mandate. *Machine Learning and Knowledge Extraction*, 5(3): 1023–1035. https://doi.org/10.3390/make5030053

Ogbuokiri, B., Ahmadi, A., Nia, Z.M., Mellado, B., Wu, J., Orbinski, J., Asgary, A. & Kong, J. 2024. Vaccine hesitancy hotspots in Africa: an insight from geotagged twitter posts. *IEEE Transactions on Computational Social Systems*, 11(1): 1325–1338. https://doi.org/10.1109/TCSS.2023.3236368

Tan, Y.Y., Chow, C.-O., Kanesan, J., Chuah, J.H. & Lim, Y.L. 2023. Sentiment analysis and sarcasm detection using deep multi-task learning. *Wireless Personal Communications*, 129(3): 2213–2237. https://doi.org/10.1007/s11277-023-10235-4

Venkit, P.N., Srinath, M., Gautam, S., Venkatraman, S., Gupta, V., Passonneau, R.J. & Wilson, S. 2023. *The sentiment problem: a critical survey towards deconstructing sentiment analysis*. 13743–13763.